Thesis for the Master's degree in Molecular Biosciences
Main field of study in Biochemistry

Hanne Mali Thesen Møllergård

Photochemical internalisation (PCI) of the pro-apoptotic gene TRAIL: A study of the cellular death mechanisms

60 study points

Department of Molecular Biosciences
Faculty of mathematics and natural sciences
University of Oslo 05/2006

Abstract

Photochemical internalisation (PCI) is a method for efficient delivery of macromolecules, like genes used in gene therapy, to the cytosol of cells. Most macromolecules enter a cell by endocytosis and are trapped in the endocytic vesicles. PCI is based on photochemical treatment disrupting the endocytic vesicles, i.e. a photosensitiser localised in the membranes of endocytic vesicles ruptures these vesicles upon exposure to light, and endocytosed macromolecules are released into the cytosol. Thus, PCI leads to an enhanced biological effect mediated by the liberated macromolecules.

In the present work, this method was employed together with the non-viral vector polyethyleneimine (PEI) for delivery of the pro-apoptotic gene TNF-related apoptosis inducing ligand (TRAIL). The aim was to evaluate the potential of PCI-mediated delivery of the PEI/TRAIL complexes to enhance cancer cell death *in vitro*. Furthermore, the apoptotic death pathway following PCI of the TRAIL gene in colon carcinoma HCT-116 cells was investigated. The PCI-mediated effect was compared to the effects induced by the photochemical treatment alone or the treatment with the TRAIL gene alone.

The effect of PCI was tested with respect to TRAIL expression, induction of apoptosis and cell survival using various methods from the fields of biochemistry and cell biology. In addition, the PCI effect on the level of several key molecules involved in apoptosis was investigated using the Western blotting technique.

The results showed that PCI enhanced the expression and the cytotoxic effect of the TRAIL gene, and it also enhanced the induction of apoptosis, as compared to the other two treatments. It was also shown that in PCI, the TRAIL gene and the photochemical treatment acted additively rather than synergistically. Although the apoptotic mechanisms behind PCI of the TRAIL gene were not fully elucidated, there were indications that in HCT-116 cells apoptosis proceeds through the extrinsic (death receptor mediated) pathway, however without activation of the main executioner caspase, caspase-3. Moreover, photochemical up-regulation of the TRAIL death receptor was detected.

Acknowledgements

The work of the present study was carried out at the PCI-group, Department of Radiation Biology, Institute for Cancer Research, Rikshospitalet-Radiumhospitalet Health Enterprise in the period February 2005 to May 2006.

I would like to express my gratitude to the leader of the PCI-group, Ph.D. Kristian Berg for taking the chance of hiring me in the first place, for encouraging me to pursue further studies, and for allowing me to work on the project of my choice for this study. I am also thankful to him and to Professor Kirsten Sandvig, my superviser from the University of Oslo, for spending time they didn't have critically reading my manuscript and providing useful comments in the writing process.

I would like to thank all former and present members of the PCI-group for providing an excellent work environment, you make the Department of Radiation Biology a great place to be. Special thanks have to be sent to Ph.D. student Anette Weyergang for her endless patience in teaching me the art of Western blotting.

But first and foremost, I wish to thank my supervisor, Ph.D. Lina Prasmickaite, with all my heart. I greatly appreciate her exceptional scientific knowledge, dedication, and friendship, and I consider myself very lucky to be able to work with her on this project.

Finally I wish to thank my family, my parents, Einar and Elisabeth, and my sister Ida for always being there for me and for always supporting my choices in life. And the most important acknowlegdement goes to Eigil Almenning, my darling husband. Your love and support and patience is what keeps me going. Thank you for being as amazing as only you can be!

Hanne Mali Thesen Møllergård
May 2006

Content

Glossary

- **Anti-apoptotic protein** – A protein that antagonises apoptosis
- **Apoptosis** - Programmed cell death
- **Gene therapy** - Treatment or prevention of a disease by transfer of nucleic acids
- **Photochemical internalisation** - Delivery of macromolecules mediated by photochemical treatment employing photosensitisers that are localised in endocytic vesicles
- **Photochemical treatment (PDT)** - Treatment with a photosensitiser followed by light exposure
- **Photosensitiser** - A compound that upon light absorption induces chemical and physical reactions
- **Plasmid** - A double-stranded, usually circular, DNA molecule that replicates independently of the genome
- **Pro-apoptotic protein** – A protein that induces apoptosis
- **Promoter** – A sequence to which RNA polymerase binds in order to initiate transcription of a gene
- **Reporter gene** - A gene that is used to test the efficiency of gene transfection
- **Restriction map** – A diagram showing the positions of restriction sites within a DNA sequence
- **Transfection** - The process of successful gene transfer and expression
- **Transgene** - A gene delivered into a cell by a vector
- **Vector** - A delivery vehicle for genes or other nucleic acids

List of abbreviations

AAV	adeno-associated virus
Adv	adenovirus
$AlPcS_{2a}$	aluminum phtalocyanine with two sulfonate groups on adjacent phenyl rings
anODN	antisense oligodeoxynucleotide
APS	ammonium persulphate
ASPP	ankyrin repeats, SH3-domain, proline rich region protein (ASP protein)
ATCC	American type culture collection
BID	Bcl-2 inhibitory domain
Caspase	cysteine aspartyl-specific protease
CCD	cooled charge-coupled device
CMV	cytomegalovirus
DAPI	4′-6-diamidino-2-phenylindole
DcR	decoy receptor
DD	death domain
DED	death effector domain
dH2O	distilled water
DMSO	dimethylsulphoxide
DNA	deoxyribonucleic acid
DR	death receptor
E. coli	escherichia coli
DTT	1,4-dithio-DL-threitol
EDTA	ethylenediaminetetraacetic acid
EF-1α	elongation factor-1α
EGF	epidermal growth factor
EGFP	enhanced green fluorescent protein
EGFR	epidermal growth factor receptor
ELISA	enzyme-linked immuno-sorbent assay
EPG2	epithelial glycoprotein-2
EtBr	ethidium bromide
FCS	foetal calf serum
FLIP	FLICE inhibitory protein
HEPES	4-(2-hydroxyethyl)piperazine-1-ethanesulfonic acid
HRP	horseradish peroxidase
Hsp	heat shock proteins
HSV-TK	herpes simplex virus thymidine kinase
hTERT	human telomerase reverse transcriptase
IAP	inhibitor of apoptosis proteins
LB	luria bertani
MAP	mitogen-activated protein
MTT	3-(4,5-dimethylthiazol-2-yl)-25diphenyltetrazolium bromide
NFκB	nuclear factor kappa B
Na_3VO_4	sodium orthovanadate
$^1O_2$	singlet oxygen
O.D.	optical density
PAGE	polyacrylamide gel electrophoresis
PARP	poly (ADP) ribose polymerase
PBS	phosphate buffered saline
PCI	photochemical internalisation
PDT	photodynamic therapy
PEI	polyethylenimine
PI	propidium iodide
PI3K	phosphoinositide-3 kinase
PMSF	phenylmethylsulfonyl fluoride
PNA	peptide nucleic acid
PTEN	phosphatase and tensin homolog on chromosome ten
PVDF	polyvinylidene difluoride
RNase	ribonuclease
ROS	reactive oxygen species
RPMI	Roswell Park Memorial Institute
SDS	sodium dodecyl sulphate
siRNA	small interfering RNA
SMAC	second mitochondria-derived activator of caspase
tBID	truncated Bcl-2 inibitory domain
TBS	tris buffered saline
TEMED	2-Bis(dimethylamino)ethane
TGFβ	transforming growth factor beta
TNFα	tumour necrosis factor alpha
$TPPS_{2a}$	meso-tetra phenylporphine with two sulfonate groups on adjacent phenyl rings (LumiTrans®)
TRAIL	tumour necrosis factor related apoptosis inducing ligand
UV	ultra violet

Introduction

1 PCI – photochemical internalisation

Macromolecules have great potential as therapeutic agents, but the potential has yet to be fully exploited. Therapeutic macromolecules include proteins, such as ribosome inactivating protein toxins for the treatment of cancer, peptides and mRNA for vaccination and nucleic acids like DNA (i.e. therapeutic genes), antisense oligodeoxynucleotides (anODN), ribozymes, peptide nucleic acids (PNAs) and small interfering RNA (siRNA) for gene therapy [1]. One of the major obstacles restricting the therapeutic effect of such macromolecules is inefficient delivery into a target cell. The majority of the macromolecules enter the cell by endocytosis (fig. I1) and get trapped in endocytic vesicles (endosomes and lysosomes) from where they are unable to escape to perform a therapeutic function. Finally, the trapped molecules are degraded by lysosomal enzymes [2, 3]. Therefore, endosomal escape is recognised to be a very important step in delivery of functional macromolecules. Photochemical internalisation (PCI) is a technique facilitating liberation from the endocytic vesicles [4]. It has been successfully applied for enhancing the effect of various macromolecules, both *in vitro* and *in vivo* (table I1).

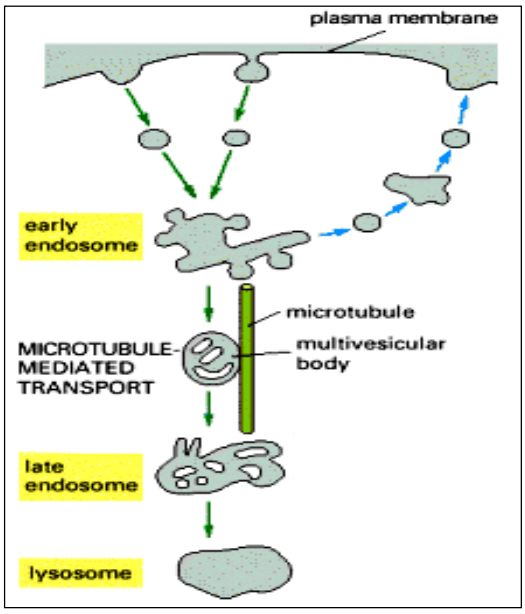

Figure I1 One model for the endocytic pathway from the plasma membrane to the lysosome (modified from [5]). Macromolecules are collected in clathrin-coated pits on the cell surface before endocytosis. The resulting clathrin-coated vesicles quickly lose their coat proteins, and the macromolecules are transported via early and late endosomes to the lysosome for degradation.

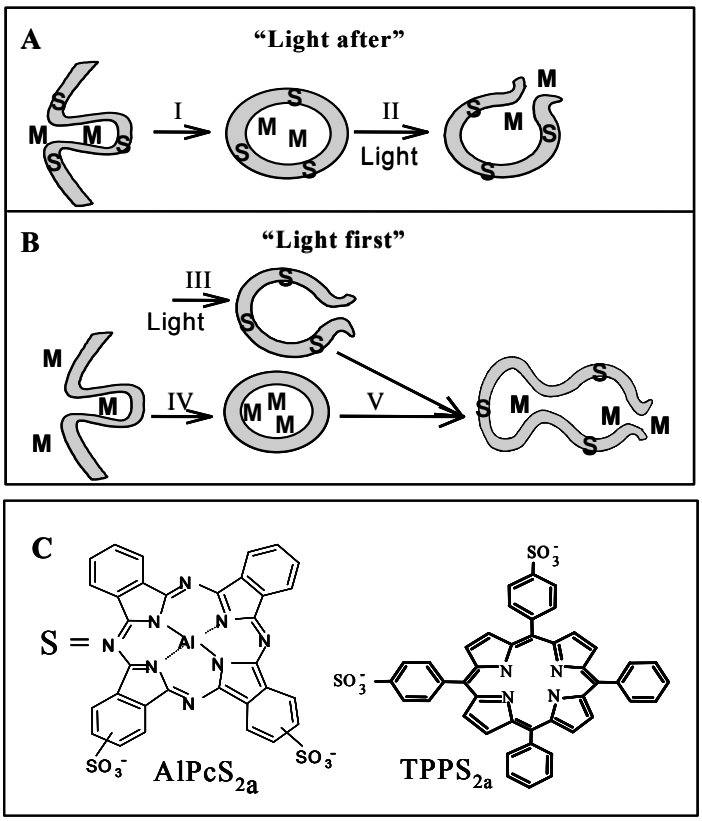

Figure I2 Schematic illustration of the principle of PCI (M = macromolecule and S = photosensitiser)

.

A) "Light after" strategy
B) "Light first" strategy

I – Uptake of macromolecules and photosensitiser via endocytosis
II + III – Light exposure followed by rupture of the endocytic vesicles (endosomes or lysosomes in which the photosensitiser is localised in the membrane) and release of the macromolecules
IV– Endocytic uptake of macromolecules in vesicles different from those containing photosensitiser
V – Fusion between ruptured vesicles and vesicles containing macromolecules resulting in release of the macromolecules

C) The most widely used photosensitisers for PCI [6]

A number of photosensitisers, including meso-tetraphenylporphine disulfunate ($TPPS_{2a,}$ LumiTrans®) and aluminium phtalocyanine disulfonate ($AlPcS_{2a}$), bind to the plasma membrane and following endocytosis they are primarily localised in the membranes of endocytic vesicles. In combination with exposure to light, these photosensitisers induce the formation of reactive oxygen species (ROS), primarily singlet oxygen ($^1O_2$). $^1O_2$ damages the membranes of endocytic vesicles, but does not affect the vesicular contents, including trapped therapeutic macromolecules, to the same extent. Therefore, functionally active

macromolecules can be released through the photochemically permeabilised membranes of the endosomes and lysosomes. This principle of delivery from endocytic compartments to the cytosol has been named PCI [4] and is illustrated in the figures I2 and I4. Importantly, PCI improves delivery and, consequently, activity of therapeutic agents only at specific, i.e. light-exposed, areas, thereby reducing adverse effects on non target sites [1].

As an alternative to the PCI-procedure illustrated in figure I2A, the light may be delivered before administration of the macromolecule, the so-called "light first" strategy (fig. I2B). When "light first" is employed, permeabilised endocytic vesicles are thought to fuse with vesicles containing the macromolecules, and thereby releasing the endocytosed macromolecules into the cytosol. This alternative strategy has been successfully tested both for gene therapy purposes and for delivery of the protein toxin gelonin *in vitro* [7].

Table II Overview of the application of the PCI-technology so far

PCI in gene therapy approaches			
Type of macromolecule	Examples	Model systems	Ref
Gene + Adeno-associated virus (AAV)	Reporter gene	Cell lines *in vitro*	[8]
Gene + Adenovirus (Adv)	Reporter genes TRAIL (apoptosis inducer)	Cell lines *in vitro*	[7-12], Engesæter et al., submitted
Gene (plasmid) + non-viral vectors	Reporter genes p53 (apoptosis inducer) HSV-tk (suicide gene) PTEN (tumour suppressor)	Cell lines *in vitro* Xenografts *in vivo* Rat eye conjunctival tissue *in vivo*	[4, 7, 13-22]
siRNA targeting:	S100A4 (promoter of metastasis)	Cell lines *in vitro*	Bøe et al., submitted
Peptide nucleic acids (PNA) targeting:	Reporter genes hTERT (involved in tumorigenesis) S100A4-protein (promoter of metastasis)	Cell lines *in vitro*	[23-25]
PCI in other tumour therapy approaches			
Type of macromolecule	Examples	Model system	Ref
Chemotherapeutic agent	Bleomycin	Cell lines *in vitro* Xenografts *in vivo*	[26]
Protein toxin	Gelonin (ribosome inactivating toxin) Saporin (ribosome inactivating toxin)	Cell lines *in vitro* Xenografts *in vivo*	[4, 7, 13, 27, 28]
Immunotoxin / affinity toxin	Moc31-Gelonin (targeting EPG-2) EGF-Saporin (targeting EGFR)	Cell lines *in vitro*	[29-31]

1.1 Photochemistry and photodynamic therapy (PDT)

The PCI technology derives from the field of photodynamic therapy (PDT) - an established treatment modality for several oncologic and non-oncologic indications such as several forms of cancer, skin actinic keratosis and age-related macular degeneration [32, 33]. PDT relies on three components: photosensitiser, light and oxygen. In cancer therapy, PDT is based on preferential uptake of photosensitiser in tumour cells followed by illumination of the tumour area, leading to ROS formation and, consequently, tumour destruction (fig. I3).

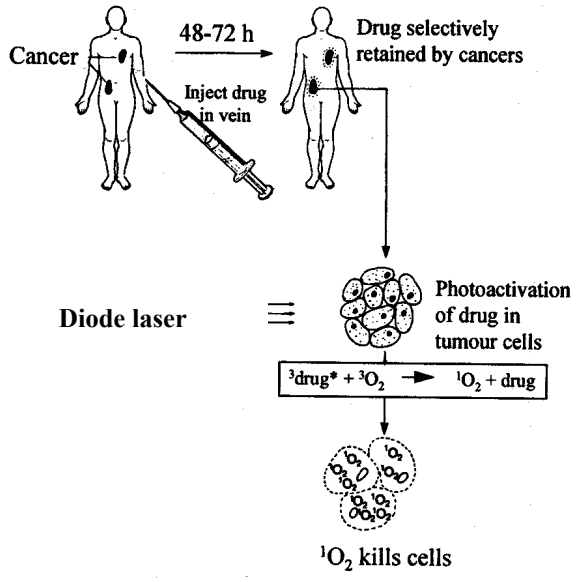

Figure I3 Schematic illustration of the basic principle of PDT. Adapted from the front page of British Journal of Cancer, 57 (5), 1988

Photosensitisers (S) are compounds that can be activated by light of the appropriate wavelength to an excited state (S*), which can further initiate photochemical/photophysical reactions. Usually the photochemical reactions proceed via $^1O_2$, a highly reactive form of oxygen generated after interaction between an excited photosensitiser (S*) and ground-state molecular oxygen (O_2) [34-36]. Schematically:

$$S \xrightarrow{\text{Light}} S^* \xrightarrow{O_2} S + {}^1O_2 \Longrightarrow \text{photochemical reactions}$$

$^1O_2$ is a very powerful oxidising agent able to oxidize proteins (the amino acids, like histidine, tryptophan, methionine, cysteine and tyrosine), DNA (guanine), unsaturated fatty acids and cholesterol [37]. This leads to the damage of various cellular structures, resulting in cytotoxicity. Since both the lifetime (< 0.04 μs) and the range of action (< 20nm) of $^1O_2$ are very short, only structures close to the photosensitiser are primarily affected [38]. Thus, the localisation of the photosensitiser determines which cellular organelles are directly affected [37], as illustrated in figure I4 for photosensitisers localised in the endocytic vesicles. Importantly, photochemical effect on DNA is not generally a dominant factor in PDT-mediated cytotoxicity, and PDT usually have a low mutagenic and carcinogenic potential [39]. Moreover, PDT with photosensitisers localised in the endocytic vesicles, like the ones used in PCI, has no known mutagenic effects on chromosomal DNA [40].

The photosensitisers used in PCI are amphiphilic molecules like $AlPcS_{2a}$ and $TPPS_{2a}$ (LumiTrans®) (fig. I2B) that upon endocytosis are mainly localised in the membranes of endocytic vesicles facing the lumen. Illumination of cells containing such photosensitisers induces $^1O_2$-mediated photochemical reactions that lead to permeabilisation of the vesicular membranes (fig. I4). This results in release of the lysosomal content, including lysosomal enzymes and the photosensitisers, into the cytosol [41]. These properties of the photosensitisers may therefore be used to release functional endocytosed molecules, such as therapeutic macromolecules, from endosomes and lysosomes upon illumination (fig. I4) [4].

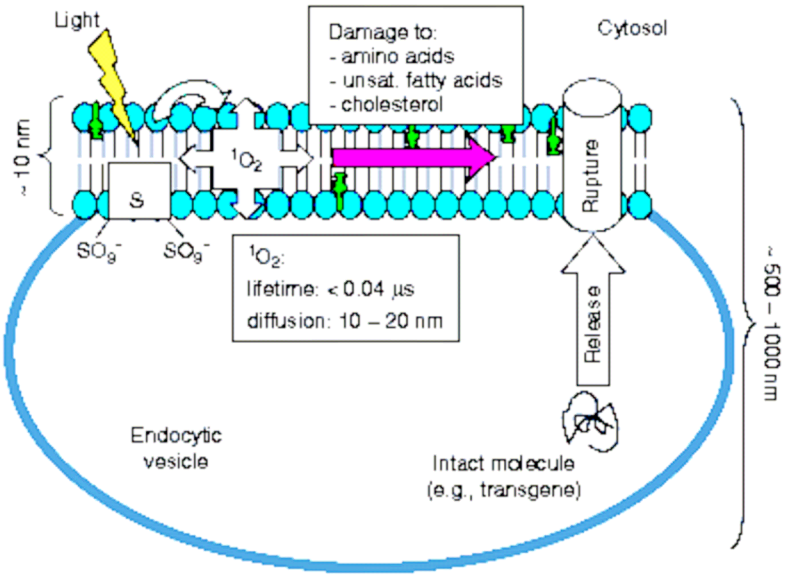

Figure I4 Schematic representation (not to scale) of the main events thought to occur in the endocytic vesicles following photochemical treatment with the photosensitisers (S) like $AlPcS_{2a}$ and LumiTrans® used for PCI [6].

Several photosensitisers with different localisation have been compared regarding their efficiency to induce the PCI-effect [11, 42], and it was confirmed that the localisation of the photosensitisers in endocytic vesicles, and especially in the endocytic membranes, is crucial for PCI. This indicates that endosomal release, and not the general photochemical effects, is responsible for the PCI-mediated enhancement of the effect of various macromolecules.

1.2 PCI in cancer therapy

Originally, PCI has been developed for use in cancer therapy approaches relying on macromolecules with anti-tumour activity (as illustrated in table I1). There are several reasons for this:

i) Being a selective, light-dependent method PCI ensures delivery of molecules inducing cell death specifically to tumour cells

ii) Photosensitisers tend to accumulate in tumour cells (as shown in fig. I3)

iii) Photochemical treatment usually also induce cytotoxic effects (discussed in chapter 1.1). Cytotoxicity is not desirable in situations where cells/tissues have to be preserved, however, in cancer therapy aiming to kill tumour cells, such cytotoxicity is advantageous.

Therefore, PCI in combination with macromolecules triggering cell death might result in enhanced cytotoxicity and a synergistic anti-tumour effect.

The “toxic” macromolecules, which are being used in combination with PCI, can induce cell death by direct inhibition of protein or DNA synthesis (e.g. protein toxins like gelonin, saporin and chemotherapeutics like bleomycin, table I1). Alternatively, cell death can be induced by stimulation of a death pathway or suppression of pro-survival signalling in the cell, shifting the balance in favour of death. There are two main death pathways, necrosis and apoptosis (discussed in chapter 2), and stimulation of apoptosis is one of the most exploited approaches in cancer therapy due to deregulated apoptosis in cancer cells (chapter 2.1.1). In addition, photochemical treatment (PDT) is usually highly efficient in inducing apoptosis (chapter 2.2) [43-48]. Therefore, combining PCI with pro-apoptotic macromolecules might result in enhanced apoptosis in cancer cells, and the aim of the present study was to investigate different aspects of such a combination, as a gene encoding an apoptosis-inducing protein has been employed as a pro-apoptotic macromolecule. Such a therapeutic strategy,

where genes or other nucleic acids are used as drugs is called gene therapy (described in fig. I5) and will be discussed in chapter 1.2.1.

One of the most attractive and successful strategies for PCI is its use in gene therapy, facilitating the delivery of nucleic acid-based macromolecules. A number of publications have already demonstrated enhanced delivery, expression [8, 12-15, 18-22, 49] and therapeutic effect ([14-16, 19, 22] and Engesæter et al., submitted) of foreign genes (transgenes) following PCI. Moreover, PCI-dependent potentiation of other types of nucleic-acids, like PNA [23-25] and siRNA (Bøe et al., submitted) targeting proteins involved in tumorigenesis, has been documented. This indicates that PCI can be combined with a variety of nucleic-acid based macromolecules relevant for cancer therapy.

1.2.1 Gene therapy

Gene therapy (fig. I5) is the treatment of a disease by using genes or other types of nucleic acids as therapeutic agents with the aim to replace, alter, suppress or supplement genes which are defective, missing or not naturally existing in the organism [50]. Most of the clinical gene therapy trials to date (~ 67 %) are focused on cancer (fig. I6). Since the majority of cancer gene therapy protocols rely on killing cancer cells rather than on their genetic correction, PCI is an ideal tool for cancer gene therapy.

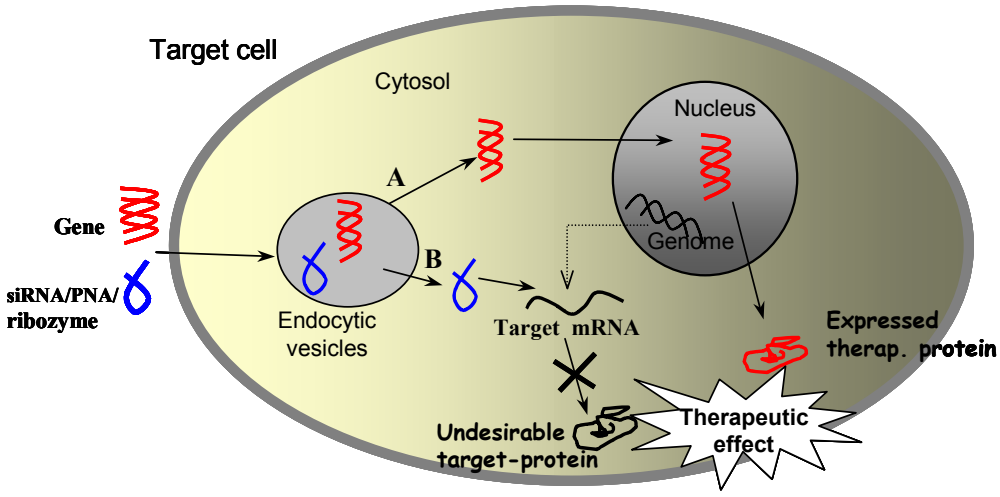

Figure I5 Illustration of the principles of gene therapy. Therapeutic nucleic acids (genes or siRNA/PNA/ribozymes) are delivered into a cell, usually via endocytosis. After liberation into the cytosol, the gene (A) is transported into the nucleus and expressed into a protein, which performs a desirable therapeutic function. Alternatively, siRNA/PNA/ribozyme (B) attack the target mRNA inhibiting the expression of an undesirable cellular target protein resulting in a therapeutic effect.

To transfer nucleic acid-based molecules into a cell, the molecules are usually packed into delivery vehicles, named vectors. Vectors enable delivery into target cells and their nuclei, provide protection from gene degradation and ensure transgene transcription in the cell [51]. Vectors can be divided into two groups, viral and non-viral [50, 51]. Physical methods for gene delivery, e.g. electroporation and gene gun are also available, and are often categorised among the non-viral vectors [52].

A **B**

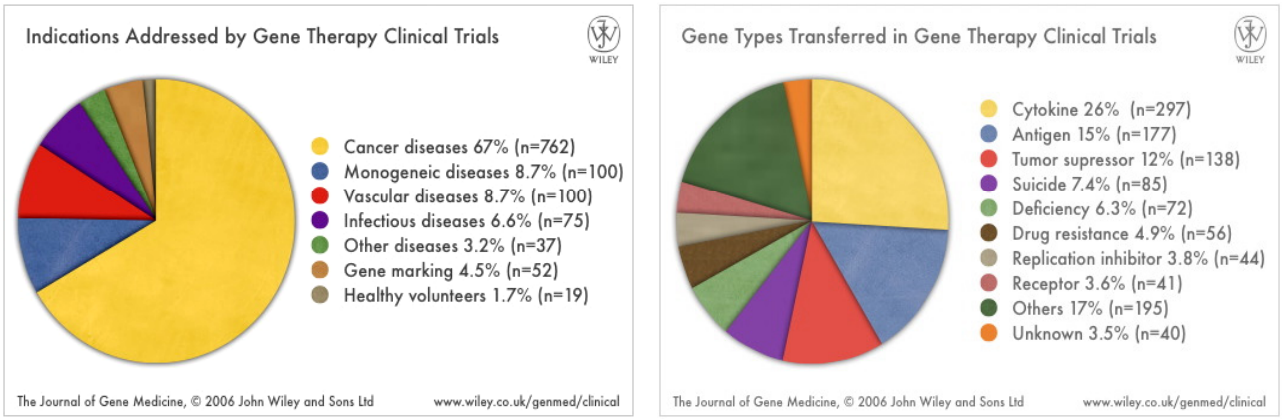

Figure I6 Overview of gene therapy clinical trials to date regarding indications (A) and gene types (B) from The Journal of Gene Medicine (www.wiley.co.uk/genmed/clinical)

Viral vectors are recognised to be the most efficient gene delivery vehicles, however, the safety remains a major concern, as these vectors are known to trigger a host immune response [53]. Viral vectors are derived from natural viruses (e.g. retroviruses, adenoviruses (Adv), adeno-associated viruses (AAV) and others) that have innate mechanisms for efficient transfer of genetic material into a cell [52]. It is possible to take advantage of this, and by introducing a foreign gene into the virus, to deliver this gene with high efficiency into the target cells. Viral vectors are being developed by genetic modification of the viral genome, i.e. deletion of the essential viral genes (making them replication deficient) followed by the insertion of a therapeutic gene into the viral genome [52].

The non-viral vectors are safer than viral, but also less efficient. A wide variety of non-viral vectors have been developed, including cationic polymers and cationic lipids. These bind to plasmid DNA carrying a foreign gene, via ionic interactions [51, 52]. The formed complexes, called polyplexes and lipoplexes, respectively, possess a positive net charge, facilitating binding to the negatively charged cell membrane and uptake into the cell by

endocytosis [3, 54]. The non-viral vectors can also be used for delivery of other types of nucleic acids like siRNA, anODN or ribozymes [51, 55].

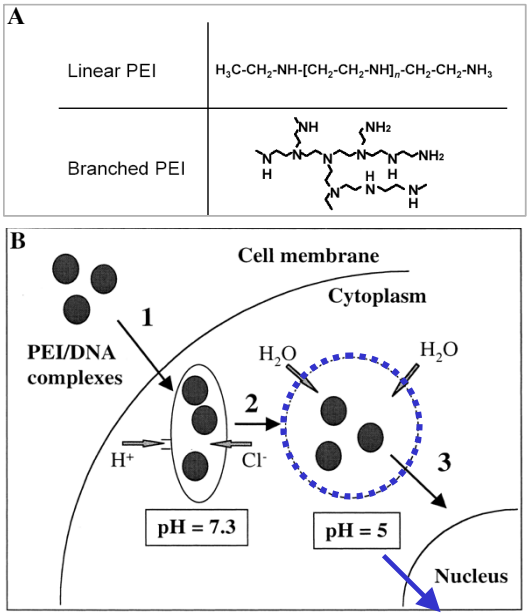

Figure I7 The structure of PEI (A) and an illustration of its endosomolytic activity (B).

Endosomal release and transport into the nucleus (fig. I5) seem to be the major barriers for gene therapy, especially for non-viral vectors [3, 56]. Although some cationic lipids and polymers (like polyethylenimine (PEI), fig. I7) have mechanisms to overcome the endosomal barrier, endosomolytic agents or strategies like PCI can improve the efficiency of such vectors [16, 18], indicating that these vectors alone are not ideal for gene delivery. Interestingly, the fact that the efficiency of the viral vectors like Adv and AAV can also be improved by PCI [8, 11], indicate that the endosomal barrier is an obstacle even for viral vectors.

In the present work PEI has been employed to deliver a pro-apoptotic transgene. PEI is one of the most widely used polymers for non-viral gene transfection *in vitro* and *in vivo* and has an advantage over other polycations in that it combines strong DNA compaction ability with an intrinsic endosomolytic property (illustrated in figure I7B) [57]. PEI is a cationic polymer with primary, secondary and tertiary amine groups, allowing for binding to DNA through ionic interactions at physiological pH, and the structure may be linear or branched (fig. I7A). Upon internalisation into endosomes via endocytic uptake [58], PEI has been shown to permeabilise the endosomal membrane. The proposed mechanism is that of a "proton sponge", preventing the acidification of the endosomes, consequently causing vesicle swelling and eventual bursting (fig. I7B) [59].

1.2.2 Cancer gene therapy, therapeutic principles

Cancer gene therapy aims to eliminate, as selective as possible, cancer cells. This can be achieved either via immune-mediated destruction (by delivery of transgenes triggering an immune response to tumours) or via direct effect on tumour cells (by delivering transgenes triggering cell death). The latter approach will be discussed herein.

The destruction of cancer cells can be achieved by introducing a "suicide" gene, i.e. a gene that encodes for (or leads to) a toxic product. "Suicide" genes have been used in ~7.5 % of all clinical gene therapy trials to date (fig. I6B) and the Hsv-TK (Herpes simplex virus thymidine kinase) is the most widely used gene. This gene encodes an enzyme, Hsv-tk, which converts a non-toxic product, ganciclovir, into a toxic metabolite leading to cell death [60].

Another alternative is the introduction of a gene or other nucleic acid-based molecules that affects survival and/or death-associated cellular mechanisms. The aim is to reduce pro-survival signals and/or stimulate death signals. A very good example is to target molecules causing apoptosis (which was also the aim of this study). In many cancers, the mechanisms for activation of apoptosis are impaired (discussed in chapter 2.1.1) leading to uncontrolled cell growth and resistance to conventional therapies that usually relies on functional apoptosis [61, 62]. Therefore, the targeting of apoptosis is a promising approach in cancer gene therapy. This can be achieved by the delivery of:

i) Genes stimulating apoptosis, such as p53 [63] or the TNF family genes like TRAIL [64, 65] used in the present study.
ii) siRNA-, ribozyme- or PNA-molecules that inhibit expression of anti-apoptotic genes like the apoptosis-inhibitiors BCL-2, survivin or IAP (Inhibitor of Apoptosis Proteins) family genes [65].

Other approaches leading to suppressed tumour growth are based on the delivery of:

iii) Tumour suppressor genes like PTEN which inhibits the pro-survival PI3K-Akt signalling pathway [19].
iv) siRNA, ribozyme or PNA for down-regulation of genes essential for viability, growth and survival of cells (e.g. the hTERT gene or genes involved in signalling via Ras, EGFR, TGFβ etc.) [66].

1.2.3 PCI in cancer gene therapy

Till now, PCI in gene therapy has been mostly combined with nucleic acids relevant for cancer therapy and has been used with most of the strategies discussed above.

When PCI was combined with the Hsv-TK gene *in vitro*, increased expression of the toxic Hsv-tk protein was demonstrated. Moreover, enhanced cell death was observed following ganciclovir-administration in PCI-treated adenocarcinoma cells compared to Hsv-TK/ganciclovir gene therapy alone [16].

PCI has already been used to deliver pro-apoptotic genes such as p53 and the tumour necrosis factor (TNF) related apoptosis inducing ligand (TRAIL). Ndoye et al. [14, 22] have demonstrated that PCI enhanced transfer of p53 (complexed to the nonviral PEI-based vector) and stimulated cell death via apoptosis both *in vitro* in p53-deficient carcinoma cell lines of the pharynx and the pancreas and *in vivo* in a head and neck cancer xenograft model with mutated p53. Engesæter et al. (submitted) have employed PCI for delivery of the TRAIL gene, and demonstrated significant PCI-dependent stimulation of apoptosis and activation of various apoptosis-related molecules in two different carcinoma cell lines *in vitro*. However, in the study of Engesæter et al., an adenoviral vector was employed for delivery of the TRAIL gene, while in the present work a similar PCI-based approach was studied employing the non-viral vector PEI.

PCI has also been used for delivery of PNA, targeting proteins associated with tumorigenesis. Folini et al. [24] employed PNA against hTERT (the human telomerase reverse transcriptase, contributing to cell growth), demonstrating marked inhibition of telomerase activity and reduced survival of a prostate cancer cell line *in vitro*. Recently, another study using PCI and PNA against another tumour-associated gene, S100A4, demonstrated PCI-induced silencing of the gene in various cancer cell lines [25].

2 Apoptosis

Apoptosis and necrosis are the main cell death pathways (fig. I8). The term “apoptosis” (from the Greek words *apo* = from and *ptosis* = falling in the meaning of leaves falling from trees or petals falling from flowers) was proposed by John F. Kerr and colleagues in 1972 [67]. Apoptosis is one of the main types of programmed cell death (although the term “programmed cell death” also covers processes like mitotic catastrophe, caspase-independent cell death and autophagy [68]). Apoptosis is an active and controlled process executed by cysteine aspartyl-specific proteases (caspases). It is different from another main death form,

necrosis, which is an un-programmed and accidental cell death in which caspases are not involved. In necrosis the cells suffer a major insult, leading to loss of membrane integrity, swelling and disruption of the cells and subsequent inflammation (fig. I8) [69].

Apoptosis is characterized by distinct morphological changes, hallmarks of apoptosis. These include condensation and fragmentation of nuclear chromatin, loss of mitochondrial membrane potential, cleaveage of caspase targets, cell shrinkage and alterations of the plasma membrane finally resulting in the phagocytosis of apoptotic cells. Phagocytosis subsequently prevents an inflammatory response and neighbouring cells remain unaffected [70]. It is generally accepted that executioner caspases are responsible for the apoptotic hallmarks.

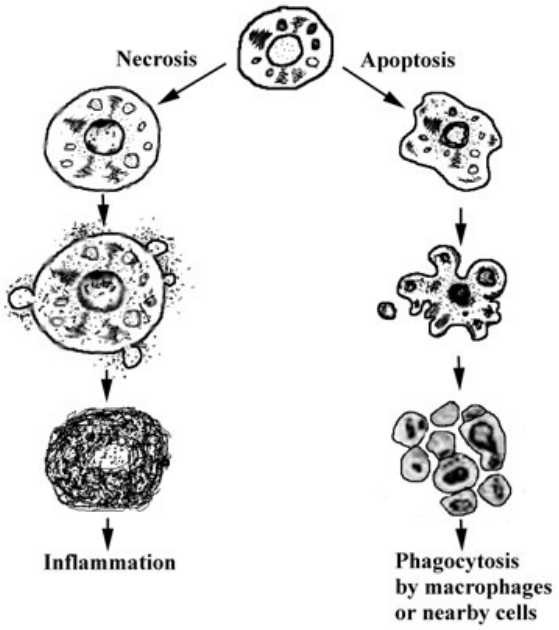

Figure I8 Illustration of the main cell death pathways [71].

Apoptosis is involved in many important cellular processes, including normal cell turnover, the immune system and embryonic development [65]. Apoptosis is also evident in cells exposed to stressful stimuli or damage, thereby preventing the maintenance and proliferation of potentially dangerous cells. Inappropriate apoptosis, leading to either increased or reduced cell death, has been implicated in many human diseases including cancer [65, 70].

2.1 Apoptosis pathways

There are two main signalling pathways that initiate the apoptotic suicide program in mammalian cells: the extrinsic (mediated by death receptors (DR) on the cell surface) and the

intrinsic (mediated by mitochondria) pathways (fig. I9). Both pathways involve caspases, but differ in the way the death signal is transduced.

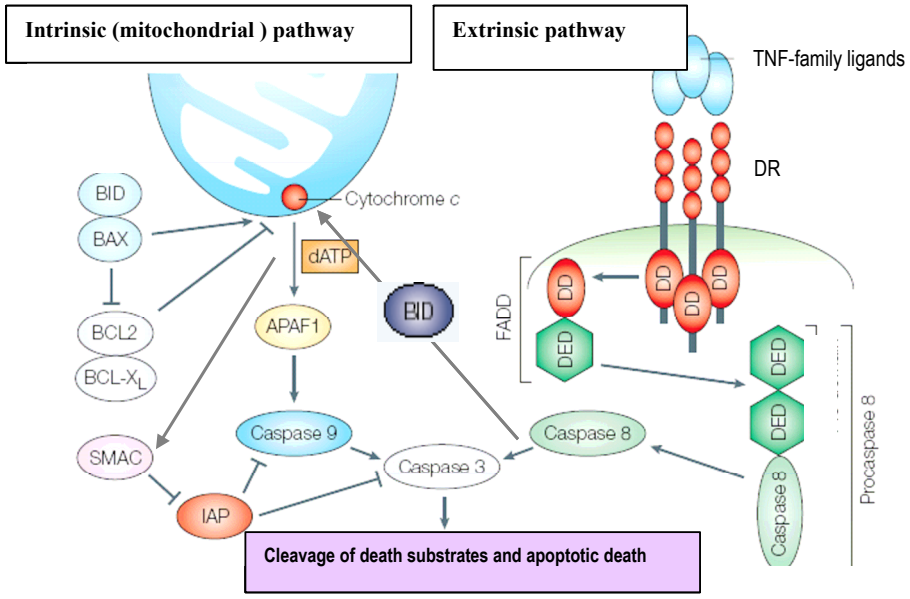

Figure I9 Simplified illustration of the main signalling pathways of apoptosis (modified from [72])

The extrinsic pathway is initiated by the members of the TNF-superfamily, like TNFα, FAS-ligand and TRAIL. Binding of such ligands to their respective receptors (DR) results in aggregation (trimerisation) of the receptor and clustering of the intracellular death domains (DD) (fig. I9). This leads to the recruitment of the adaptor protein FADD and the subsequent binding (via the death-effector domain (DED)) and cleavage of inactive procaspase-8 (an initiator caspase which is activated by cleavage). Activated caspase-8 will then cleave caspase-3, -6, and 7 (executioner caspases, caspase-3 being the most important), leading to cleavage of the death substrates such as structural and regulatory proteins like lamins, cytokeratins and poly (ADP-ribose) polymerase (PARP) [69, 72].

The intrinsic pathway is triggered as a response to DNA damage, cell cycle checkpoint defects, hypoxia, loss of survival factors or other types of severe cell stress including PDT (discussed below in chapter 2.2). This pathway involves activation of the pro-apoptotic arm of the Bcl-2 gene superfamily, which in turn engages the mitochondria to cause the release of apoptogenic factors such as cytochrome *c* and SMAC into the cytosol (fig. I9). Cytochrome *c* subsequently binds the adaptor protein APAF-1, forming an "apoptosome" that activates caspase-9 (initiator caspase) leading to activation of the executioner caspases-3, 6 and 7. SMAC promotes apoptosis by binding to inhibitor of apoptosis proteins (IAP), thereby preventing these factors from attenuating caspase activation (fig. I9) [69, 72].

The two signalling pathways also communicate with each other; caspase-8 activated by the extrinsic pathway can cleave the pro-apoptotic Bcl-2 family member Bid to its active form tBid, promoting cytochrome *c* release from the mitochondria and activation of the intrinsic pathway (fig. I9). Caspase-8 mediated Bid-processing thereby provides a bridge between the two pathways, causing an amplification of the extrinsic signal and a subsequent augmentation of apoptotic cell death [69].

Two different cell types have been described with respect to apoptotic mechanisms. In type I cells, caspase-8 activation via the extrinsic pathway is sufficient to kill cells. In type II cells (like the HCT-116 cells [73] used in the present study) however, cell death is dependent on amplification of the signal via activation of the intrinsic pathway [74, 75].

2.1.1 Apoptosis in cancer

Table I2 Mechanisms of resistance to apoptosis, potential targets for cancer therapies (modified from [76] and [77])

Pathways and molecules involved in resistance to apoptosis	
Expression of anti-apoptotic molecules	Down-regulation and mutation of pro-apoptotic genes
Anti-apoptotic BCL2 family members (BCL2, BCL-$X_{L,}$) – inhibit apoptosis at the mitochondria level (fig. I9)	BAX – involved in mitochondrial apoptosis (figs. I9, I11)
FLIP - prevents apoptosis through death receptors	APAF1-binds released cytochrome *c* (figs. I9, I11)
Soluble receptors (sCD95, DcR) - act as decoys for death ligands (figs. I9, I10)	Caspase-8 - executioner caspase (figs. I9, I11)
IAP family (survivin, cIAP2, XIAP)- inhibit caspases (fig. I9)	Death receptors (CD95, DR4, DR5) (fig. I9)
Deficiency in the apoptotic p53 pathway	Stimulation of survival signalling via the PI3/AKT pathway
↓ p53 – central in apoptosis	↑ PI3K
	↓ PTEN (tumour supressor)
↓ ASPP – stimulates p53 function	↑ AKT
Other mechanisms	
Activation of NF-kB (chapter 2.2.1)	
Induction of heat shock proteins (Hsp) (chapter 2.2.1)	

In many cancers, the normal process of eliminating unwanted cells (i.e. apoptosis) is deregulated. Tumour cells acquire resistance to apoptosis by down-regulation or mutation of pro-apoptotic genes and/or by the increased expression of anti-apoptotic genes (table I2) [61, 76]. Therefore, apoptosis can be restored or triggered by cancer gene therapy approaches targeting the defects in apoptosis signalling as already discussed in chapters 1.2.2 and 1.2.3.

2.2 PDT and apoptosis

Although PDT can lead to apoptosis or necrosis, or a combination of these two mechanisms, PDT is highly efficient in inducing apoptosis in many cases [45]. It appears as if low doses of PDT favour apoptosis, while high doses favour necrosis [45, 78]. The efficiency of PDT as an inducer of apoptosis depends on the cells, the treatment conditions, and, particularly, on the photosensitiser and its subcellular localisation, as has been demonstrated both *in vitro* and *in vivo* [43-48, 79]. Generally, photosensitisers that are localised in the mitochondria are the most efficient for induction of apoptosis following PDT [48]. However, photosensitisers that are localised in lysosomes, like the ones used in PCI, have also been shown to initiate the apoptotic death program [48, 79]. The kinetics of apoptosis induction seems also to depend on the localisation of the photosensitiser. Noodt et al. [48] showed that the mitochondria-localised photosensitisers induce rapid (within a few hours) apoptosis, while lysosomal photosensitisers like the PCI-relevant LumiTrans® or $TPPS_4$, induce late apoptosis (more than 12 h after PDT). This indicates that there is no universal mechanism for the apoptotic signalling following PDT.

Usually, PDT initiates the intrinsic (mitochondrial) apoptotic pathway (fig. I10) whereas the role of the extrinsic pathway following PDT is controversial [45]. Recent studies indicate that disruption of lysosomes releases lysosomally located cathepsins to the cytosol, where they cleave Bid leading to apoptosis via the intrinsic pathway (fig. I10) [80, 81]. Since the photosensitisers used in PCI mediate lysosomal/endosomal damage, it is likely that PCI treatment will function similarly, i.e via the intrinsic pathway.

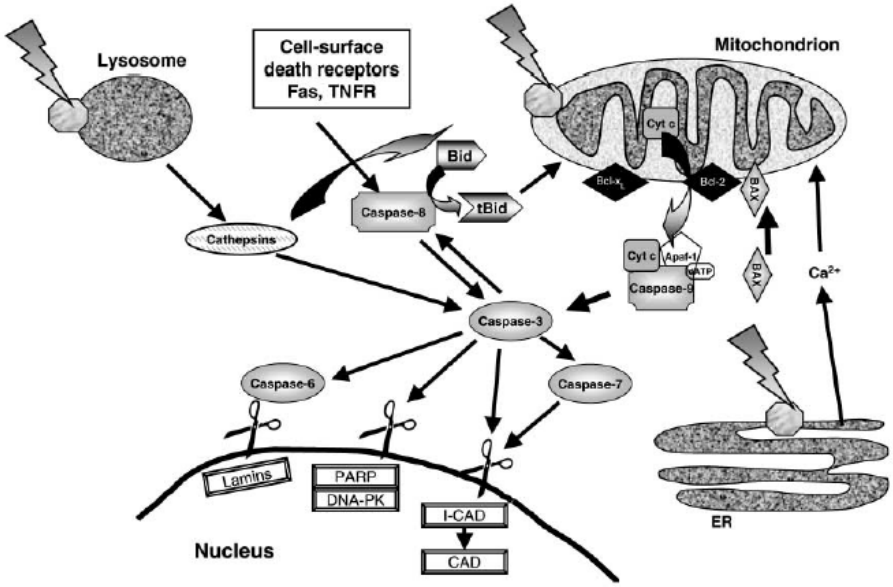

Figure I10 Major molecular events leading to apoptosis following PDT with differently localised photosensitisers [45]

2.2.1 PDT and pro-survival signalling

It has been shown that PDT can also induce anti-apoptotic signals, e.g. activate the transcription factor nuclear factor–kappa B (NF-κB) [78, 82] or induce heat-shock proteins (Hsp) [83]. NF-κB often acts as a survival factor and can prevent apoptosis by up-regulation of anti-apoptotic genes like IAP (fig. I9) [82, 84]. HCT-116 cells (also used in this study) have been used to show that photochemical activation of NF-κB might partially protect from apoptosis initiated by PDT with photosensitisers localised in membranes and lysosomes [78]. In addition, photochemical induction of heat shock proteins like Hsp-70 might also counteract apoptosis [85]. Hsp prevent apoptosis by direct interaction with different key apoptotic proteins, e.g. Hsp70 bind directly to Apaf-1, thereby preventing the recruitment of procaspase-9 and subsequent activation of procaspase-3 (figs. I9 and I10) [86-90]. Lately it has been shown that the PCI-relevant PDT treatment also induces Hsp-70 [83], indicating that both apoptotic and anti-apoptotic signals might be initiated by photochemical treatment.

2.3 Tumour necrosis factor (TNF) related apoptosis inducing ligand (TRAIL)

Employment of TRAIL in order to promote apoptosis (extrinsic pathway) is a promising approach currently undergoing preclinical and early clinical studies for various malignancies [72, 91]. TRAIL is especially attractive due to its ability to induce apoptosis in tumour cells of diverse origin, with little toxicity toward normal cells [92, 93]. Although the

TRAIL protein initially seemed to be an ideal molecule for achieving a selective and powerful anti-tumour effect, there are limitations to its clinical use, e.g. instability of the TRAIL protein and the toxicity observed in non-malignant liver cells with some recombinant forms of the protein [94, 95]. Thus, TRAIL gene therapy has been proposed as a way of achieving high intra-tumoral concentrations of TRAIL for a sustained period of time, and this strategy has been used in the present study.

TRAIL is a type II transmembrane protein, exposing its c-terminal domain into the extracellular space [92, 96], and inducing apoptosis through interaction with its death receptors, DR4 and DR5. Though five human receptors for TRAIL have been identified – the death receptors DR4 and DR5, the decoy receptors DcR1 and DcR2 and a soluble receptor osteoprotegrin (OPG) - only DR4 and DR5 contain functional death domains (DD) (fig. I11) able to signal apoptosis via the extrinsic pathway (fig. I9). The other three receptors bind to TRAIL but do not have functional DD (fig. I11), therefore do not initiate apoptosis and may infer resistance to TRAIL-mediated apoptosis by competing with DR4 and DR5 [97].

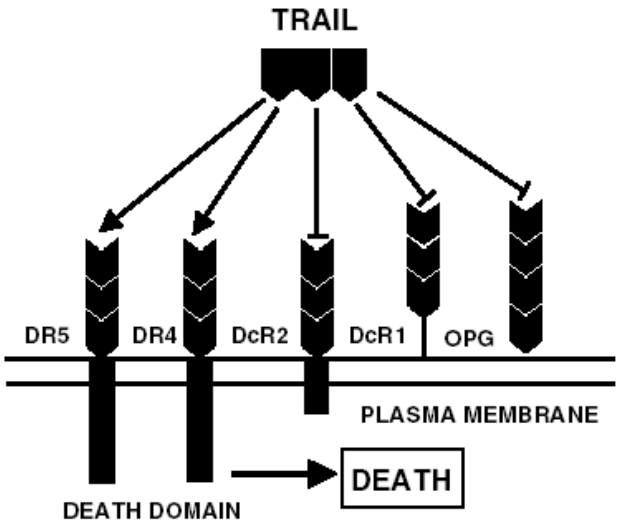

Figure I11 TRAIL and its receptors [74].

In addition to induction of apoptosis, TRAIL binding to its receptor may also lead to activation of the transcription factor NF-κB, which can prevent apoptosis by stimulation of anti-apoptotic genes e.g. IAP (table I2, fig. I9). Therefore, in many cells, TNF/TRAIL negatively regulates its own cytotoxicity by NF-κB activation [98].

Normal cells are generally resistant to TRAIL, which is advantageous in respect to cancer therapy. However, lately it has also been reported that some tumour cells might be, or might become, resistant to TRAIL treatment [77, 99]. Various factors could contribute to such resistance e.g. over expression of DcRs (a mechanism proposed for normal cells) and apoptosis inhibitors (IAP), activation of NF-κB and MAP kinases, [77, 100] low expression level of the DRs [101], and elevated levels of heat shock proteins like Hsp-70 [86].

Accumulating evidence suggest that a combination of TRAIL gene therapy with e.g. chemotherapy or radiotherapy may overcome such resistance [102-106]. Moreover, it has been demonstrated that the combination of TRAIL-therapy with PDT (based on other photosensitisers than those used in PCI) can also augment induction of apoptosis [107]. Combination therapies might sensitise cells to TRAIL by various mechanisms:

i) Up-regulation of pro-apoptotic molecules like DRs [108]
ii) Stimulation of caspase-3 and caspase-8 [108]
iii) Activation of the mitochondrial (intrinsic) pathway [107]
iv) Down-regulation of apoptosis inhibitors like c-FLIP [103, 104]
v) Suppression of the NF-κB pathway [100, 109]

Hence, it seems that combining TRAIL gene therapy with other therapeutic approaches will play a major role in TRAIL-based therapies in the future. In this respect, the photochemical treatment initiating PCI may be reckoned as a form of PDT, and therefore it was of interest to study whether this photochemical stimulus could enhance TRAIL mediated apoptosis in our experimental system.

Aim of the study

The overall aim of the present study was to evaluate the potential of PCI-mediated delivery of a therapeutically relevant gene, the pro-apoptotic gene TRAIL, carried by the nonviral vector polyethylenimine (PEI) to enhance cancer cell death *in vitro*. Furthermore, to investigate the apoptotic death pathway following PCI-mediated transfection of the TRAIL gene in colon carcinoma HCT-116 cells.

In this regard, the partial aims were:

i) To evaluate PCI of the PEI/TRAIL polyplexes in respect to:

- Reduction of cell survival
- Induction of apoptosis
- Effect on different apoptosis-related proteins.

ii) To compare the effect of PCI-mediated TRAIL gene transfection with the effects achieved by photochemical treatment (PDT) alone or TRAIL gene transfection alone.

Materials and methods

1 Materials

1.1 Reagents

Table M1 List of reagents

Reagent name	Origin
Acrylamide/Bis	Bio-Rad Laboratories (Hercular, CA, USA)
Agarose	SIGMA-Aldrich (St Louis, MO, USA)
Amersham ECL plus™ Western Blotting detection reagents	GE Healthcare (Little Chalfont, Buckinghamshire, UK)
Ampicillin	SIGMA-Aldrich
APS	Bio-Rad Laboratories
Benzonase	Merck (Darmstadt, Germany)
β-glycerolphosfate	Fluka Chemie AG (Buchs, Switzerland)
Biotinylated Protein Ladder Detection Pack	Cell Signaling Technology (Beverly, MA, USA)
DC protein assay kit II	Bio-Rad Laboratories
DMSO	SIGMA-Aldrich
DTT	Fluka Chemie AG
EDTA	SIGMA-Aldrich
Enz-check Caspase-3 assay kit #2	Molecular Probes (Eugene, OR, USA)
EtBr	SIGMA-Aldrich
FCS	PAA laboratories Gmbh (Pasching, Austria)
Glutamin	SIGMA-Aldrich
Glycerol	BDH Laboratory supplies (Poole, UK)
HEPES	SIGMA-Aldrich
HRP-labelled anti-goat secondary antibody	Serotec (Oxford, UK)
HRP-labelled anti-mouse secondary antibody	GE Healthcare
HRP-labelled anti-rabbit secondary antibody	Promega (Madison, USA)
Human TRAIL ELISA kit	Biosource (Camarillo, CA, USA)
Kanamycin	SIGMA-Aldrich
LB-Agar	Bio 101 (Carlsbad, CA, USA)
LB medium	Bio 101
LumiTrans®	PCI Biotech AS (Oslo, Norway)
MTT	SIGMA-Aldrich
Na_3VO_4	SIGMA-Aldrich
Na-deoxycholic acid	SIGMA-Aldrich
PBS	SIGMA-Aldrich
pEGFP-N1 (plasmid encoding EGFP)	Clontech Laboratories (Palo Alto, CA, USA)
pEGFP-TRAIL (plasmid encoding the EGFP-TRAIL fusion protein)	Kind gift from Prof. B. Fang (The University of Texas, TX, USA)
PEI 22 kDa, linear	Kind gift from Prof. E. Wagner (Ludwig-Maximilians University, Munich, Germany)
Penicillin/Streptamycin solution	SIGMA-Aldrich
Phosfatase inhibitor cocktails I and II	SIGMA-Aldrich
PI	SIGMA-Aldrich

Reagent name	Origin
Plasmid midi-prep purification kit	Qiagen Gmbh (Hilden, Germany)
PMSF	Fluka Chemie AG
Ponceau S	SIGMA-Aldrich
pORF-hTRAIL (plasmid encoding the TRAIL protein)	Invivogen (San Diego, CA, USA)
Powdered skimmed milk	Nestlé food service (Vevey, Switzerland)
Primary antibodies against caspase-3, caspase-8 and caspase-9 (mouse monoclonal)	Cell Signaling Technology
Primary antibody against α-tubulin (mouse monoclonal)	Calbiochem (San Diego, CA, USA)
Primary antibody against DR5 (goat polyclonal)	Santa Cruz Biotechnology (Santa Cruz, CA, USA)
Primary antibody against PARP (rabbit serum)	Calbiochem
Protease inhibitor coctail	SIGMA-Aldrich
Protein Standards KaleidoscopeTM	Bio-Rad Laboratories
Restriction enzymes (NotI, NheI, NcoI, EcoRI)	New England Biolabs (Beverly, MO, USA)
RPMI 1640 cell medium	SIGMA-Aldrich
SDS	Bio-Rad Laboratories
TEMED	Bio-Rad Laboratories
Tergitol NP-40	SIGMA-Aldrich
Tris-Base	Bio-Rad Laboratories
Trypsin-EDTA	SIGMA-Aldrich

1.2 Cell lines and bacteria

The human colon carcinoma cell lines HCT-116 (catalogue no CCL-247) and WiDr (catalogue no CCL-218) were from ATCC (Rockville, MD, USA).

SoloPack® gold Competent E-coli cells (XL-10 gold strain) were from Stratagene (La Jolla, CA, USA)

2 Methods

2.1 General cell treatment

2.1.1 Cell culture

HCT-116 and WiDr cells were subcultured twice a week in RPMI 1640 medium supplemented with 10 % foetal calf serum (FCS), 100 U/ml penicillin, 100 μg/ml streptomycin and 2 mM glutamine (complete growth medium) at 37^{o}C in a humidified atmosphere containing 5 % CO_2. The cells were routinely kept between passage 4 and 30, and they were tested regularly for mycoplasma infection.

When seeded out for experiments, the cells were detached by trypsinisation, pelleted (180 xg for 3 min with a table centrifuge (Beckman Coulter, Fullerton, CA, USA)) and

resuspended in complete growth medium. The amount of cells in the suspension was counted by using a "glasstic®slide 10 with grids" (Hycor Biomedical Inc., Garden Grove, CA, USA) and the appropriate amount of cells (table M2) was seeded out for experiments.

2.1.2 PCI-procedure

To induce PCI, the photosensitiser LumiTrans®, (meso-tetraphenylporphine with two sulfonate groups on adjacent phenyl rings, $TPPS_{2a}$) was used. The absorbtion spectrum of the photosensitiser is shown in figure M1A.

For PCI-based gene transfection with the "light after" strategy (described in fig. M2A), cells were seeded out (as described in table M2) 6 h prior to addition of LumiTrans® (0.4 μg/ml). After incubation over night, the cells were washed 3x to remove any excess of the photosensitiser before the addition of the PEI/plasmid DNA polyplexes.

The polyplexes at N/P ratio 4 (N/P = molar ratio of PEI nitrogen to DNA phosphate) were prepared by mixing plasmid and PEI solutions prepared separately. Per ml of transfection medium: 5 μg of plasmid DNA and 26 μl of PEI solution (0.1 mg/ml) was each diluted in 20 mM HEPES buffer (pH 7.2) to a working volume of 50 μl. The PEI-mix was added to the DNA-mix (a pipette was used for gentle mixing) and the solution was incubated in room temperature for 20 min. The polyplex solution was diluted with complete growth medium to 1 ml (final plasmid concentration 5 μg/ml) or 2 ml (final plasmid concentration 2.5 μg/ml), and the appropriate volume for transfection (indicated in table M2) was added to the cells.

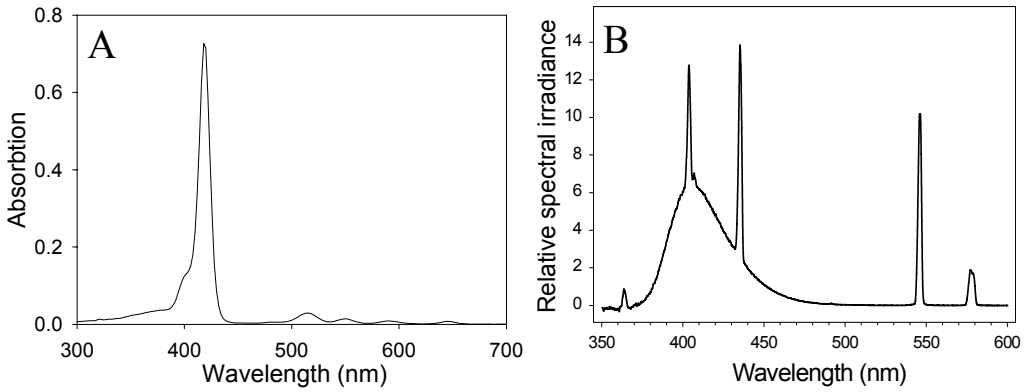

Figure M1 The absorbtion spectrum of LumiTrans® (A) and the emission spectrum of the LumiSource® lamp.

After 4 h of incubation allowing for endocytosis of the polyplexes, the cells were washed once (to remove polyplexes that were not endocytosed) and exposed to light from the LumiSource® lamp (PCI Biotech AS, Olso, Norway). The LumiSource®, which is designed for excitation of the LumiTrans®, emits light from four light tubes of λ = 375-450 nm with a peak at 435 nm (fig. M1B) and has a fluence rate of 8.5 W/m^2.

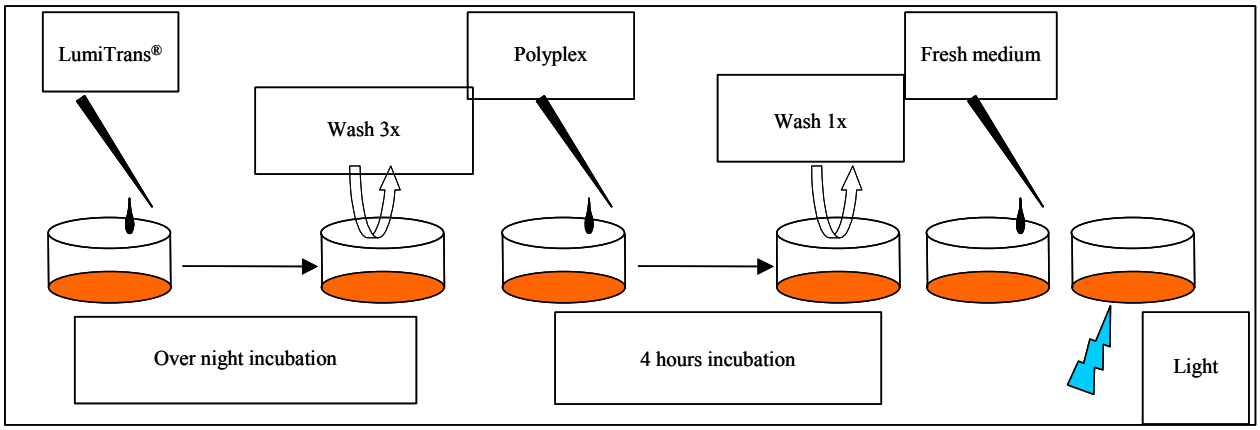

Figure M2 Outline of a standard PCI-based gene transfection ("light after" strategy) with non-viral vectors

For PCI-based gene transfection with the "light first" strategy (described in fig. M2B), cells were also seeded out (as described in table M2) 6 h prior to addition of LumiTrans® (0.4 μg/ml). After incubation over night, the cells were washed 3x to remove any excess of the photosensitiser before 4 h of incubation followed by exposure to light from the LumiSource® (fig. M2B) and subsequent addition of the PEI/plasmid DNA polyplexes as described above. The cells were incubated for 4 h before they were washed once to remove excess polyplexes.

The cells were finally analysed for various parameters at different time points after light exposure. Control "no PCI" cells were treated identically except that light was not applied, and control "PDT" cells were exposed to the photochemical treatment without polyplexes.

To pellet the cells for further analysis, centrifugation was performed at 1100 xg or 2200 xg (depending on the rotor) for ~30 s by using the table centrifuge from Beckman Coulter.

Table M2 Conditions for experimental cell culture

Type of experiment	Type of plate, dish or flask*	Total amount of cells seeded out	Volume of medium during incubation	Volume of medium during transfection
SubG1-assay and EGFP flow cytometry	12-well plate	80 000	1 ml	0.45 ml
Hoechst staining and EGFP fluorescence microscopy	6-well plates	160 000	2 ml	0.6 ml
Western blotting	Falcon 3003-dish	1 300 000	7 ml	5 ml
Caspase3 enzymatic assay and TRAIL ELISA assay	25 cm^2 flask	400 000	5 ml	1.5 ml
MTT-assay	MTT-assays were usually done in parallel with the other experiments and therefore in the same type of plate or dish. However, when the 25 cm^2-flasks were used, the MTT-assay was carried out in 6-well plates.			

*Flasks and plates were from Nunc (Roskilde, Denmark), dishes from Becton Dickinson Labware (Franklin Lakes, NJ, USA)

2.2 Production and purification of the plasmids pORF-hTRAIL and pEGFP-TRAIL

SoloPack Gold competent E. coli cells were transformed with the plasmid according to the manufacturer's instructions. Briefly, 10-50 ng plasmid DNA was added to the competent cells, and the cells were heat-pulsed at 42°C for 60 s. After 1 h incubation at 37°C, the transformed cells were selected on LB-agar plates containing 50 μg/ml of either ampicillin (for pORF-hTRAIL) or kanamycin (for pEGFP-TRAIL). Transformed bacterial cells were kept as glycerol stocks (1:1) at –80°C.

To produce the plasmids, transformed bacterial cells were grown overnight in LB-medium containing the appropriate antibiotics. The resulting biomass was centrifuged, and the plasmids were isolated from the bacterial pellet by using the midi-prep plasmid purification kit according to the manufacturer's instructions. The plasmid concentration was calculated by measuring optical density (O.D.) of the plasmid solution in a quartz cuvette (100 μl, 1 cm light path) at 260 nm using the ultrospec 2100 pro UV/Visible spectrophotometer (Amersham Biosciences).

The quality of the produced plasmids was verified by digestion with restriction enzymes (fig. M3 shows the plasmid restriction maps) followed by separation of the DNA fragments on a 0.8 % agarose gel (run at 80 V for 30 min). λ DNA-Hind III digest was used as the size marker. The DNA fragments were visualized by staining the gel with EtBr (0.5 μg/ml)

followed by exposure to UV-light. Images were obtained by the DC40/DC120 camera and the 1D Image analysis software from Kodak (Rochester, NY, USA).

Finally, the stock solution obtained was diluted to approximately 1 mg/ml and sterile filtered through a 0.22 µm pore filter (Corning Inc., Acton, MA, USA).

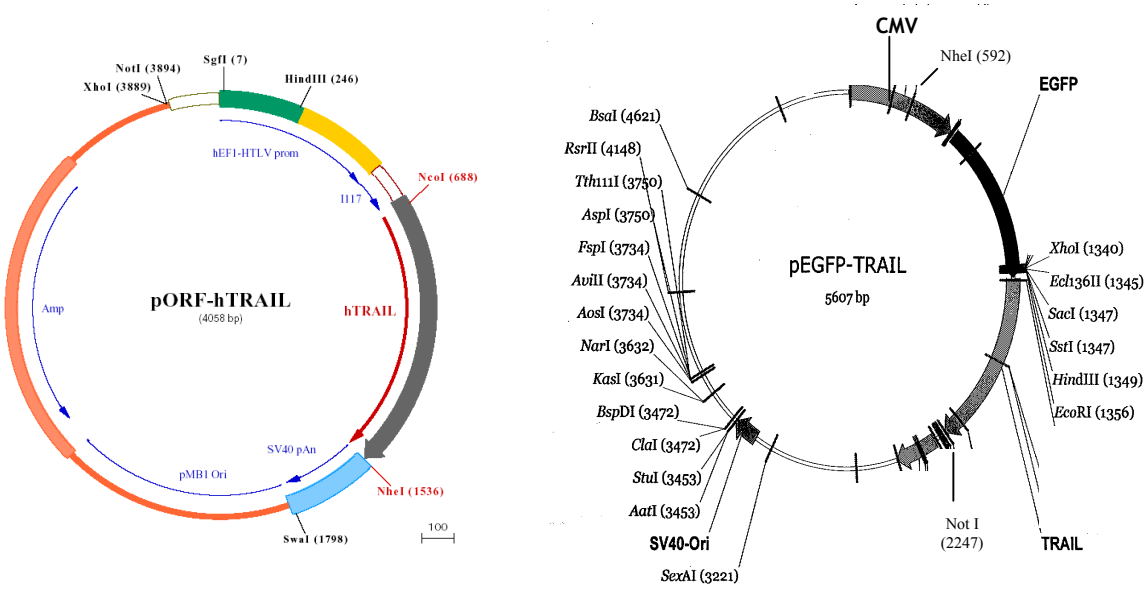

Figure M3 Restriction maps of the plasmids produced in this study (supplied from Invivogen (pORF-hTRAIL) and Prof. B. Fang (pEGFP-TRAIL)).

2.3 Evaluation of transgene expression

In the present work expression of the reporter (EGFP) and the therapeutic (TRAIL) transgenes were evaluated. The EGFP transgene encodes a fluorescent protein, which was detected by fluorescence microscopy (described in chapter 2.3.1) and flow cytometry (described in chapter 2.3.2) as a marker for transfection efficiency. Expression of the therapeutic TRAIL transgene was evaluated by a quantitative sandwich enzyme immunoassay (described in chapter 2.3.3).

2.3.1 Analysis of EGFP transgene expression by fluorescence microscopy

EGFP-positive cells can be identified by fluorescence microscopy, which allows to see the intracellular localisation of the EGFP protein as well as the distribution of the EGFP-positive cells in the whole cell population.

HCT-116 cells were transfected with the pEGFP-N1 plasmid and exposed to light (PCI) or kept in the dark ("No PCI"). Two days later, the cells were observed by a Zeiss (Oberkochen, Germany) Axioplan fluorescence and phase-contrast microscope equipped with

a 20x-magnification air objective. An HBO/100W mercury lamp was used for excitation. To detect EGFP, a 450-490 nm band pass excitation filter, a 510 nm dichroic beam splitter and 510-540 nm long pass emission filter were used. Micrographs were recorded by means of a cooled charge-coupled device (CCD) camera (Photometrics Inc., Tucson, AZ) and analysed with the AnalySIS^D 5.0 software (Olympus Biosystems Gmbh, Hamburg, Germany).

2.3.2 Analysis of EGFP transgene expression by flow cytometry

In flow cytometry, single cells are analysed for fluorescence. Therefore, the percentage of cells expressing EGFP from a large cell population can be quantified.

HCT-116 cells were treated according to the PCI procedure described in chapter 2.1.2 and harvested by trypsinisation 24, 48 or 72 h after light exposure. After centrifugation, the cells were resuspended in 400 μl complete growth medium and filtered through a 50 μm-pore mesh nylon filter to remove cell aggregates. To discriminate between viable and dead cells, 1 μl of PI (0.5 mg/ml stock), which stains only dead cells, was added, and the cells were analysed by means of a FACS Calibur flow cytometer (Becton Dickinson, San Jose, CA, USA) measuring EGFP fluorescence through a 510-530 nm filter and PI fluorescence through a 655-669 nm filter after excitation with an argon laser at 488 nm. For each sample 10 000 events were collected. Dead cells were discriminated from viable cells by gating on the PI fluorescence signal. Cell doublets were discriminated from single cells by gating on PI pulse width versus pulse area. The data were analysed with the CELLQuest software (Becton Dickinson).

An MTT-assay (described in chapter 2.5.1) was performed in parallel to evaluate the effect of the treatment on cell survival.

2.3.3 Analysis of TRAIL transgene expression by an ELISA assay

The level of the TRAIL protein expressed from the pORF-hTRAIL plasmid was measured in both growth medium and cell lysates by using the Human TRAIL ELISA kit based on a biotinylated anti-hTRAIL antibody in combination with a streptavidin-horse radish peroxidase (HRP) conjugate and a substrate for HRP. HRP-generated yellow colour develops in proportion to the amount of TRAIL.

HCT-116 cells were treated as described in chapter 2.1.2. At 24 h after light exposure, the medium with floating cells was collected and centrifuged to pellet the floating cells and to separate the cells from the growth medium (supernatant). The supernatant was stored at -80^{o}C until analysis. The adherent cells were scraped in PBS by means of a rubber policeman

(Corning) and combined with the pelleted cells. After wash with PBS, the cells were lysed in a lysis buffer provided with the kit, and the cell lysates were also stored at - 80^{o}C.

The amount of TRAIL in each sample was determined in both cell lysate and supernatant (medium) using the according to the manufacturer's instructions. Briefly, the lysate/supernatant were transferred to anti-hTRAIL-coated microplate wells and after 2 h incubation and wash, biotin-conjugated anti-hTRAIL was added for further 1 h incubation. After wash, a streptavidin-HRP-conjugate was added followed by wash and addition of a "chromogen" solution, which is a substrate for HRP. Yellow colour was subsequently formed, which was detected at 450nm using a microplate reader (Victor^2 1420 multilabel counter from Perkin Elmer, (Wellesley, MA, USA)) measuring fluorescence, absorbance and luminescence. The intensity of the colour is proportional to the amount of TRAIL bound in the initial step and, therefore, reflects the amount of TRAIL in a sample. The amount of expressed TRAIL in each sample was quantified from a standard curve based on O.D. measurements of the known amounts of the TRAIL-protein provided as a standard. The amount of expressed TRAIL was normalised to the total protein amount in each sample. The total amount of protein in the cell lysates was determined as described in chapter 2.5.2.

2.4 Methods for detection of apoptotic cells

Apoptosis was measured using three different approaches; cells were stained with Hoechst 33342 for visualisation of apoptotic nuclei, the level of active caspase-3 was measured and flow cytometric measurements of DNA-content were performed.

2.4.1 Hoechst staining

The Hoechst 33342 dye stains DNA in living cells and can be used to visualise (microscopically) normal cells, where DNA is distributed in an even and diffuse pattern throughout the nucleus, and apoptotic cells, where DNA is fragmentary and concentrated in strongly fluorescent granules.

HCT-116 cells were treated as described in chapter 2.1.2 and analysed 24 and 48 h after light exposure. Hoechst 33342 (10 μl of 0.562 mg/ml stock) was added to the medium, and after 5 min the cells were observed by an inverted Zeiss microscope, Axiovert 200 equipped with air-objectives (20x magnification) and a filter for DAPI (365/12 nm band pass excitation filter, a 395 nm beam splitter, and a 397 nm long pass emission filter). Pictures were composed by the use of Carl Zeiss AxioCam HR, Version 5.05.10 and AxioVision 3.1.2.1 software. Pictures were processed in AnalySIS^D 5.0 software.

2.4.2 Caspase-3 enzymatic assay

Activation of caspase-3 indicates caspase-dependent apoptosis, as this is the main executioner caspase (see introduction, chapter 2). Caspase-3 activity was measured by the EnzCheck Caspase-3 Assay kit #2 based on a caspase-substrate coupled to rhodamine 110, which starts fluorescing when cleaved by active caspase-3.

HCT-116 or WiDr cells were treated as described in chapter 2.1.2. Both floating and adherent cells were harvested 6, 18, or 48 h (for HCT-116) and 18 h (for WiDr) after light exposure. The pelleted cells were washed once with PBS and stored at –80^{o}C before further analysis. Caspase-3 activity was determined according to the instructions of the kit manufacturer. Briefly, the cells were lysed during one freeze-thaw-cycle and the cell lysates of each sample were added to the microplate wells followed by addition of the enzymatic substrate. After incubation at room temperature for ~ 40 min, the samples were analysed for rhodamine 110 fluorescence using the fluorescein settings (excitation filter 485 nm, emission filter 535 nm, 1.0 s measurement time) in the Victor^{2} 1420 multilabel counter.

An MTT assay (chapter 2.5.1) and a protein assay (chapter 2.5.2) were performed in parallel to be able to relate the fluorescence (representing caspase-3 activity) to cell survival and to the amount of total protein in the cell lysates, respectively.

2.4.3 SubG1-assay

The SubG1-assay is based on the fact that apoptotic cells lose part of their DNA due to the DNA fragmentation during apoptosis. Those cells may be detected as a “Sub-G1” population because they have less DNA than a normal cell in the G1 cell cycle phase. Staining DNA of fixed cells with PI allows for distinguishing between normal cells (with normal DNA content) and apoptotic cells (with reduced DNA content) by analysing PI fluorescence intensity histograms [110].

HCT-116 cells were treated as described in 2.1.2 and both floating and adherent cell were harvested 24, 48 or 72 h after light exposure. The pelleted cells were fixed in 500 µl of ice-cold 100% methanol and kept at -20^{o}C at least overnight. Before analysis, the fixed cells were pelleted, washed once with warm (37^{o}C) PBS and resuspended in warm PBS containing RNaseA (100 µg/ml) to remove RNA, which would interfere with PI-staining of DNA. After 30 min incubation at 37^{o}C, the cells were filtered as described in chapter 2.3.2. To stain DNA, 1 µg/ml of PI was added and the DNA content was analysed by the FACS Calibur flow

cytometer, measuring PI fluorescence through a 655-669 filter after excitation with an argon laser at 488 nm. For each sample 5000 – 20 000 events were collected. PI fluorescence pulse area was used as a measure of DNA content. Cell doublets were discriminated by gating on PI pulse width versus pulse area. The data were analysed with the CELLQuest software.

2.5 Measurements of cell viability and protein/DNA content

2.5.1 MTT-assay

3-[4.5-dimetylthiazol-2-y]-2.5 difenyltetrazolium bromide (MTT) is a substrate for mitochondrial dehydrogenases resulting in the formation of formazan crystals of purple colour. The intensity of the colour is assumed to be proportional to the number of viable cells[111]. It should, however, be noted that the MTT-results may be influenced by cell proliferation, i.e. viable cells will divide and subsequently constitute an increasingly large fraction of the population over time.

HCT-116 or WiDr cells were treated as described in 2.1.2 and the medium was removed after the appropriate time points (usually 18, 24, 48, 72 h after light exposure). Growth medium containing MTT (0.25 mg/ml) was added to each well including a well without cells (used as a negative control). After incubation for ~3 h, the medium was removed and the formazan crystals were dissolved in an appropriate volume of DMSO. The samples were transferred to a microplate and, if necessary, diluted with DMSO to keep the absorbance within the linear range. The absorbance at 570 nm was measured by using a Multiscan EX platereader (Global Medical Instrumentation, Ramsey, MN, USA).

2.5.2 Protein content measurement

When measuring the activity (e.g. of caspase-3) or expression level of a certain protein (e.g. TRAIL), the measured values have to be normalised against the total protein content in the corresponding sample. Moreover, knowing protein concentration in each sample is important for protein analysis by gel electrophoresis (chapter 2.6.2.), because an equal amount of protein from each sample has to be applied on the gel (i.e. equal loading).

The protein content in the sample can be determined by a colorimetric assay, where the intensity of the colour is proportional to the amount of protein. The protein concentration can thus be calculated from a standard curve based on absorbance of the known amounts of a standard protein like bovine serum albumin (BSA).

The protein concentration was measured by using the DC protein assay kit II (based on the Lowry assay [112]) according to the manufacturer's instructions. Briefly, 5 µl of each

sample lysate were added to a microplate well followed by addition of 25 µl of A' (consisting of copper tartrate solution and surfactant solution) and 200 µl of B (Folin phenol reagent). Following ~15 min incubation at room temperature with gentle agitation, blue colour was formed and the absorbance at 750 nm was measured by using the Multiscan EX platereader.
In parallel, absorbance of standard BSA (concentration range 0-2.0 µg/µl, prepared in the lysis buffer) was measured.

2.5.3 DNA-measurement

The SDS-lysis buffer (described in the appendix) that was used for preparation of the samples for protein analysis by SDS-PAGE/Western blotting (described in chapter 2.7) is not compatible with the DC protein colorimetric assay (chapter 2.5.2). Therefore, another method had to be used in order to assure equal loading of cells from each sample on a gel. Thus, DNA (i.e. O.D. at 260 nm) instead of protein was measured in each cell lysate.

The lysates were prepared as described in chapter 2.7.1, and a blank sample was made by a 2x dilution of the complete lysis buffer (see appendix for details) in distilled water (dH_2O). All samples and the blank were diluted 25x, and O.D. at 260 nm was measured by using the Ultrospec 2100 pro UV/Visible spectrophotometer, which was also used to translate O.D. into DNA concentration (ng/µl). Each sample was measured three times, and the average was used as the DNA concentration.

2.6 Statistical analysis and calculation of synergy

When two (or more) treatments are combined, the final therapeutic effect can be:

i) Greater than the sum of effects of individual treatments. This is called synergy and is advantageous for combined cancer therapy.
ii) Lower than the sum of effects of individual treatments, indicating that the effects induced by one treatment interfere with the effects of the other treatment. This is antagonism.
iii) Equal to the sum of effects of individual treatments indicating that they do not influence each other and therefore lead to a so-called additive effect.

PCI is a combination of two treatments, photochemical treatment (PDT) and, in the present study, transfection of PEI/pORF-hTRAIL polyplexes. The interaction of PDT and pORF-hTRAIL transfection in PCI was evaluated following Steel and Peckham [113]:

-ln of survival after each treatment was calculated, i.e. y(L) = -lnS(L), where S is the relative survival after a light dose L. Cell survival S, which was calculated from the experimental data for each light dose (L) based on the MTT-assay (chapter 2.5.1).

For each light dose including and for non-illuminated cells (0s), -lnS of the following treatments was calculated:

y^{PDT} - Photochemical treatment (PDT) alone
y^{TRAIL} - Transfection of PEI/pORF-hTRAIL polyplexes alone
y^{PCI} - Transfection of PEI/pORF-hTRAIL polyplexes combined with PDT (PCI)

Then the difference between the –lnS values was calculated. The purely additive effect of the combined treatments is supposed to be:

$$Y^{additive}(L) = y^{TRAIL}(L) + y^{PDT}(L) = -(\ln S^{TRAIL}(L) + \ln S^{PDT}(L))$$

The extra effect obtained by combining these two treatments is $\Delta y(L) = y^{PCI} - y^{additive}$. When Δy is zero, there is no extra effect obtained by combining these treatments (i.e. no synergy, no antagonism). Positive Δy indicates synergy (the effect after PCI is stronger than the simple sum of the effect of the two treatments). Negative Δy indicates antagonism.

2.7 Protein analysis by SDS-polyacrylamide gel electrophoresis and Western blotting

2.7.1 Preparation of cell lysates with the SDS-lysis buffer

HCT-116 cells were treated as described in chapter 2.1.2. The cell samples were prepared 2, 4, 8, 18, 24 or 45 h after light exposure by the following procedure (performed keeping the dishes and the samples on ice):

1. The medium, containing the floating cells, was collected, and the floating cells were pelleted by centrifugation. The cell pellet was washed once with ice-cold PBS, and ~10 µl of complete SDS-lysis buffer* was added to the pellet.
2. The adherent cells were washed once with ice-cold PBS, and 150 µl of complete SDS-lysis buffer was added to the cells. Then the cells were scraped by means of a rubber policeman.

3. The cells from step 1 and step 2 were collected in one tube, and after addition of 0.7 µl of Benzonase (to digest DNA, which makes the lysates viscous), the tubes were vortexed for 3 s and incubated for 5- 10 min on ice to perform lysis.

The samples were divided into ~50 µl aliquots and stored at –80^{o}C until use, avoiding multiple freeze-thaw cycles. One additional aliquot of 20 µl was designated to the DNA-measurements (chapter 2.5.3).

*Buffers are described in the appendix

2.7.2 SDS-polyacrylamide gel electrophoresis (SDS-PAGE)

To separate proteins according to their size (molecular weight) SDS-PAGE gel electrophoresis was used. SDS (sodium dodecyl sulphate) unfolds the proteins and gives them a negative charge, allowing them to pass through the gel towards the anode during electrophoresis. Large proteins travel more slowly than small proteins through the pores of the polyacrylamide gel when current is applied. Two different gels are cast on top of each other: a stacking (top) gel with a low amount of polyacrylamide for stacking the proteins before separation (to obtain clear bands); and a separating (bottom) gel with a higher amount of polyacrylamide for separation of the proteins. Depending on the size of the protein to be analysed, the amount of polyacrylamide in the separating gel may be varied (table M3). Along with the samples, a molecular weight standard is always applied on the gel, which is used to determine the size of the separated proteins from the sample.

SDS-PAGE gels were cast using the Mini protean 3 electrophoresis system from Bio-Rad Laboratories (see table M4 for the recipe). To make two gels, 15 ml of the separating gel and 10 ml of the stacking gel was used.

Table M3 Amount of acrylamide for analysis of different proteins

Protein	Size (kDa)	% Acrylamide in separating gel
DR5	50 - 60	12
PARP	113 + 89	10
Caspase-3	35 + 19/17	15
Caspase-8	57 + 43 + 18	12
Caspase-9	47 + 37/35	12

Table M4 Recipes for acrylamide gels

Separating gel	% Acrylamide			Stacking gel	% Acrylamide
	10	12	15		4
dH_2O (ml)	7.28	6.5	5.4	dH_2O (ml)	6.4
1.5 M Tris-HCl pH 8.8 (ml)	3.75	3.75	3.75	1.5 M Tris-HCl pH 6.8 (ml)	2.5
10 % SDS stock (ml)	0.15	0.15	0.15	10 % SDS (ml)	0.1
40 % Acrylamide/Bis (ml)	3.75	4.5	5.63	40 % Acrylamide/Bis (ml)	1
10 % APS (µl)	75	75	75	10 % APS (µl)	50
TEMED (µl)	7.5	7.5	7.5	TEMED (µl)	10
Total volume (ml)	15	15	15	Total volume (ml)	10

An aliquot of each sample to be analysed was thawed and heated at 95°C for 5 min. The sample volume that had to be applied in the different wells of a gel (taking care that equal protein amount from each sample was applied) was calculated based on the DNA-measurements previously performed (see chapter 2.5.3). The most concentrated sample was applied using the maximal volume (45 µl), while the remaining samples were applied in a smaller volume according to the DNA measurements. A sample with both the coloured protein marker Kaleidoscope™ (6 µl) and a biotinylated protein marker (3 µl) in 21 µl of the 2x sample buffer* was included for each gel.

The electrophoresis was performed in a running buffer* at 200 V with a current of 100-200 mW for 45 min. The mini protean cell (Biorad) was placed in a tray filled with ice to prevent heating, which could destroy the gels and the proteins.

*Buffers are described in the appendix

2.7.3 Western blotting and immunodetection

After being separated by the SDS-PAGE, the proteins were transferred from the gel to a Hybond-P membrane (PVDF-membrane, Amersham Biosciences) and detected by using specific antibodies. In the wet-blot procedure the gel-membrane "sandwich" is soaked in a transfer buffer*, and current moves the proteins from the gel to the membrane.

Before transfer, the Hypond-P membranes (~7.0 x 9.0 cm size) were soaked in methanol and equilibrated in the transfer buffer together with the gels. Sponges and filters were also soaked in the buffer, and the transfer chambers were then assembled in the following order:

Black plate – sponge – filter – gel – membrane– filter – sponge – transparent plate

The protein transfer was performed at 100 V for 70 min on ice, with continuous stirring. Successful transfer was confirmed visually by verifying that the Kaleidoscope™ protein marker was transferred from the gel to the membranes.

Table M5 Conditions for immunostaining after Western blotting

Primary antibody	Dilution and buffers for the primary antibodies		Dilution and type of the secondary antibodies	
Anti-DR5	1:200	Blocking buffer	1:2000	Anti-goat
Anti-Caspase-8	1:1000	Wash buffer with 5 % BSA	1:5000	Anti-mouse
Anti-Caspase-9	1:1000	Blocking buffer	1:5000	Anti-mouse
Anti-Caspase-3	1:1000	Blocking buffer	1:5000	Anti-mouse
Anti-PARP	1:2000	Wash buffer with 5 % BSA	1:5000	Anti-rabbit

The membranes were transferred into 50-ml vials with the side that had faced the gel during transfer, facing inwards towards the buffer ("protein side up"), and a blocking buffer* was added to avoid unspecific binding. Blocking was performed by rotation of the vials for 1 h at room temperature. The blocking buffer was replaced by a solution containing a primary antibody diluted in either blocking buffer or wash buffer* with 5 % BSA (see table M5), and the membranes were rotated at 4°C. They were then washed 3x5 min in wash buffer and incubated with a secondary antibody conjugated to HRP for 1 h at room temperature. The details for the antibody-incubations are found in table M5. The membranes were subsequently washed and incubated with the Amersham ECL plus™ Western Blotting detection reagent. This reagent creates a chemifluorescence signal upon reaction with HRP. Finally the proteins were visualised by detection of the chemifluorescence using the Molecular Dynamics Storm 860 Scanner and the ImageQuant software from GE Healthcare.

*Buffers are described in the Appendix

2.7.4 Verification of equal loading after Western blotting

After transfer, Ponceau staining was performed to confirm that an equal amount of cells was applied in each well. The Hybond-P membranes were soaked in Ponceau S-solution (0.1 % in 5 % acetic acid) for ~ 5 min before destaining in water. The membranes were subsequently scanned using a ScanJet 6200C from Hewlett Packard Co. (Palo Alto, CA, USA).

An abundant protein (α-tubulin) was also used as a loading control and was detected by the help of antibodies as described in chapter 2.7.3.

Results

1 Verification of the plasmids carrying the TRAIL gene

Two different plasmids - pORF-hTRAIL and pEGFP-TRAIL - have been used in the present study to deliver the TRAIL gene. pORF-hTRAIL carries the TRAIL gene controlled by the human Elongation factor-1α (EF-1α) promoter, while pEGFP-TRAIL carries the EGFP-TRAIL fusion gene controlled by the CMV promoter. For verification, the produced plasmids were digested with different combinations of restriction enzymes. Subsequently the obtained plasmid fragments were separated on an agarose gel to identify the size of the DNA fragments. The used enzymes and the size of the expected DNA fragments are presented in tables R1 and R2, and the separation of the resulting DNA-fragments is shown in figures R1 and R2.

Figure R1 shows the DNA bands that correspond to the expected fragments from pORF-hTRAIL (according to table R1), indicating successful production and purification of the correct plasmid.

Table R1 Combination of restriction enzymes for digestion of pORF-hTRAIL. The listed expected size of DNA is based on the restriction map of pORF-hTRAIL (fig. M3).

Sample	Restriction Enzyme	Expected size of DNA after digestion (bp)
1	None, λ-Hind III standard (1 μg)	23 130 – 9 416 – 6 557 – 4361 – 2 322 – 2 027
2	NotI	4058
3	NheI	4058
4	NotI + NheI	1700 + 2358
5	NotI + NcoI	854 + 3206
6	None	4058 (circular: relaxed + supercoiled)
7	None, λ-Hind III standard (2 μg)	23 130 – 9 416 – 6 557 – 4361 – 2 322 – 2 027

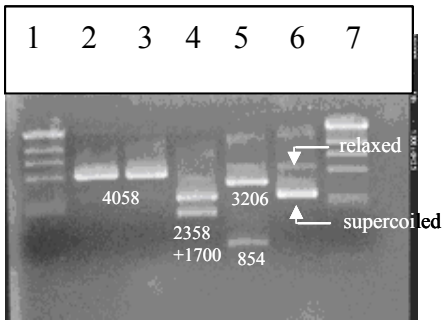

Figure R1
Fragments of digested pORF-hTRAIL (as described in table 1) separated by gel electrophoresis. Lane numbers correspond to sample numbers in table 1. For each sample ~1 μg of plasmid DNA was digested for 1 h at 37°C and separated on the 0.8% agarose gel.

The digestion of pEGFP-TRAIL (shown in fig. R2) in most of the cases gave the correct DNA fragments, according to table R2. Only in the cases when NheI was used (lanes

2 and 4) some extra bands were observed (indicated by "?" in fig. R2), which might be the result of incomplete cleavage by NheI. Despite that, it can be assumed that the produced plasmid corresponds to pEGFP-TRAIL.

Table R2 Combination of restriction enzymes for digestion of pEGFP-TRAIL. The listed expected size of DNA is based on the restriction map of pORF-hTRAIL (fig. M3).

Sample	Restriction Enzyme	Expected size of DNA after digestion (bp)
1	NotI	5607
2	NheI	5607
3	EcoRI	5607
4	NotI + NheI	1655 + 3952
5	NotI + EcoRI	891 + 4716
6	None	5607 (circular: relaxed + supercoiled)
7	None, λ-Hind III standard (2 μg)	23 130 – 9 416 – 6 557 – 4361 – 2 322 – 2 027

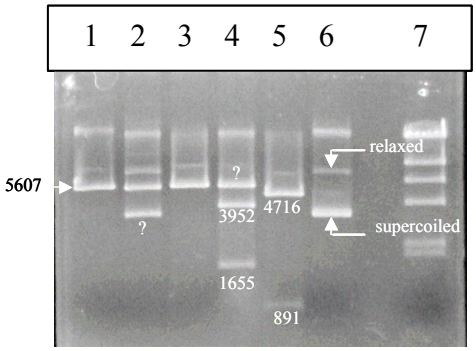

Figure R2
Fragments of digested pEGFP-TRAIL (as described in table 2) separated by agarose gel electrophoresis. Lane numbers correspond to sample numbers in table 2 and for each sample ~0.8 μg of DNA was digested for 1 h and applied on the 0.8 % agarose gel.

2 Analysis of the expression and effect of the photochemically internalised genes

2.1 Expression of the EGFP reporter gene

Expression of a reporter gene gives an indication about the efficiency of a transfection method. Therefore, the expression level of a reporter gene, like EGFP, can be used to predict the expression of a therapeutic gene like TRAIL transfected by the same method and under the same conditions. Thus, to choose the transfection conditions that could be used for the therapeutic TRAIL gene and to confirm that PCI works under these conditions, a reporter plasmid (pEGFP-N1, carrying the reporter EGFP gene) was employed first. Herein PCI means transfection with a PEI/plasmid DNA polyplex followed by the photochemical treatment (PDT) used to initiate endosomal release of the polyplexes (described in Materials and methods, chapter 2.1.2).

It was first demonstrated that PCI enhances the expression of the reporter EGFP gene delivered as a polyplex with the nonviral vector PEI into HCT-116 cells. A dose of

photochemical treatment (PDT) killing 30-50% of the cells was selected to initiate PCI, since previous studies [17] have indicated that these photochemical doses are optimal for PCI of

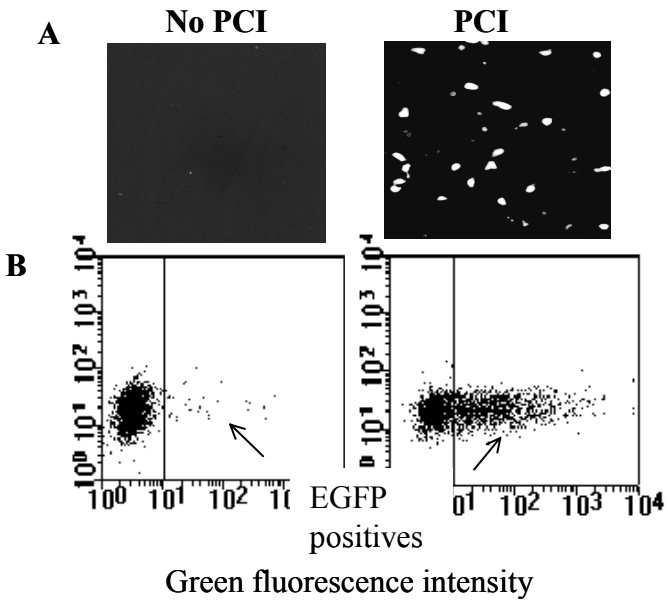

Figure R3 The effect of PCI on expression of the reporter EGFP gene delivered by PEI into HCT-116 cells. Fluorescence microscopy (A) and flow cytometry (B) analysis of EGFP-expressing cells performed 2 days after treatment. The cells were transfected with pEGFP-N1 (5 μg/ml) and either kept in the dark (No PCI) or exposed to light (PCI).

plasmids.

Figure R3 illustrates the transfection efficiency with the pEGFP-N1 alone and in combination with PCI, showing an obvious effect of PCI on EGFP expression in HCT-116 cells. Fluorescence microscopy of HCT-116 cells receiving the pEGFP-N1 revealed that the cells expressed EGFP when exposed to PCI treatment, but not without PCI (fig. R3A).

For quantification of the number of cells expressing the EGFP transgene, cells were analysed by flow cytometry. Dot-plots (fig. R3B) show the populations of EGFP-negative (left part of the plot) and EGFP-positive cells (right part of the plot) without or with PCI, indicating that PCI can enhance polyplex-based transfection by several folds.

To test several PCI light doses and to find the time point when the EGFP level is the highest, HCT-116 cells were transfected with the PEI/pEGFP-N1 polyplexes followed by exposure to light for 0s, 80s and 110s (PCI). The cells were analysed for EGFP expression 1, 2 and 3 days after the treatment (fig. R4, upper panel). In parallel, cell survival was evaluated (fig. R4, lower panel) to correlate the PCI effect on EGFP expression with the photochemical effect on cell killing. Figure R4 (upper panel) presents the quantitative results of the flow cytometry data.

Normally, the cells have no endogenous EGFP, therefore there were no cells with green fluorescence after PDT alone, as can be seen by the lack of the black bars (fig. R4, upper panel). EGFP expression in cells transfected with the pEGFP-N1 (grey bars, fig. R4 upper panel), but not exposed to light (0s), did not change significantly with time, resulting in ~ 4% EGFP-positive cells. On the contrary, EGFP expression in cells transfected with pEGFP-N1 and exposed to light (i.e. PCI) was significantly increased (resulting in 10-25% EGFP-positive cells) depending on the light dose and on when the analysis was performed (fig. R4, upper panel).

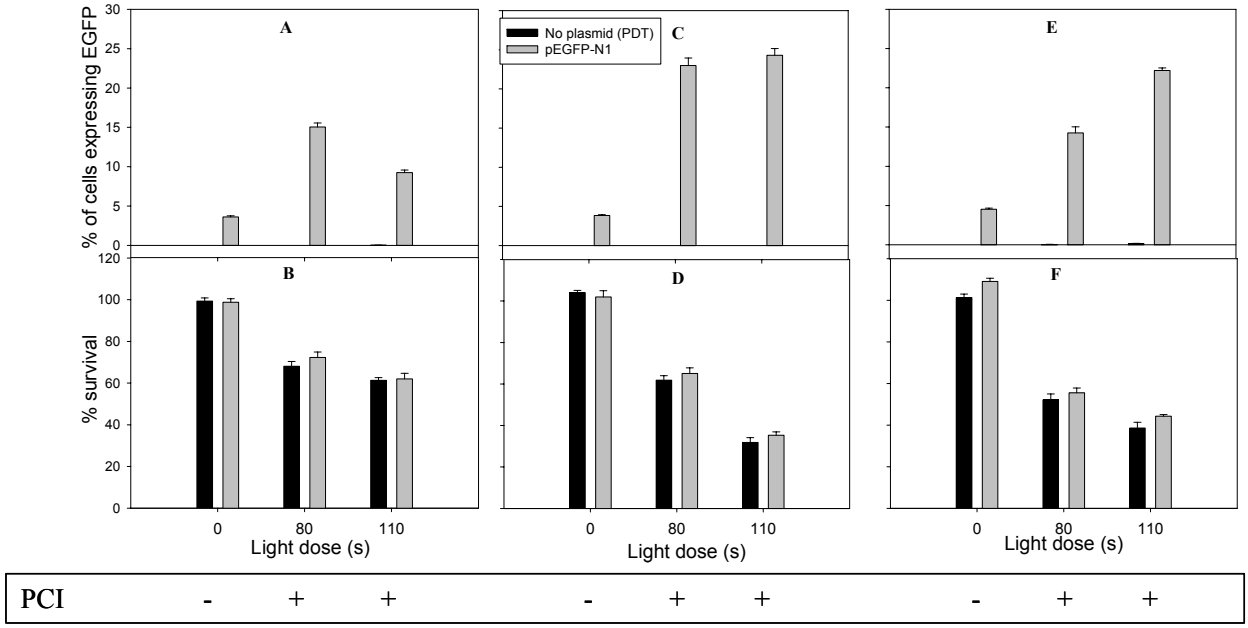

Figure R4 The effect of PCI on expression of EGFP (upper panel: A, C, E) and on cell survival (lower panel: B, D, F) in HCT-116 cells. "PDT" indicates cells exposed only to photochemical treatment as indicated in the figure. "pEGFP-N1" means the cells were treated with the PEI/pEGFP-N1 polyplexes (2.5 μg/ml pEGFP-N1) followed by the photochemical treatment. On day 1 (A, B), 2 (C, D) and 3 (E, F) after treatment, the cells were analysed for EGFP expression by flow cytometry or for cell survival by the MTT assay. MTT-results are shown relative to untreated cells. The error bars represent the standard error (SE) of three parallels in the same experiment.

These data indicated that EGFP expression reaches the maximum approximately 2 days after PCI, although the PCI-dependent enhancement could be seen already 1 day after PCI. Moreover, the effect of the higher light dose (110s) on EGFP expression seems to be "delayed" in respect to the lower light dose (80s). This might indicate that longer illumination, which leads to higher cytotoxicity (Fig. R4D,F), has a stronger temporal-inhibitory effect on EGFP translation than shorter illumination.

The toxicity induced by PDT, as measured by the MTT assay, was also most pronounced 2 days after the treatment (fig. R4, lower panel, black bars). Moreover,

PEI/pEGFP-N1 polyplexes did not induce any additional cytotoxicity (no difference between the black and grey bars in fig. R4, lower panel), indicating that the polyplexes are not toxic when they carry a reporter gene, and that the toxicity observed is determined only by the photochemical treatment.

These results indicated that the tested transfection conditions were suitable for PCI, and could be used for PCI with the therapeutic, pro-apoptotic gene TRAIL.

2.2 Expression and effect of the therapeutic TRAIL gene

The effect of PCI on the expression of the therapeutic TRAIL gene delivered with the PEI/pORF-hTRAIL polyplexes was measured with an ELISA-assay as described in Materials and methods (chapter 2.3.3). The level of TRAIL protein following transfection alone or in combination with PCI was evaluated both in the growth medium (excreted soluble TRAIL) and in the lysate of HCT-116 cells (cellular TRAIL) as shown in figure R5.

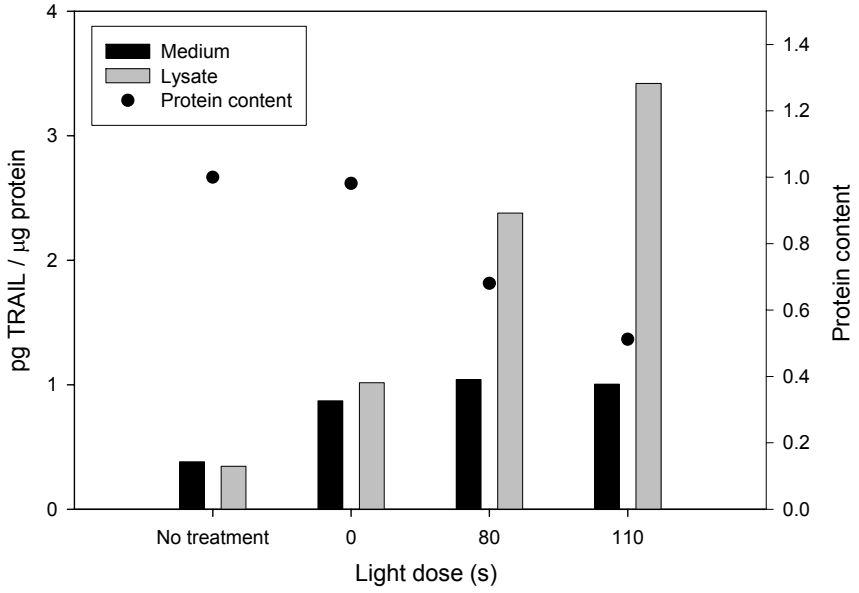

Figure R5 The effect of PCI on the level of TRAIL expression in HCT-116 cells. The cells were treated with the photosensitiser followed by the incubation with the PEI/pORF-hTRAIL polyplexes (2.5 µg/ml pORF-hTRAIL) and exposure to light as indicated in the figure. The amount of TRAIL in the cell lysates and in the medium was measured 1 day after the treatment. Protein content in the lysates (relative to untreated cells) was used as an indication of cell survival (dots, right y-axis). The graph represents one experiment with one sample per treatment.

Untreated cells had little endogenous TRAIL protein (~ 0.5 pg TRAIL in both the medium and the cell lysate per µg protein in the lysate) (fig. R5). Upon transfection with pORF-hTRAIL without PCI (0s illumination), ~ 1 pg TRAIL per µg protein in the cell lysate

was found in both medium and lysate, while with PCI, the expression of TRAIL in the cell lysate increased by 2.5 and 3.5-fold after light doses of 80s and 110s, respectively. However, the level of TRAIL protein secreted into the growth medium remained stable, ~ 1 pg TRAIL per μg protein regardless of the light dose. Photochemical treatment alone (PDT) did not influence the TRAIL expression (data not shown).

These results indicated that PCI enhances the level of TRAIL protein in HCT-116 cells transfected with pORF-hTRAIL. The enhancement corresponded to the fold enhancement observed with the EGFP reporter gene (fig. R4A). Moreover, most of the TRAIL protein was shown to stay in the cells and was not excreted into the medium.

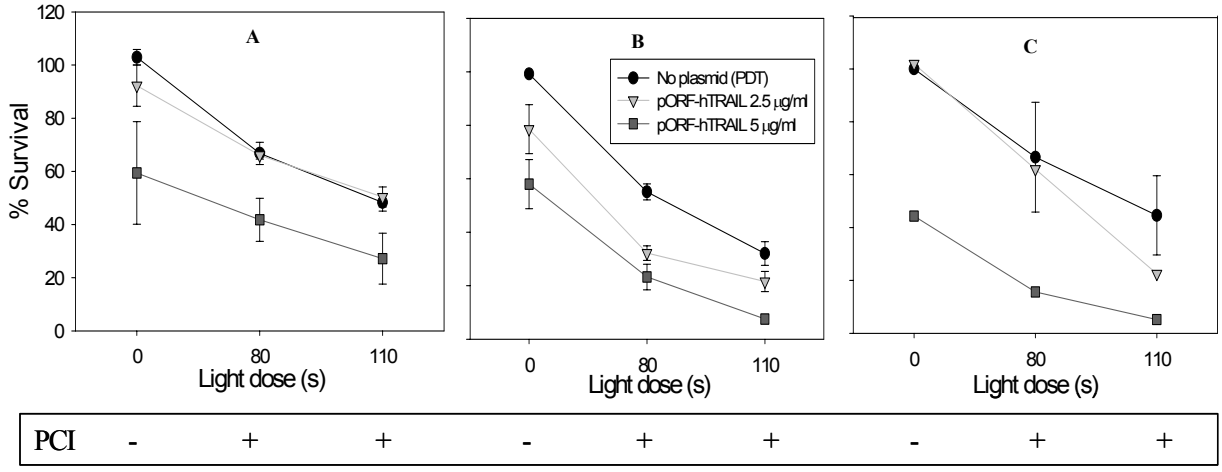

Figure R6 The effect of PCI of pORF-hTRAIL on the survival of HCT-116 cells. "pORF-hTRAIL" means treatment with PEI/pORF-hTRAIL polyplexes (2.5 μg/ml and 5 μg/ml) followed by the photochemical treatment as indicated. "PDT" means only photochemical treatment. Survival was measured 1, 2 and 3 days (A, B and C) after treatment. The error bars represent the SE of 1-4 experiments with one sample per treatment. Lack of error bars indicates one experiment.

To be certain that the expressed pro-apoptotic TRAIL protein was functional and could induce cell death, the cytotoxic effect of PCI of pORF-hTRAIL was evaluated and compared to the cytotoxic effect of the photochemical treatment (PDT) alone. Two different concentrations (2.5 μg/ml and 5 μg/ml) of pORF-hTRAIL were employed, and the decrease in cell survival was analysed 1, 2 and 3 days after treatment. As can be seen in figure R6, transfection with pORF-hTRAIL killed HCT-116 cells both alone and in combination with PCI, with an overall enhancement of cell death when PCI was applied. One day after treatment (fig. R6A) the survival curves for PDT and PCI with 2.5 μg/ml of pORF-hTRAIL

were overlapping, indicating that only photochemical treatment and not TRAIL at this dose caused the cytotoxicity. However, when the pORF-hTRAIL dose was doubled, an obvious effect of the TRAIL protein was observed leading to ~40 % cytotoxicity without PCI and up to ~70 % cell death with PCI using the highest light dose (110s). For comparison, PDT induced ~45 % death at the same light dose. Two days after treatment (fig. R6B) both 2.5 μg/ml and 5 μg/ml of pORF-hTRAIL had a pronounced effect on cytotoxicity, leading to ~20 % and ~40 % cell death, respectively, without PCI and increasing to >70 % and >90 % cell death, respectively, with PCI. For comparison, PDT-induced cytotoxicity was lower (black dots in figure R6B). Three days after treatment, only 5 μg/ml of pORF-hTRAIL gave a significantly higher cytotoxicity compared to PDT-induced cytotoxicity.

Table R3 Statistical evaluation of the toxicity induced by PCI transfection of the TRAIL gene versus the toxicity induced by single treatments: PDT alone or transfection with pORF-hTRAIL alone. Negative Δy indicates an antagonistic effect of PCI, Δy of zero indicates a purely additive effect and positive Δy indicates synergy. P-values were obtained using the paired t-test. The points marked with * are statistically significant ($p<0.05$) while the ¤ implies that there was only one sample and therefore it was not possible to calculate SE or p-values.

A 2.5 μg pORF-hTRAIL / ml		Δy	SE	p-value
Day 1	0 s	-0.03	0.03	
	80 s*	-0.09	0.04	**0.034**
	110 s	-0.17	0.10	0.488
Day 2	0 s	0.04	0.03	
	80 s*	0.45	0.07	**0.002**
	110 s*	0.45	0.15	**0.020**
Day 3	0 s	-0.03	¤	
	80 s	0.33	¤	¤
	110 s	0.97	¤	¤
B 5 μg pORF-hTRAIL / ml		Δy	SE	p-value
Day 1	0 s	0.07	0.04	
	80 s*	-0.12	0.19	0.415
	110 s	0.02	0.04	0.673
Day 2	0 s	0.02	0.03	
	80 s*	0.27	0.18	0.196
	110 s*	0.45	0.25	0.162
Day 3	0 s	-0.01	¤	
	80 s	0.22	¤	¤
	110 s	1.01	¤	¤

These data indicated that the photochemically internalised TRAIL gene was functional, and could lead to cell death in a light-dose dependent manner. In addition, the resulting cytotoxicity was much higher when 5 μg/ml of pORF-hTRAIL was employed

compared to 2.5 μg/ml of pORF-hTRAIL, which gave a quite good effect, but only 2 days after treatment.

The survival data presented in figure R6 were also used to calculate whether pORF-hTRAIL and photochemical treatment act synergistically in PCI, or whether a purely additive effect of the combined pEGFP-hTRAIL and PDT on cell death is achieved (table R3). Interestingly, statistically significant synergy (positive Δy) was only detected with the lowest dose (2.5 μg/ml) of pORF-hTRAIL, and only 2 days after PCI (see table R3). There was also an indication of synergy 3 days after PCI for both concentrations, but since only one experiment was performed the result was not statistically significant.

Summarising, the data indicated that 5 μg/ml of pORF-hTRAIL combined with PCI gives a stronger overall effect on cell death, whereas 2.5 μg/ml of pORF-hTRAIL gives a lower, but synergistic effect on cell death. Synergy might be very important in therapeutic situations when the highest specificity of the treatment is needed. Thus, in the present study both 2.5 μg/ml and 5 μg/ml of pORF-hTRAIL were used depending on the specific goal of the experiment.

2.3 Expression of the EGFP-TRAIL reporter-therapeutic fusion gene

The effect of PCI on the expression of the fusion gene, containing both the reporter EGFP gene and the therapeutic TRAIL gene, was studied employing PEI/pEGFP-TRAIL polyplexes. The fusion gene would allow for tracking of EGFP-expressing cells, that should also express the TRAIL protein, and to analyse apoptosis in the EGFP-positive and the EGFP-negative cells. The PCI effect on EGFP expression was tested by flow cytometry (fig. R7A), while the PCI effect on TRAIL protein expression was tested by the MTT assay, measuring the killing potential of TRAIL (fig. R7B).

The results (obtained 2 days after treatment) showed that the expression of EGFP from pEGFP-TRAIL was negligible compared to EGFP-expression from the pEGFP-N1 under the same conditions (fig. R7A). The intensity of the EGFP fluorescence detected after PCI of the pEGFP-TRAIL was also lower than the intensity after transfection with pEGFP-N1, and similar results were obtained 1 or 3 days after treatment (data not shown). This might suggest that the processing of the fusion gene EGFP-TRAIL does not result in properly folded EGFP, which could fluoresce green.

The TRAIL-moiety of the fusion gene seemed to be expressed to a larger extent than the EGFP moiety. However, transfection with pEGFP-TRAIL without PCI induced ~ 20 % cell death, which was approximately 2-fold less than the > 40 % toxicity induced by pORF-hTRAIL (fig. R7B). PCI of the pEGFP-TRAIL did not lead to higher cytotoxicity either,

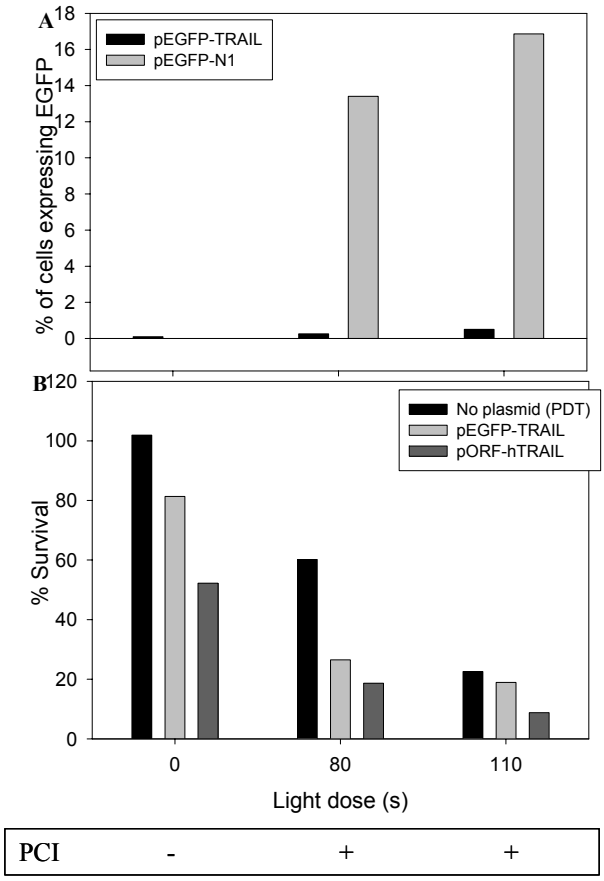

Figure R7 The effect of PCI on EGFP expression (A) measured by flow cytometry, and on cell survival (B) measured by the MTT assay after transfection with pEGFP-TRAIL. For comparison, EGFP expression following transfection with pEGFP-N1 (A) and survival following transfection with pORF-hTRAIL (B) is presented. Analysis was performed 2 days after treatment. All plasmids were at a concentration of 5 μg/ml. Survival was relative to untreated cells. One representative experiment out of three is presented.

compared to PCI of pORF-hTRAIL. This indicated that the pORF-hTRAIL plasmid is more potent than pEGFP-TRAIL in inducing cell death both alone and in combination with PCI. Therefore, pORF-hTRAIL was chosen for the following studies of apoptosis and molecular mechanisms.

3 Analysis of apoptosis

The previous section showed that the cells produced an enhanced level of the TRAIL protein following PCI of pORF-hTRAIL (fig. R5) resulting in enhanced cell death (fig. R6).

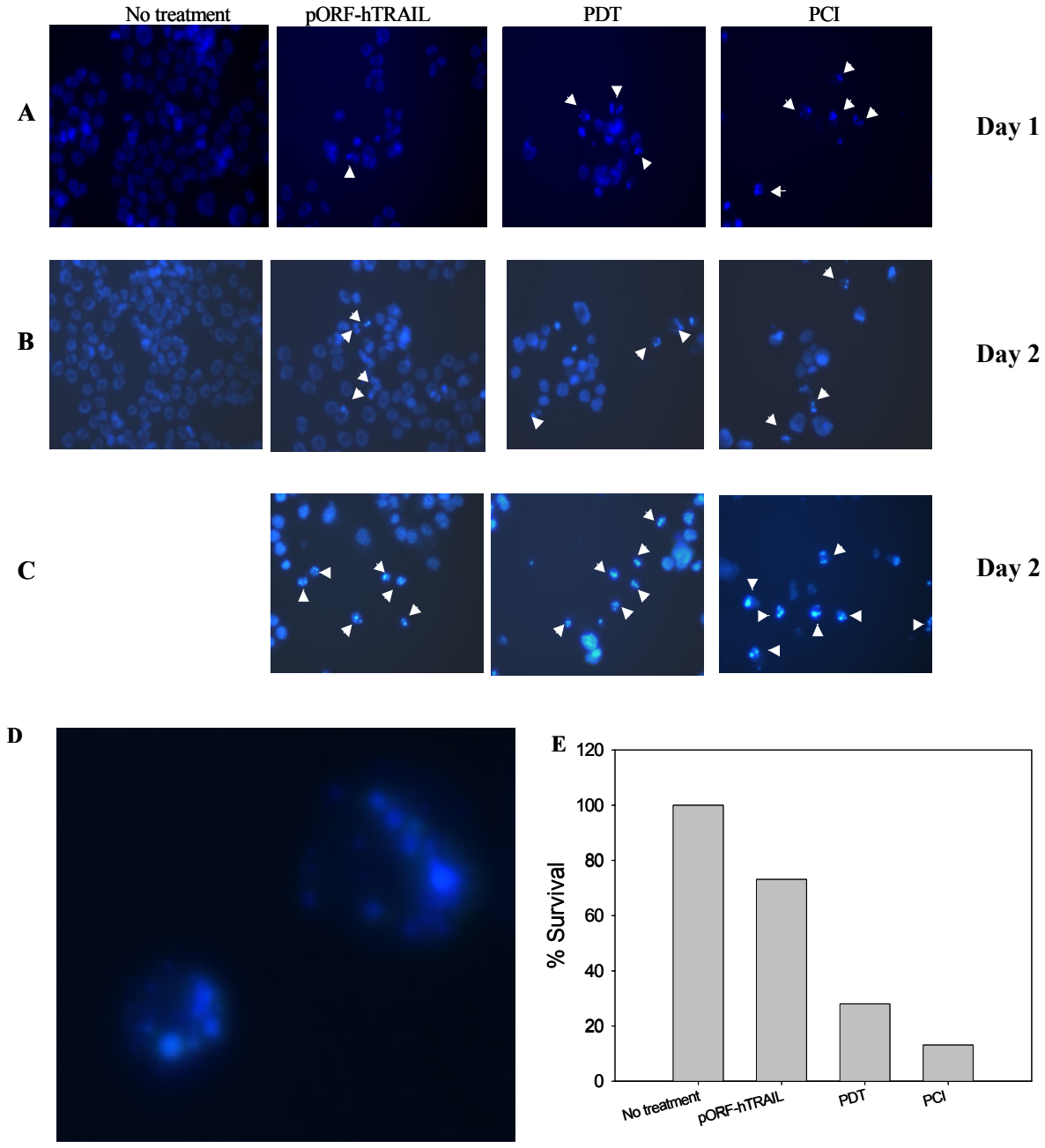

Figure R8 Fluorescence microscopy micrographs showing apoptotic nuclei in HCT-116 cells treated as indicated in the figure and stained with Hoechst 33342 immediately before analysis (A-C, C shows cells floating in the medium) 1 and 2 days after treatment as indicated. Close up of two apoptotic nuclei (D) (from the upper right corner of "PDT" in B). Corresponding cell survival was measured by means of the MTT assay (E) 2 days after treatment and releated to untreated cells. "pORF-hTRAIL" indicate cells transfected with the PEI/pORF-hTRAIL polyplexes without PCI. "PDT" indicates cells treated photochemically without plasmid. 5 μg/ml of pORF-hTRAIL was used where indicated. Arrows point to cells with apoptotic nuclei.

To investigate the intensity of apoptosis after PCI-transfection of pORF-hTRAIL compared to transfection without PCI and to PDT alone, apoptosis was assayed by three different methods: fluorescence microscopy of cells stained with Hoechst 33342, quantification of caspase-3 enzymatic activity and analysis of the fraction of cells in SubG1.

3.1 Fluorescence microscopy of Hoechst 33342-stained cells

To visualise the apoptotic cells (i.e. apoptotic nuclei) the cells were transfected with the pro-apoptotic pORF-hTRAIL alone or in combination with PCI, or the cells were exposed to photochemical treatment alone (PDT) followed by staining with the Hoechst 33342 as described in Materials and methods (chapter 2.4.1). Figure R8 shows cells analysed 1 (fig. R8A) and 2 (fig. R8B,C) days after treatment. The arrows point to the cells containing condensed clumped DNA, indicating apoptotic nuclei like the ones shown in figure R8D.

As can be seen, untreated cells had no apoptotic nuclei. However, when the cells were transfected with pORF-hTRAIL without PCI, some cells with apoptotic nuclei could be observed already after 1 day, and the amount of cells in apoptosis increased after 2 days. This implies that some time is needed before the internalised pORF-TRAIL is expressed into the TRAIL protein and before the TRAIL protein induces apoptosis. When transfection with pORF-TRAIL was combined with PCI, most of the cells had condensed nuclei already after 1 day. PDT also seemed to be efficient at inducing apoptosis, as judged by apoptotic nuclei 1 day after PDT, but to a slightly lower extent than the PCI-treatment.

It should be noted that the cell survival (fig. R8E) was low in this particular experiment: PDT killed ~ 70 % of the cells and PCI killed almost 90 %. This can also be seen in the micrographs, where the amount of cells is dramatically decreased in the PDT/PCI-samples compared to the untreated cells. Low cell survival might also indicate that the difference between PCI- and PDT-induced apoptosis might be higher under photochemical conditions optimal for PCI (i.e. killing ~ 50 % of the cells [17])

These data illustrated that all three treatments – PCI-transfection of pORF-hTRAIL, transfection of pORF-hTRAIL alone, and photochemical treatment (PDT) – lead to the morphological changes characteristic of apoptosis, and that these changes can already be detected 1 day after treatment becoming more evident 2 days after treatment, which corresponds to the earlier presented data (figs. R4 and R6).

3.2 Activation of Caspase-3

Caspase-3 is the main executioner caspase (Introduction, chapter 2.1), and its activity

can hence be used as a measure of induced apoptosis. To evaluate the activation of caspase-3 following transfection with pORF-hTRAIL polyplexes (alone or in combination with PCI) and PDT alone, an enzymatically based caspase-3 assay was used as described in Materials and methods (chapter 2.4.3). This assay consists of a substrate for active caspase-3, which is linked to a fluorescing protein, and, upon cleavage of the substrate, fluorescence appears and can be measured. The fluorescence is proportional to the caspase-3 activity.

As can be seen in figure R9, in HCT-116 cells the activation of caspase-3 1 day after treatment was very low (not exceeding 1.5-fold) regardless of treatment, even though the effect on cell survival was obvious: PDT employing 110s of light killed ~ 50 %, and PCI of pORF-hTRAIL employing the same light dose killed ~ 60 % of the cells. Analysis

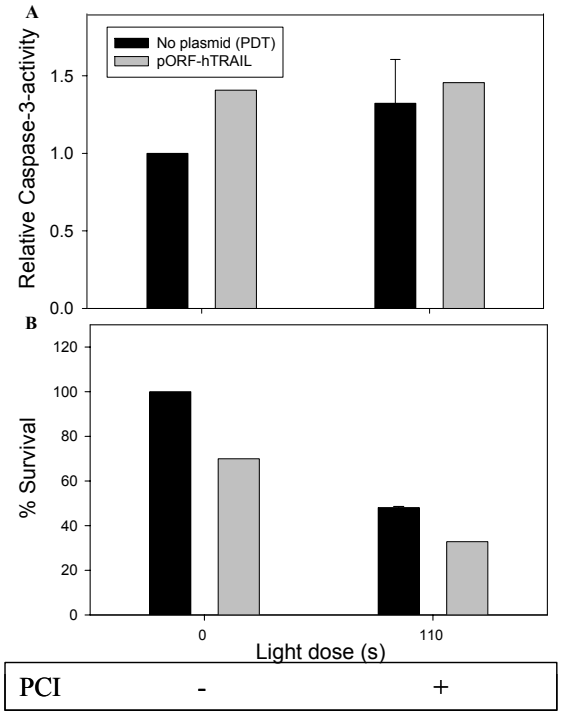

Figure R9 The effect of transfection with 2.5 μg/ml pORF-hTRAIL (alone or in combination with PCI) and treatment with PDT alone on caspase-3 activation (A) and on cell survival (B) in HCT-116 cells. The activity of caspase-3 and cell survival was measured 1 day after treatment and is relative to untreated cells. Error bars represent the SE of 1-3 different experiments with one sample per treatment. Lack of error bars indicates one experiment.

performed 4 hours and 2 days after treatment also showed similar results to the ones presented in figure R9 (data not shown).

To investigate whether the low activation of caspase-3 was a phenomenon of the HCT-116 cells, or an artefact related to the detection method, similar experiments were performed on another cell line – the colon carcinoma WiDr cells. These cells are generally

less sensitive to transfection with PEI/plasmid polyplexes than HCT-116 (data not shown), therefore, 5 μg/ml of pORF-hTRAIL was used for transfection of the WiDr cells.

Figure R10 shows that in the WiDr cells, the activity of caspase-3 increased with increasing light dose. PCI using 110s illumination (killing ~ 70 % of the cells) induced a 10-fold increase in the activity of caspase-3, whereas the corresponding PDT-dose (killing ~

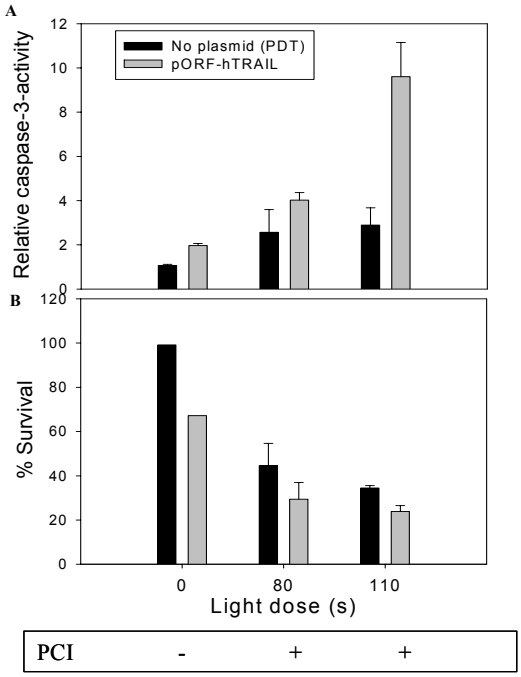

Figure R10 The effect of transfection with 5μg/ml pORF-hTRAIL (alone or in combination with PCI) or PDT alone on caspase-3 activation (A) and on cell survival (B) in WiDr cells. The activity of caspase-3 and cell survival was measured 1 day after treatment and related to untreated cells. Error bars represent the SE of two different experiments.

60 % of the cells) induced only a 3-fold increase. This indicated that the caspase-3 enzymatic assay detects the activation of caspase-3. Therefore, one may assume that in HCT-116 cells caspase-3 is not notably activated, neither by PCI of pORF-hTRAIL nor by PDT alone or pORF-hTRAIL alone. These results also indicated that there is a difference between these two cell lines regarding the apoptotic pathway, and in the way different apoptosis-related components respond to PCI/PDT.

3.3 SubG1-analysis

To quantify the fraction of cells undergoing apoptosis, the cells containing less DNA (i.e. SubG1 cells) were identified by flow cytometry as described in Materials and methods (chaper 2.4.2). Figure R11A shows histograms illustrating how the SubG1 cell fraction was

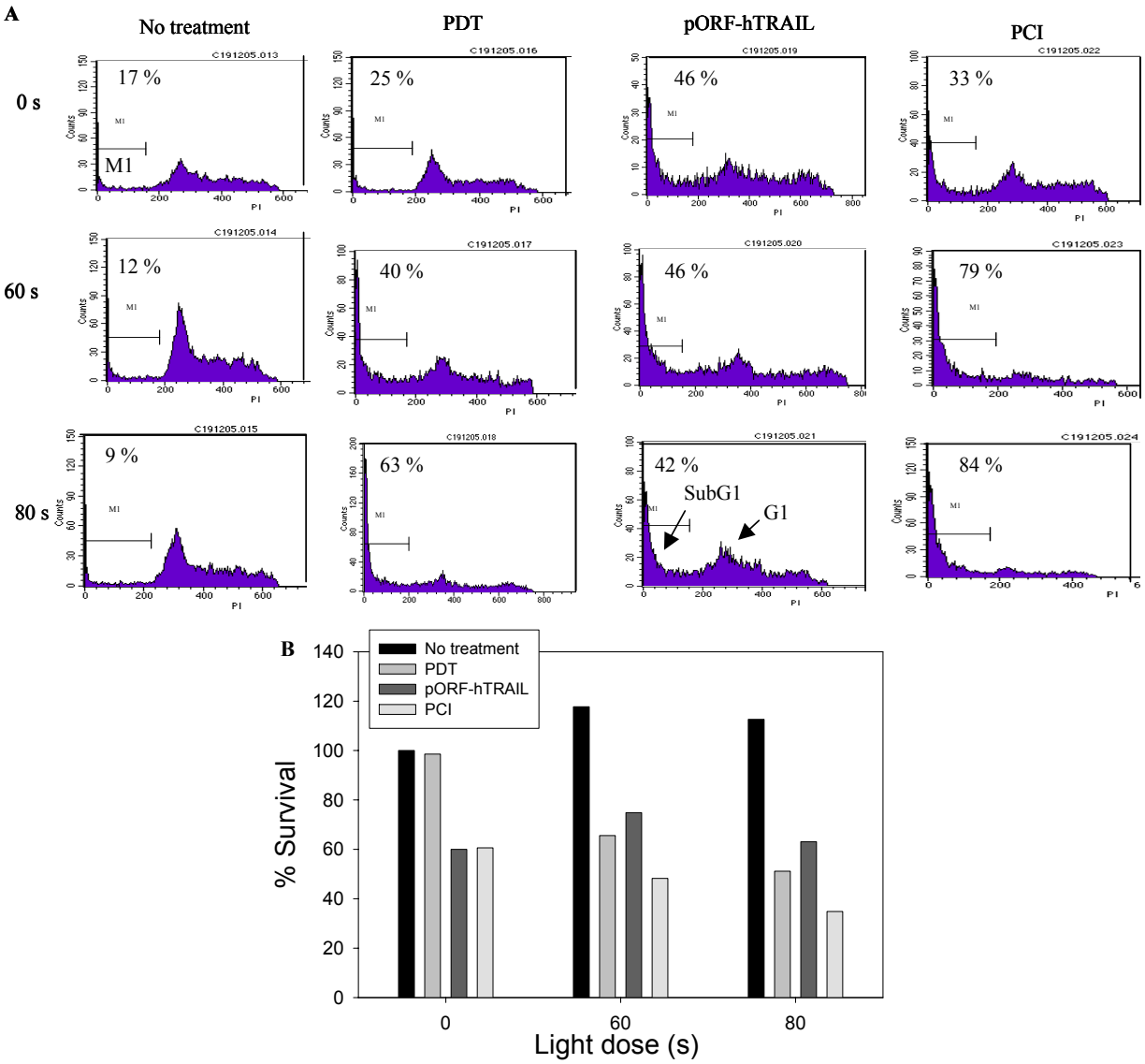

Figure R11 Histograms from flow cytometry analysis of SubG1 cell fraction (A) in HCT-116 cells 2 days after treatment (data from one representative experiment) and corresponding cell survival (B). The numbers in A indicate the percentage of cells in SubG1. "pORF-hTRAIL" indicate cells transfected with PEI/pORF-hTRAIL polyplexes without photosensitiser. 5 μg/ml of pORF-hTRAIL was used.

calculated. In each histogram, the amount of cells (y-axis) is plotted against the intensity of PI-fluorescence indicating the cellular DNA content (x-axis). The fraction of cells in SubG1 (indicated by the vertical bar "M1") has less DNA than cells in G1. As can be seen, the percentage of cells in SubG1 (found by using the CellQuest software) depended on the treatment. PCI seemed to be the most efficient, resulting in the largest SubG1 cell fraction (fig. R11A). This correlated to the survival data presented in figure R11B, showing the strongest killing efficiency of PCI transfection of pORF-hTRAIL compared to PDT alone or pORF-hTRAIL alone.

In figure R12, the combined result of SubG1-analysis from four different experiments (upper panel), and the corresponding cell survival (lower panel) is presented. The SubG1 data reflects apoptotic death, and the cell survival data reflects the overall toxicity, i.e. death via both apoptosis and necrosis. The SubG1 fraction and the survival were measured 1, 2 and 3 days after various treatments.

The results showed that the fraction of apoptotic cells generally increased with increasing concentration of pORF-hTRAIL and with increasing light dose (fig. R12, upper panel). The toxicity curves depicted a similar dependency. In general, the strongest effects on apoptosis and cell death were detected 2 days after treatment (fig. R12C, D). As can be seen

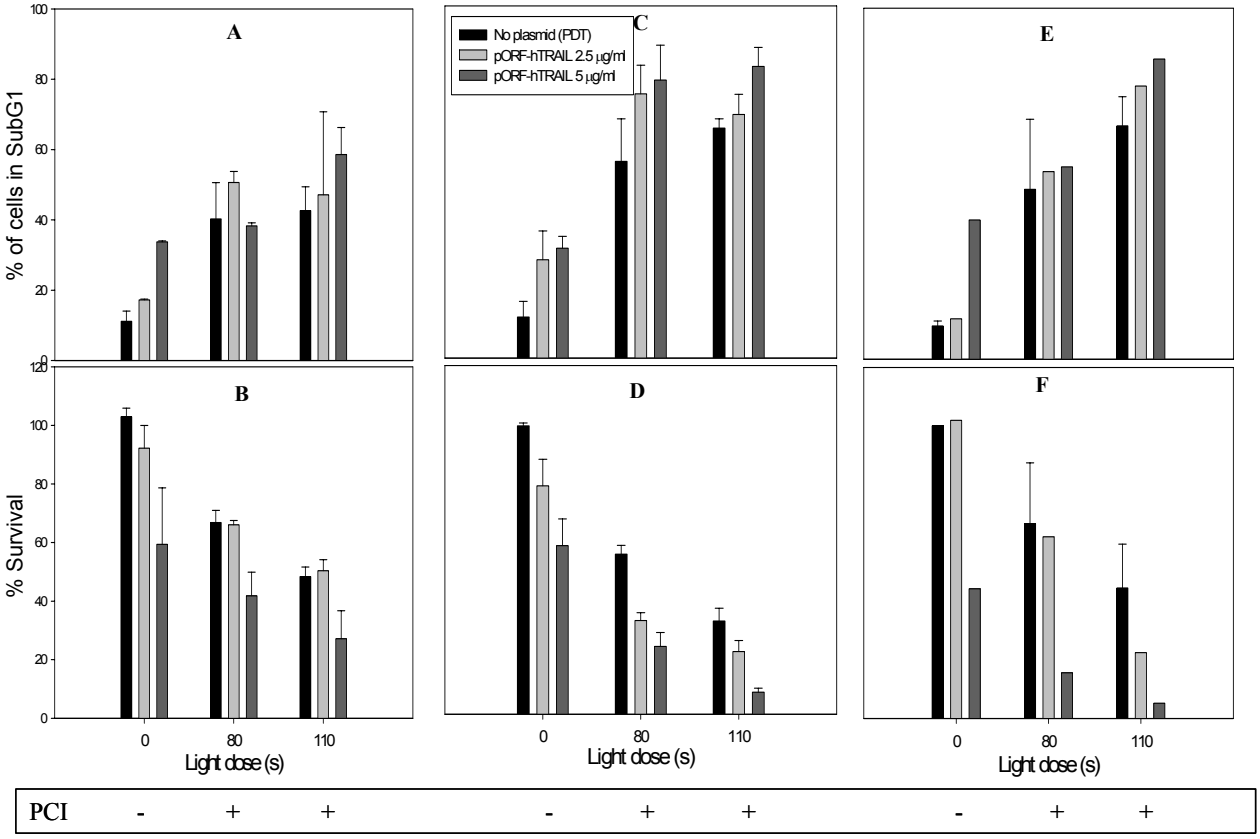

Figure R12 Quantification of SubG1-fraction (upper panel) and corresponding cell survival (lower panel) in HCT-116 cells after transfection with pORF-hTRAIL (2,5 µg/ml or 5 µg/ml, alone or in combination with PCI) (using two different light doses). The samples were analysed 1 (A+B), 2 (C+D), and 3 (E+F) days after treatment. The survival data are based on the same data as in figure 6 and are relative to untreated cells. The error bars represent the SE of 1-4 experiments with one sample per treatment. Lack of error bars indicates one experiement.

in figure R12 (upper panel), pORF-hTRAIL transfection alone (using 2.5 µg/ml or 5 µg/ml of pORF-hTRAIL) led to ~ 20 % and ~ 40 % apoptotic cells, respectively. When PCI was employed, the fraction of apoptotic cells increased significantly, resulting in 70-80 %

apoptotic cells (fig. R12C,E). However, the photochemical treatment alone (PDT) was also quite efficient in inducing apoptosis (fig. R12, upper panel, black bars) though slightly less so than PCI. The induction of apoptosis correlated to the toxicity data: PCI eliminated 70-90 % of the cells (fig. R12D,F), while PDT induced 40-60 % cytotoxicity (fig. R12D,F) depending on the light dose and on the analysis time.

3.3.1 PCI of the TRAIL gene employing the "light first" strategy

As an alternative to the regular PCI-procedure, where the illumination is performed after treatment with the polyplexes, the illumination may be performed before administration of the PEI/DNA polyplex ("light first", fig. I2) [7]. This approach was briefly tested and both

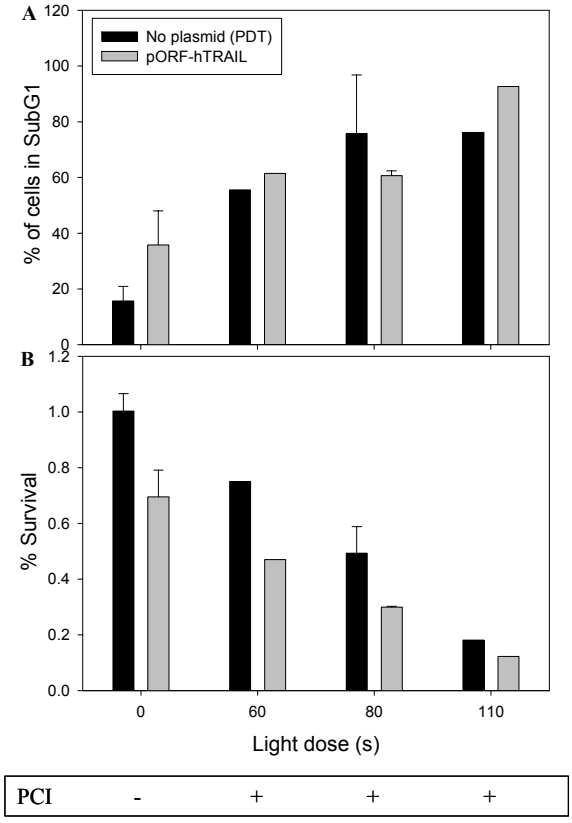

Figure R13 SubG1-fraction (A) and corresponding cell survival (B) measured two days after treatment with "light first" PCI-procedure. The concentration of pORF-hTRAIL was 5 μg/ml. The survival was relative to untreated cells. One experiment was conducted with the light doses 60 and 80s, and one with 80 and 110s. Error bars represent the SE of two independent experiments with one sample per treatment.

SubG1 and cell survival were analysed to see whether "light first" would improve the therapeutic effect of PCI with pORF-hTRAIL. The data showed that the fraction of cells in

SubG1 increased depending on the light dose (fig. R13A). However, only a negligible difference between PCI and PDT could be observed (fig.R13A), even though there was a strong effect of PCI compared to the PDT effect on the overall cell death (fig. R13B). Comparison of figures R12 and R13 revealed that "light first" does not lead to higher cytotoxicity than "light after", and therefore the "light first" approach was not explored further.

4 Effect of PCI on the level of apoptosis-related molecules – a study by Western blotting

In order to investigate the apoptotic death pathway at the molecular level in HCT-116

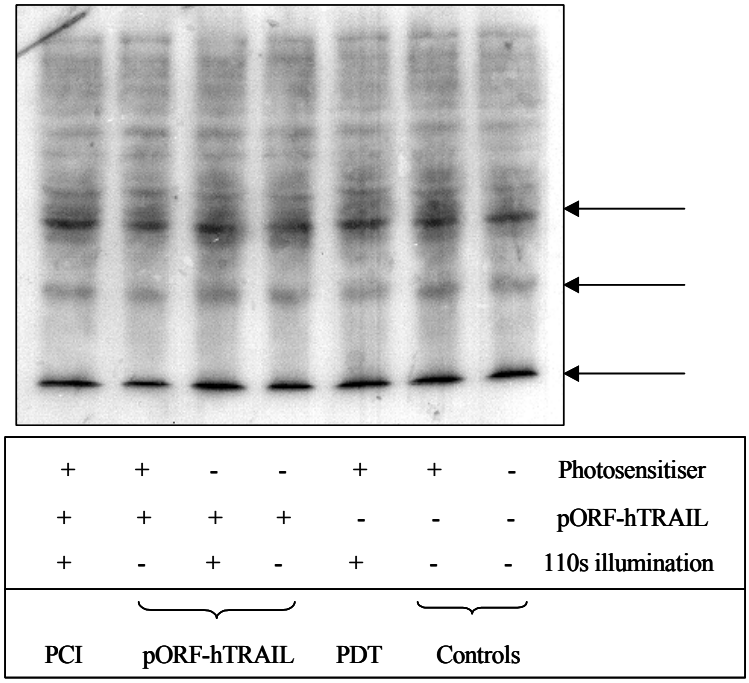

Figure R14 Representative Ponceau staining of a membrane used for Western blotting (the same as in figures R18 and R20, 45 h). Samples were treated as indicated. 5 μg/ml of pORF-hTRAIL was used.

cells after transfection with PEI/pORF-hTRAIL polyplexes (alone or in combination with PCI) or photochemical treatment (PDT), the involvement of various apoptosis-related molecules was analysed at different time points after treatment. The idea was to find out whether, and how fast, the level of key apoptosis-related proteins was affected by the treatments.

The proteins selected for further analysis were:

- DR5, main death receptor (DR) for the TRAIL-protein
- Caspase-8, the main initiator caspase in DR-mediated apoptotic pathways

- Caspase-9, the main initiator caspase for mitochondria-mediated apoptosis
- Caspase-3, the main executioner caspase
- PARP, a key death substrate (apoptosis inducing enzyme) cleaved by executioner caspases

The activation of caspases can be detected by the reduced level of procaspases and by the appearance of cleaved fragments, i.e. active caspases. Both pro- and cleaved forms of caspases can be detected by Western blot analysis, as it was attempted to show below.

For evaluation of the treatment effect on the level of selected proteins, it is important that the same amount of total protein is applied from all the samples, regardless of treatment. Thus, equal loading was first confirmed by Ponceau staining, where all the separated proteins

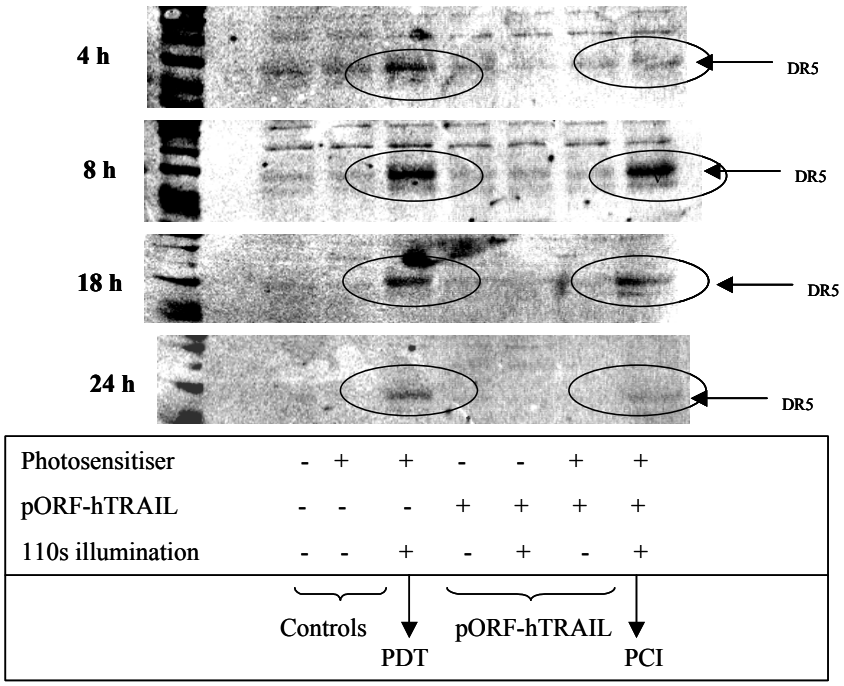

Figure R15 Expression of DR5 (MW ~50 kDa) in HCT-116 cells analysed 4, 8, 18 and 48 h after treatment. The samples were treated as indicated in the figure. A pORF-hTRAIL concentration of 5 μg/ml was used.

on a representative gel are visualised (as shown in fig. R14). Especially the strongest bands (indicated with arrows) appear to be equal independent of the treatment, indicating that an equal amount of total protein was applied in each well. Alternatively, equal loading can be confirmed by detection of an abundant cellular protein like α-tubulin, as it is demonstrated in figure R18B.

4.1 Death receptor 5

DR5 is involved in initiation of the extrinsic apoptotic pathway characteristic for the TRAIL protein. Consequently, the level of DR5 might influence TRAIL-mediated apoptosis and, therefore, DR5 expression was evaluated in this study. The expression of DR5 was clearly up-regulated by photochemical treatment (110s illumination), i.e. both PCI-and PDT-treated cells showed an elevated level of DR5 as can be seen in figure R15 (the circles point out the strongest bands corresponding to DR5). The cells treated with PDT alone seemed to have a slightly higher up-regulation of DR5-level than the cells treated with PCI. The up-regulation was notable already 4 h after light exposure, peaked after 8 h and persisted until 48 h, though at a lower level.

These data suggest that the photochemical treatment used in PCI also stimulate the expression of DR5 and thus might sensitise the cells to apoptosis via death receptors.

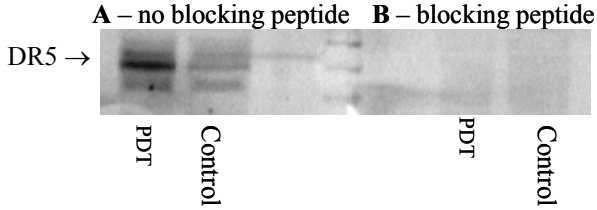

Figure R16 Effect of a blocking peptide on the detection of the DR5-bands in Western blots. "PDT" means the cells were treated with the photosensitiser followed by 110s illumination, "control" means untreated cells. Blots are without (A) or with (B) the DR5-specific blocking peptide added in 5x excess to a 1:5000 dilution of the primary antibody.

To confirm that the photochemically up-regulated bands observed in figure R15 were DR5 bands, a DR5 blocking peptide was used (fig. R16). The blocking peptide is recognised by the primary antibody and therefore blocks the binding of the primary antibody to DR5. As a result, DR5 bands cannot be seen on Western blots, as was demonstrated in figure R16B. The band that was stronger in PDT-treated cells than in untreated cells, and thus were expected to be the DR5 band (fig. R16A), disappeared when the blocking peptide was applied (fig. R16B) indicating that this band was indeed DR5.

4.2 Caspase-8

To investigate the involvement of the extrinsic pathway following various treatments, the level of the main initiator caspase of the extrinsic pathway, caspase-8, was analysed. As can be seen in figure R17, the level of procaspase-8 did not change significantly regardless of

treatment. However, bands corresponding to cleaved fragments, i.e. active caspase-8, were observed in the PCI-treated samples 18 h after treatment, and were still apparent after 45 h (fig. R17, cleavage product indicated with circles). After 24 h, cleavage products were detected after PCI (fig. R17, 24h A+B). PDT also gave rise to bands corresponding to active caspase-8 (fig. R17, 24h B), but these bands were only present in this one blot (missing in fig. R17, 24h A), and had disappeared 45 h after PDT.

These data suggested that PCI of the PEI/pORF-hTRAIL polyplexes is more efficient in activating caspase-8 as compared to PDT alone or pORF-hTRAIL alone.

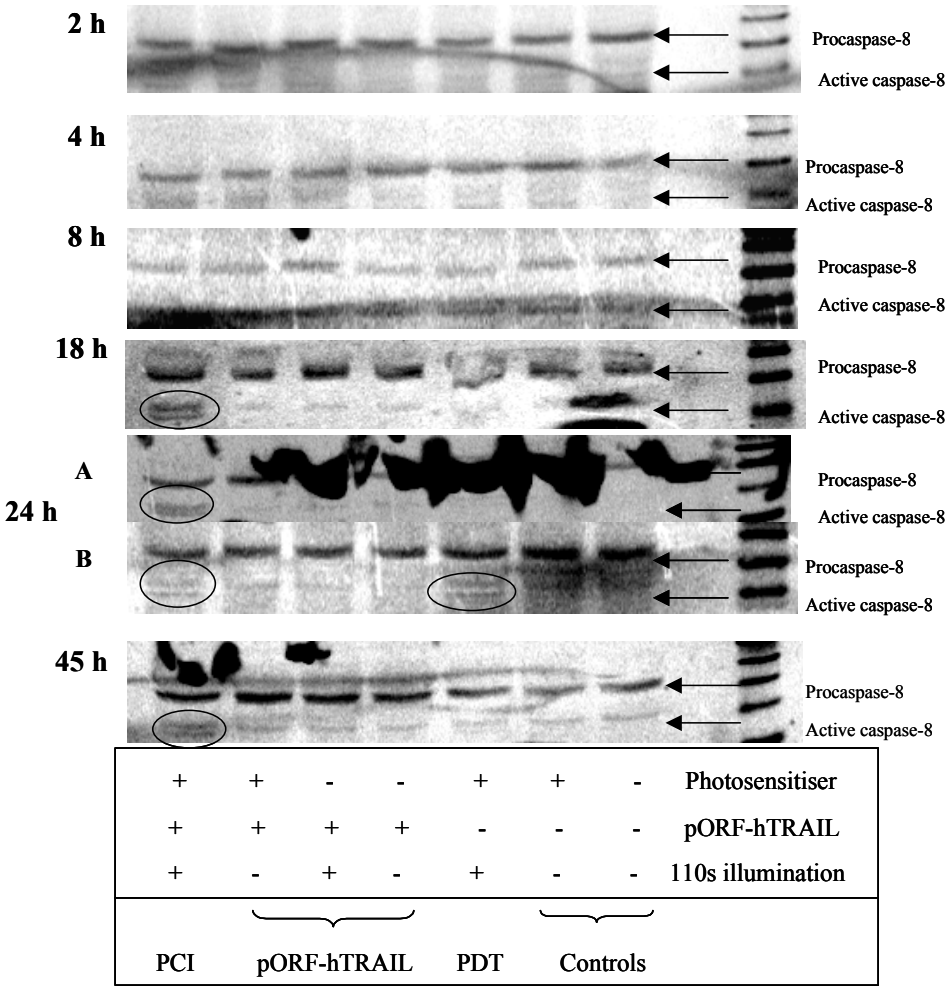

Figure R17 The level of caspase-8 in HCT-116 cells analysed 2, 4, 8, 18, 24 and 45 h after treatment. The cells were treated as indicated in the figure, and the level of both procaspase-8 (MW 57 kDa) and caspase-8 (MW 43/41 kDa) was detected. 5µg/ml pORF-hTRAIL was used where indicated

4.3 Caspase-9

To investigate the involvement of the intrinsic pathway following various treatments, the level of the main initiator caspase of this pathway, caspase-9, was analysed. However, the procaspase-9 and the cleaved (active) fragments proved to be difficult to analyse by the antibodies used in the present study. Figure R18 shows that the bands corresponding to pro- and active caspase-9 were very weak, making it difficult to observe changes after various treatments. Moreover, it seemed that both procaspase-9 and the large fragment of active caspase-9 were present in all the samples regardless of treatment.

Procaspase-9 was more easily detected in another experiment using membranes

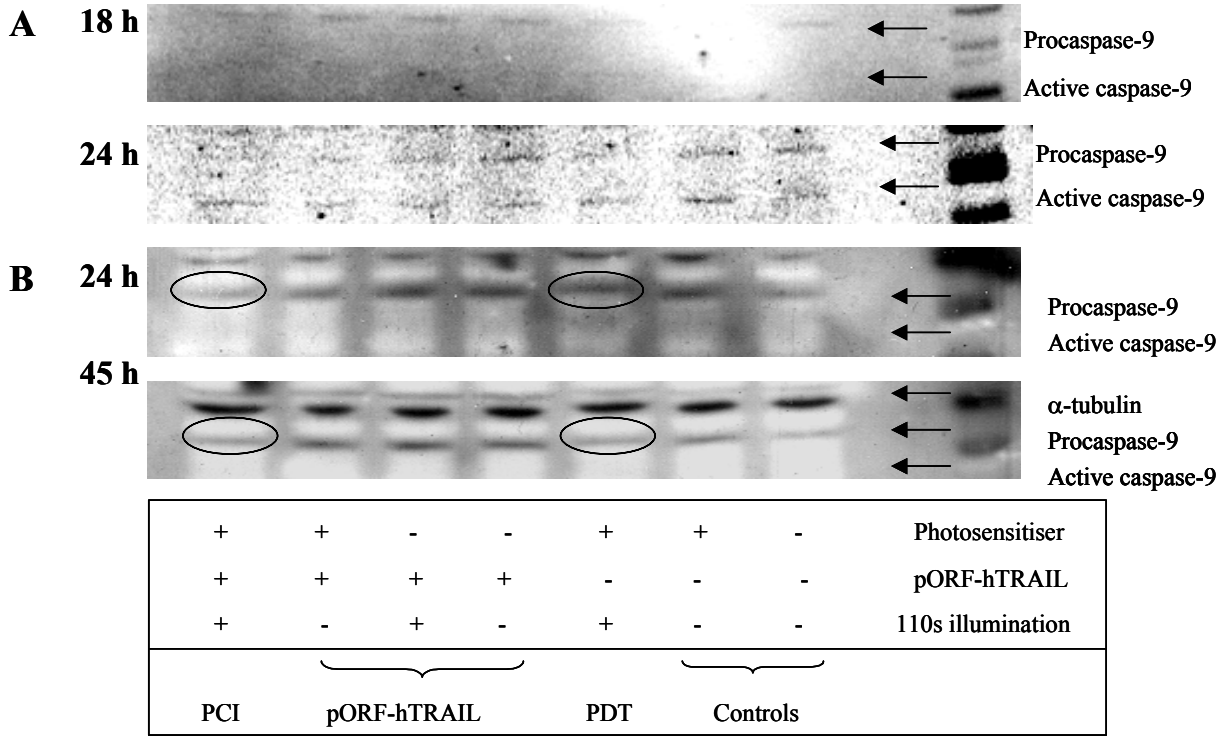

Figure R18 The level of procaspase-9 (MW 47 kDa) and active caspase-9 fragment (MW 35/37 kDa) in HCT-116 cells 18, 24 and 45 h after treatment. A and B present different membranes (i.e. different Western blots). As a loading control, α-tubulin (MW 50 kDa) was used (B, 45h). Circles indicate samples with lower level of procaspase-9 than in samples not exposed to the photochemical treatment. The cells were treated as indicated in the figure. 5 μg/ml pORF-hTRAIL was used where indicated. The membranes shown in B were previously used for PARP-detection (fig. R20).

different from the ones previously used (fig. R18B). There seemed to be some changes in the intensity of the procaspase-9 bands depending on the treatment, the fragments of active caspase-9 were not detected though. In general, reduced levels of procaspase-9 (indicating

caspase-9 activation) were observed after PCI and PDT as compared to samples where no photochemical treatment was applied (except untreated cells, which might be an artefact) (fig. R18B). To check if the reduction in the level of procaspase-9 was in fact the result of the

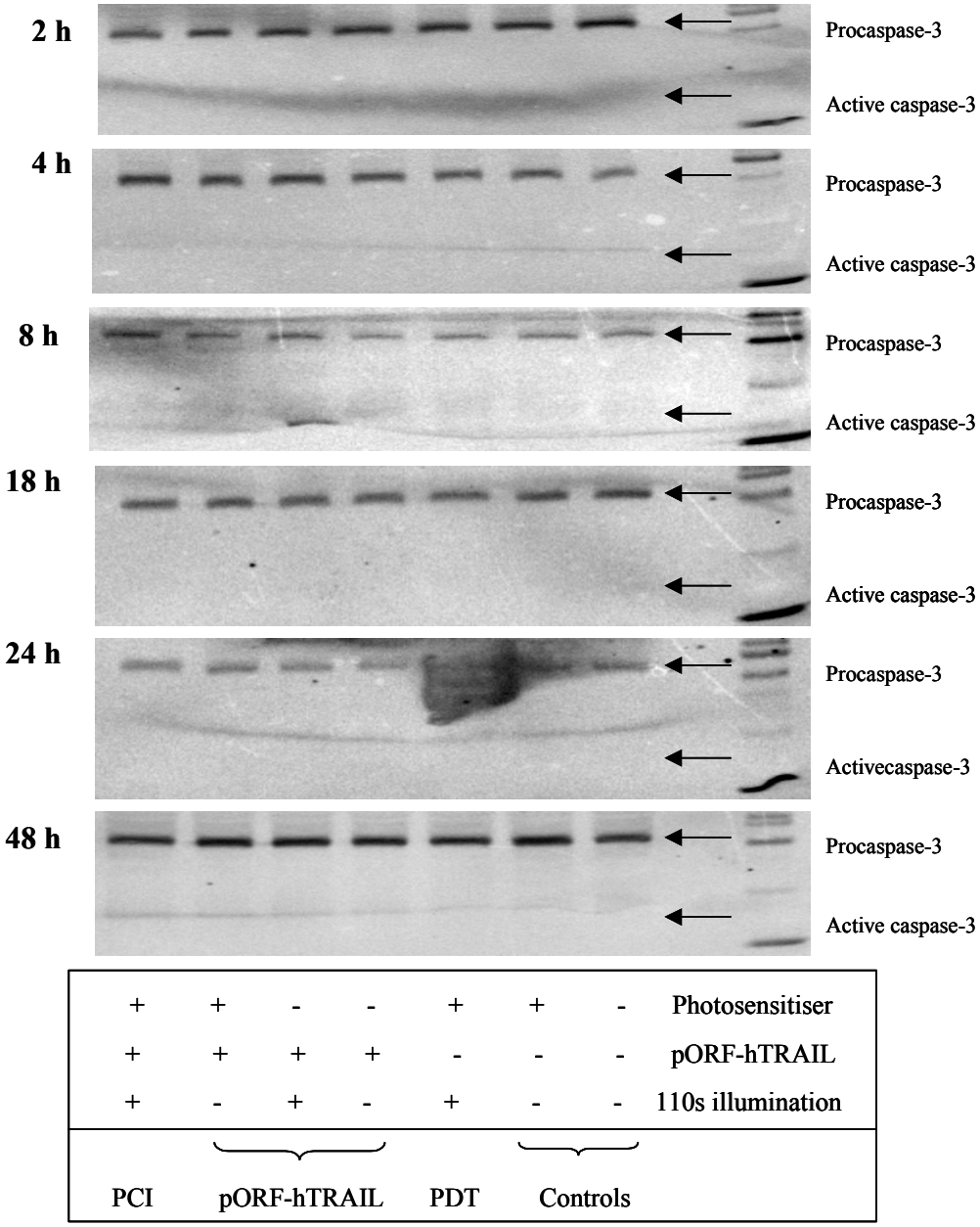

Figure R19 The level of caspase-3 in HCT-116 cells analysed 2, 4, 8, 18, 24 and 45 hours after treatment. The cells were treated as indicated in the figure, and the level of procaspase-3 (35 kDa) was detected. 5μg/ml pORF-hTRAIL was used where indicated

PDT/PCI treatment and not due to less protein loaded on the gel, one of the membranes (fig. R18B, 45h) was used to detect α-tubulin as a loading control. As can be seen in the image from 45 h (fig. R18B), the intensities of the α-tubulin bands were quite similar for all

the samples. This indicated that the same amount of total protein from the PCI/PDT samples, and from the samples not exposed to photochemical treatment were loaded on the gel, confirming the result obtained with Ponceau staining (fig. R14).

All together this indicates that caspase-9 might be activated by photochemical treatment, as could be expected according to the literature [45], as well as by PCI. However, the results are not convincing and indicate that more sensitive detection methods are generally needed to capture the activation of this caspase.

4.4 Caspase-3

To investigate the activation of the main executioner caspase, caspase-3, the levels of procaspase-3 and cleaved (active) caspase-3 were evaluated. The enzymatic caspase-3 assay (chapter 3.2) did not reveal significant caspase-3 activation in HCT-116 cells. Likewise, Western blot analysis did not show any cleaved forms of caspase-3 (fig. R19). Only the bands corresponding to procaspase-3 were observed in all the samples, and the level of procaspase-3

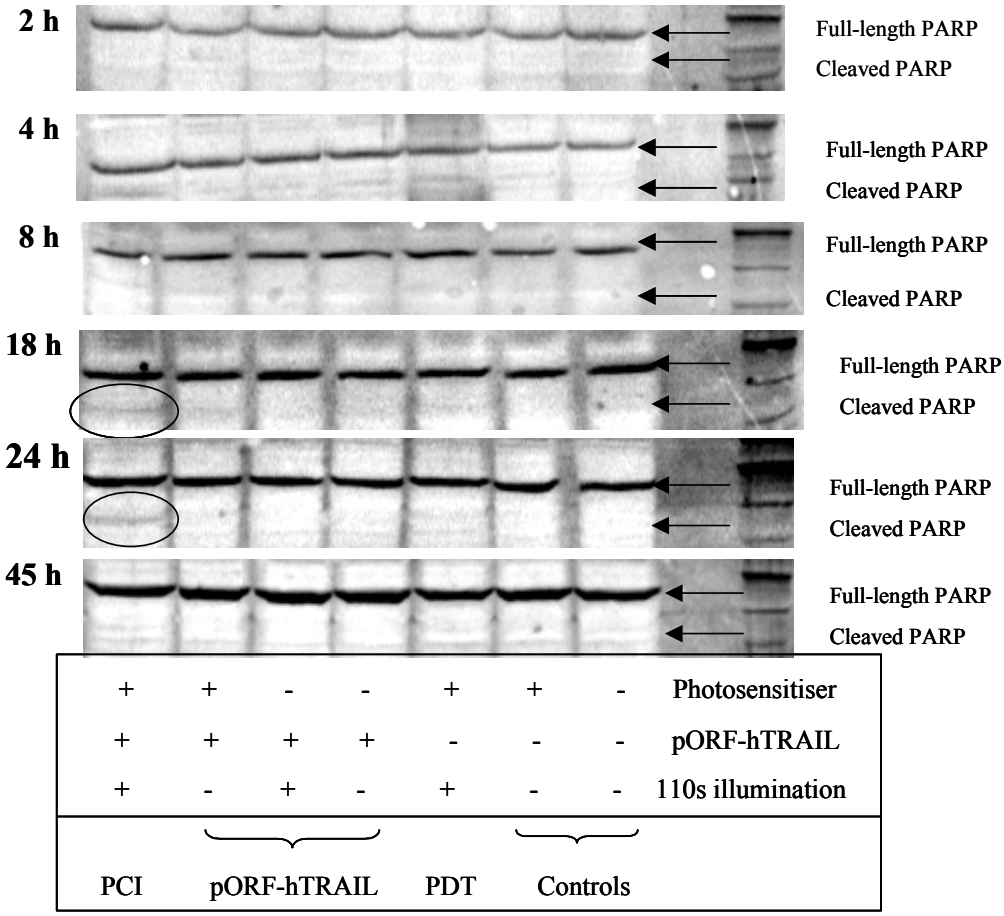

Figure R20 The level of PARP in HCT-116 cells 2, 4, 8, 18, 24 and 45 h after treatment. The cells were treated as indicated in the figure, and the level of both full-length PARP (113 kDa) and active PARP fragment (89 kDa, indicated by circles) was detected. 5 μg/ml of pORF-hTRAIL was used.

did not change following various treatments. These data confirmed that caspase-3 is not strongly activated by the tested treatments in HCT-116 cells.

4.5 PARP

Cleavage of the apoptosis-inducing enzyme Poly (ADP-ribose) polymerase (PARP) is one of the final stages in the apoptotic death pathway, performed by executioner caspases like caspase-3. Therefore, the level of PARP was evaluated at different time points after transfection of PEI/pORF-hTRAIL polyplexes (alone or in combination with PCI) and after PDT. As can be seen in figure R20, full length PARP was present in all the samples, indicating that none of the treatments induced complete cleavage of PARP. Despite generally weak bands, it appeared that only PCI induced PARP cleavage (indicated in fig. R20 with circles), which could be detected 18 and 24 h after treatment. These data support the earlier observations that PCI of PEI/pORF-hTRAIL polyplexes could induce apoptosis more efficiently than transfection with only pORF-hTRAIL or PDT alone.

Discussion

Photochemical internalisation (PCI) is a well-tested strategy for delivery of macromolecules to target cells, which enables the macromolecules to escape from endocytic vesicles where they would otherwise be degraded. Efficacy of macromolecular therapy is therefore highly improved employing PCI. This strategy also provides specificity i.e. allows targeting of macromolecular therapies only to illuminated areas. Therefore, PCI is especially attractive for delivery of cytotoxic molecules as used in cancer treatment.

The aim of the present study was to evaluate the potential of PCI for enhancement of the delivery, expression and, consequently, the effect of a therapeutically relevant gene, aimed at inducing apoptotic death in cancer cells. In that respect, PCI was used for delivery of the pro-apoptotic gene TRAIL in the form of polyplexes consisting of the pORF-hTRAIL plasmid and the nonviral vector PEI. This work was partially based on another similar study by Engesæter et al. (submitted), who delivered the TRAIL gene by the help of PCI, however, employing an adenoviral vector. The authors demonstrated that PCI of the TRAIL-adenovirus significantly enhanced the induction of apoptosis and led to a synergistic increase in cell death. On this basis, it was relevant to study whether comparable results could be achieved with a "safe", i.e. non-viral vector.

Here it was demonstrated that in the colon carcinoma cell line HCT-116, PCI enhances both the expression of TRAIL (at least 3.5-fold, fig. R5) and the cytotoxic effect compared to cytotoxicity induced by pORF-hTRAIL polyplexes without PCI (fig. R6) or photochemical treatment (PDT) without pORF-hTRAIL (figs. R6 and R12). It was also demonstrated by several different assays for detection of apoptosis that PCI was the strongest inducer of apoptosis as compared to the other two treatments. Although studies of apoptosis at the molecular level, e.g. investigating activation of various caspases, did not show an obvious effect of any of the treatments, only PCI (to some extent also PDT) resulted in low, but detectable effects. For example, indications of active caspase-8 or cleaved PARP (figs. R16 and R19) were stronger after PCI than after PDT, whereas transfection with pORF-hTRAIL without PCI did not show any effect. These data do not exclude the possibility that individual treatments, like PDT or transfection with pORF-hTRAIL, also induce the hallmarks of apoptosis, but, the data indicate that the effect of the individual treatments was below the PCI-mediated level, and below the detection limit of the employed assays.

The strongest effect on cell death was registered when a relatively high dose (5 μg/ml) of pORF-hTRAIL was combined with PCI. In this case, cell death was approaching 100% two-three days after PCI (fig. R6). However, the high dose of pORF-hTRAIL without PCI also killed ~50% of the cells. This might be not desirable in many therapeutic situations, where non-target cells have to be preserved. In this regard, it has been shown before [16] that a relatively low dose of plasmid DNA and the PEI vector (with a low PEI:DNA ratio compared to the ratio employed if PEI is used alone [54, 114]) might be especially attractive for specific killing, since only PCI-treated cells are affected. Low concentrations of PEI would not be expected to have an effect on cell death, as low doses of PEI are unable to release the plasmid unless PCI is performed. This allows for high therapeutic specificity, in that only tumour cells are affected due to PCI, while the normal cells are preserved due to the absence of PCI. In the present study, such a low concentration was found to be 2.5 μg/ml pORF-hTRAIL, which induced only 10-20 % killing without PCI and 70 % killing with PCI (fig. R5). In addition, the low concentration induced a synergistic killing effect when combined with PCI. It should be noted that generally, an additive or only slightly synergistic effect (using 2.5 μg/ml pORF-hTRAIL) was obtained when pORF-hTRAIL was delivered by the help of PCI. This means that the enhanced cytotoxicity achieved by PCI-mediated transfection of the pORF-hTRAIL polyplexes was mostly a sum of cytotoxicities induced by the two individual treatments: photochemical treatment and transfection of pORF-hTRAIL. One would, however, expect a more pronounced synergistic effect on cell death following PCI of pORF-hTRAIL based on the following facts:

i) PCI enhanced the level of the expressed TRAIL protein so that more TRAIL was available for initiation of apoptosis in PCI-treated cells

ii) Photochemical treatment initiating endosomal release also stimulated the expression of the TRAIL death receptor DR5 (responsible for induction of apoptosis by TRAIL), which could sensitise the PCI/PDT-treated cells to TRAIL.

The lack of significant synergistic effect could have several explanations as discussed below:

1) The expressed TRAIL protein stays associated with the cells and is not excreted into the medium (fig. R5). This “entrapment” of the TRAIL protein could be one of the explanations for the lower-than-expected cytotoxic effect of PCI despite of up-regulated DR5. The cellular “entrapment” of TRAIL indicates that it does not induce a bystander killing effect on the

neighbouring cells that do not receive or express the TRAIL gene. The "entrapped" TRAIL could also explain why the best cytotoxic effect was registered two days after treatment, while the effect tended to weaken at the later time points (fig. R6). Possibly, the expressed TRAIL kills only the TRAIL-producing cells diminishing the number of TRAIL-producers and, consequently, the level of TRAIL with time. A study by Kim et al. [115] showed that the TRAIL gene delivered by an adenoviral vector was substantially more efficient in inducing apoptosis when a secretable form of TRAIL was used. Likely, PCI effect on cell death could be greatly improved with a plasmid encoding secretable TRAIL, which would allow for spreading of the cytotoxic protein and thereby maintenance of the killing effect.

2) The photochemical treatment initiating the PCI-event might also induce pro-survival signals. Pro-survival molecules like Heat shock proteins (Hsp), Inhibitor of apoptosis proteins (IAP) or the transcription factor NF-κB could be mentioned in that respect (Introduction, chapter 2.2.1). These molecules might interfere with apoptosis induced by the PCI-delivered TRAIL. It has already been demonstrated that the photochemical treatment as used in this study enhances the level of Hsp70 in HCT-116 cells [83]. Hsp are known to inhibit several essential steps in the apoptotic process e.g. block apoptosome formation preventing caspase-3 activation via the intrinsic apoptotic pathway [86, 90]. Additionally, it has been shown by microarray analysis that photochemical treatment initiating PCI also up-regulates genes like XIAP (inhibiting caspase-3, -7 and -9) and some genes from the NF-kB pathway in WiDr colon carcinoma cells (Prasmickaite, unpublished results). Studies have also shown that PDT with other photosensitisers than those used in PCI can induce pro-survival signals [116, 117], especially when sub-lethal doses of PDT are employed. Based on these data, one could expect that such up-regulation might occur also in HCT-116 carcinoma cells, which would imply enhanced level of anti-apoptotic molecules following PCI of TRAIL gene. If the photochemical stimulation of anti-apoptotic factors counterbalances the PCI-enhanced expression of TRAIL, the cytotoxic effect of PCI with pORF-hTRAIL might be lower than expected. It should be noted that the similar study by Engesæter et al. (submitted) demonstrated that the TRAIL gene delivered by an adenoviral vector with PCI leads to at least 100-fold higher levels of the expressed TRAIL protein as compared to the levels achieved by PCI of the PEI/pORF-hTRAIL polyplexes. High amounts of TRAIL can induce strong apoptotic signals, which could more easily overcome the anti-apoptotic signals and therefore lead to synergistic killing, as it was shown by Engesæter et al. Moreover, recently Rudner et al [118] proposed a model suggesting that high doses of TRAIL do not require the

intrinsic pathway for apoptosis propagation even in type II cells like the HCT-116. However, for low doses of TRAIL or weak TRAIL-signal the involvement of the intrinsic pathway is crucial. Thus, the apoptosis inhibitors like Hsp70, acting mainly on the intrinsic pathway, might have a greater impact when a low level of TRAIL is produced, which seems to be the case for PCI of pORF-hTRAIL in the HCT-116 cells. Therefore, combined therapies employing PCI of the pro-apoptotic TRAIL gene together with molecular inhibitors (e.g. siRNAs) against anti-apoptotic HSPs, IAPs or others might be an interesting approach trying to enhance cell death [119].

3) The pORF-hTRAIL plasmid, used in most of the experiments in the present study, delivers the TRAIL gene driven by the human Elongation Factor 1α (EF-1α) promoter, which is reported to be a strong promoter in most tissues [120]. So far, there are no extensive studies on how EF-1α promoter responds to the PCI-relevant photochemical treatment. The recent microarray-based study, investigating the effect of the PCI-relevant photochemical treatment on various genes/corresponding promoters in WiDr colon carcinoma cells, showed that elongation factor genes were neither suppressed, nor stimulated when measured 3 h after the photochemical treatment (1.1±0.2-fold up-regulation in respect to "no photochemical treatment", Prasmickaite, unpublished data). This suggests that gene expression driven by elongation factor promoters is not repressed by PCI-relevant treatment. Still, there is a theoretical possibility that EF-1α might be a weaker promoter in HCT-116 cells, leading to a different (e.g. shorter) expression pattern of the TRAIL gene compared to expression of e.g. the EGFP gene (fig. R4) driven by the strong CMV promoter. So far, the CMV promoter is the most tested and has demonstrated the best results with PCI [11, 83]. Moreover, the recent study by Engesæter et al., which clearly showed synergistic cell death after PCI of TRAIL carried by adenovirus, used a CMV-controlled TRAIL. Therefore, employment of another promoter, e.g. CMV, would be one of the possibilities trying to enhance the cytotoxicity mediated by PCI and the TRAIL gene carried by non-viral vectors. It should be noted that CMV-controlled TRAIL was tested in the present work (Results, chapter 2.3) without showing a notable improvement (fig. R7). However, in this case the TRAIL gene was fused to the EGFP gene, making the plasmid construct rather big and quite different from the CMV-containing constructs that have been shown to be efficient in PCI.

4) The over-expression of DR5 does not sensitise the cells to TRAIL-induced apoptosis. The recent study of Wenger et al. [121] reported that cells over-expressing the TRAIL gene might become resistant to TRAIL, and that such resistance was due to intracellular retention of the receptors. It is, however, not very likely that PCI of TRAIL-containing polyplexes result in TRAIL-protein amounts that might induce such retention. As mentioned above, PCI of TRAIL-containing adenovirus gave 100-fold more TRAIL-protein as compared to the level obtained in this study, and still, the synergistic effect on cell death was demonstrated after PCI of TRAIL-adenovirus (Engesæter et al., submitted). This indicates that the photochemically enhanced level of the TRAIL protein could hardly mediate negative effects on apoptosis via death receptors. However, the possibility that over-expressed DR5 does not necessarily lead to an enhancement of apoptosis via the TRAIL-DR pathway, due to e.g. improper localisation and/or function is worth considering.

Summarising the first part of this study, it was demonstrated that PCI of the pro-apoptotic TRAIL gene delivered by the non-viral vector PEI increases cell death. However, more studies are needed, addressing all the issues mentioned above, to obtain a synergistic killing effect of this strategy.

It was also shown that the PCI-effect on cell death was related to apoptosis. Generally, the strong induction of apoptosis as detected by the SubG1 assay (fig. R12) was not reflected on Western blots (figs. R17-20). This discrepancy might be due to overestimation of apoptotic cell fraction when measuring SubG1 cell fraction and/or due to underestimation of apoptotic hallmarks by Western blotting, indicating that the real effect on induction of apoptosis by PCI of pORF-hTRAIL might be found somewhere in between.

A weakness of the SubG1 assay is that it probably also includes cells that are e.g. pre-necrotic or late-apoptotic. Therefore employment of another assay like cell staining with annexin-V (detects loss of membrane asymmetry in apoptotic cells) followed by flow cytometric analysis [122] would allow to discriminate between early-apoptotic, late-apoptotic and necrotic cells. It can be mentioned that annexin-V staining of photochemically treated HCT-116 cells confirmed that necrosis is not a dominant death pathway after PDT with the photosensitisers used in PCI (Prasmickaite, unpublished data). However, both early- and late-apoptotic cells were detected 1-2 days after treatment, though at a lower level than detected here by measuring the subG1 cell fraction, indicating that the SubG1 assay might indeed over-estimate the apoptotic fraction.

Despite the non-conclusive results obtained by Western blotting, the evaluation of the molecular apoptosis mechanisms following PCI versus the single treatments, PDT and pORF-hTRAIL, did lead to some findings.

Most noteworthy, caspase-8 was activated by PCI, which suggests, as expected, an activation of the extrinsic apoptotic pathway by PCI of pORF-hTRAIL. It also seems like the extrinsic pathway, involving caspase-8, was activated by PDT alone, which is known to be a secondary apoptotic feature of PDT [45]. Caspase-8 appeared to be activated 18 h after combined (i.e. PCI) or 24h after individual PDT treatment. This indicates that both PCI and PDT induce relatively delayed apoptosis, which was not unexpected. Delayed apoptosis after PDT is in agreement with Noodt et al [40], who showed that other lysosomally localised photosensitisers induce apoptosis apparent only after >12 hours. One would not expect a rapid induction of apoptosis after transfection of pORF-hTRAIL either, as transcription and translation steps are required before the TRAIL protein is produced and can induce apoptosis. Moreover, there are several indications that photochemical treatment might temporally suppress translation, ([11, 123, 124], Prasmickaite, unpublished data), implying that TRAIL synthesis might be delayed in PCI-treated cells. Nevertheless, it might seem that PCI leads to a bit earlier caspase-8 activation than PDT does (fig. R17). In addition, the activation of caspase-8 seems to be prolonged after PCI as compared to PDT, most likely due to photochemically internalised and expressed TRAIL protein. The earlier caspase-8 activation after PCI might be a result of a stronger apoptotic signal after PCI, when both TRAIL- and PDT-treatments are combined, making it easier to detect the active caspase-8. Alternatively, it might indicate that caspase-8 is directly activated by photochemically internalised TRAIL, while activation of caspase-8 after PDT is a secondary event, and therefore appears later. An experimental artefact could also be an explanation, since the 18h-PDT-sample gave an unclear band on the particular Western blot (fig. R17).

The activation of caspase-8 was followed by cleavage of the key death substrate PARP (fig. R20), which unfortunately, was quite unpronounced (probably due to detection problems) and did not correspond to other data indicating significant apoptosis. Despite that, it can be concluded that only PCI led to detectable PARP cleavage, however, without detectable activation of the main executioner caspase, caspase-3. The latter result seems to be valid, as an enzymatic assay of caspase-3 activity also showed negligible activation in HCT-116 (fig. R9). In comparison, other colon carcinoma cells, WiDr, displayed substantially activated caspase-3 after both PDT and PCI where PCI induced the highest activation (fig. R10). Furthermore, a recent study by Furre et al. [125] also showed induction of apoptosis in

HCT-116 cells in a caspase-3 independent manner after photochemical treatment, however, with a photosensitiser not relevant for PCI (5-ALA-based PDT). The lack of significant caspase-3 activation in HCT-116 cells partially corresponds to the data of Engesæter et al. (submitted), demonstrating quite low activation (hardly detectable in Western blots) of caspase-3 in HCT-116 following PDT as used in this study. However, Engesæter et al. showed clearly detectable active caspase-3 in HCT cells after transduction with TRAIL-adenovirus with or without PCI. This, again, implies that adenovirus-based delivery of the TRAIL gene was much more potent than the non-viral based transfection used in this study.

All together, studies of caspase-3 activation suggest an alternative apoptotic mechanism in HCT-116 as a response to PDT or to PCI of pORF-hTRAIL, possibly involving other executioner caspases e.g. caspase-6 and caspase-7 or a combination of caspase-3 and -7, where caspase-3 does not play the major role [126]. This remains to be elucidated.

The role of the intrinsic (mitochondrial) pathway, involving caspase-9, also remains to be elucidated. Though there are some indications (reduced level of procaspase-9, fig. R18B) that caspase-9 might be activated after PDT and PCI of pORF-hTRAIL, clear activation of caspase-9 was not detected (fig. R18B). This was unexpected since, according to the literature, PDT generally activates this pathway [45, 127]. Moreover, HCT-116 cells belong to the type II cells, in which TRAIL-induced apoptosis requires signal amplification from the extrinsic to the intrinsic pathway [73, 75]. Therefore, the fact that active caspase-9 was not registered can probably be ascribed to the detection problems that remain to be solved before further conclusions can be drawn. An alternative would be to measure other hallmarks of apoptosis indicating the involvement of mitochondria e.g. change of the mitochondrial membrane potential, release of cytochrome *c* or detection of Bid/tBid [79, 128, 129]. Another possibility, that the mitochondrial pathway was not involved due to e.g. inhibitory effects of photochemically induced pro-survival molecules (like Hsp or IAP), has already been discussed above and should not be excluded.

Finally, it can be noted that transfection of pORF-hTRAIL without PCI did not show any signs of apoptosis at the molecular level, which generally indicates that this treatment was the weakest in inducing cell killing compared to PCI of pORF-hTRAIL and PDT alone, corresponding also to the survival data obtained (fig. R6).

Taken together, the data presented here showed that a pro-apoptotic gene like TRAIL combined with the nonviral vector PEI can be delivered into carcinoma cells by the help of PCI, and that this leads to both enhanced cytotoxicity and enhanced apoptosis in PCI-treated cells. However, further studies are needed in order to obtain a desirable synergistic effect as

well as to understand the molecular mechanisms behind cell killing by PCI of the TRAIL gene.

Future perspectives

The results presented in this study showed that PCI of the TRAIL gene delivered by a nonviral vector is an interesting approach, resulting in higher cytotoxicity *in vitro* as compared to the individual treatments - photochemical treatment (PDT) or non-viral transfection with the TRAIL gene. However, a stronger synergistic effect on cell death is necessary before this approach can be suitable for *in vivo* situations.

This might be achieved in a number of ways:

i) Employ a plasmid where the TRAIL gene is controlled by a strong promoter known to be induced, or at least not repressed, after PCI treatment.

ii) A secretable form of the TRAIL gene would be preferential.

iii) To investigate whether the photochemical treatment induces anti-apoptotic signals. In case anti-apoptotic signals are activated, PCI of the pro-apoptotic TRAIL gene should be combined with inhibitors of such anti-apoptotic factors.

Understanding of the PCI effect on pro-survival factors would be valuable not only in respect to TRAIL, but also in respect to other molecules delivered by PCI and aimed at inducing apoptosis.

It would also be of interest to continue studies of the molecular mechanisms behind PCI of the TRAIL gene, trying to reveal the role of each apoptotic pathway. Many of the questions could be answered by the help of a successful Western blotting protocol. The establishment of such a protocol requires individual optimisation for each protein to be analysed, and for each new antibody employed. In the present study this was solved for a very small number of proteins and there is a big room for optimisation.

Experiments employing inhibitors of various caspases would also be interesting in order to investigate further the role of different caspases in the induction of apoptosis by PCI of a pro-apoptotic gene like TRAIL.

References

1. Berg, K., et al., *Photochemical drug and gene delivery.* Current Opinion in Molecular Therapeutics, 2004. **6**: p. 279-287.
2. Fretz, M.M., et al., *Strategies for cytosolic delivery of liposomal macromolecules.* International Journal of Pharmaceutics, 2005. **298**: p. 305-309.
3. Khalil, I.A., et al., *Uptake pathways and subsequent intracellular trafficking in nonviral gene delivery.* Pharmacological Reviews, 2006. **58**: p. 32-45.
4. Berg, K., et al., *Photochemical internalization: a novel technology for delivery of macromolecules into cytosol.* Cancer Research, 1999. **59**: p. 1180-1183.
5. Albert, B., et al., *Molecular Biology of the cell*. 4th ed, ed. Gibbs, S. 2002, New York: Garland Science.
6. Prasmickaite, L., et al., *Light-directed gene delivery by photochemical internalisation.* Expert Opinion on Biological Therapy, 2004. **4**: p. 1403-1412.
7. Prasmickaite, L., et al., *Photochemical disruption of endocytic vesicles before delivery of drugs: a new strategy for cancer therapy.* British Journal of Cancer, 2002. **86**: p. 652-657.
8. Bonsted, A., et al., *Photochemical enhancement of gene delivery to glioblastoma cells is dependent on the vector applied.* Anticancer Research, 2005. **25**: p. 291-297.
9. Bonsted, A., et al., *Photochemically enhanced transduction of polymer-complexed adenovirus targeted to the epidermal growth factor receptor.* The Journal of Gene Medicine, 2005. **8**: p. 286-297.
10. Bonsted, A., et al., *Transgene expression is increased by photochemically mediated transduction of polycation-complexed adenoviruses.* Gene Therapy, 2004. **11**: p. 152-160.
11. Engesaeter, B.O., et al., *Photochemical treatment with endosomally localized photosensitizers enhances the number of adenoviruses in the nucleus.* The Journal of Gene Medicine, 2006. **In press**.
12. Hogset, A., et al., *Light-induced adenovirus gene transfer, an efficient and specific gene delivery technology for cancer gene therapy.* Cancer Gene Therapy, 2002. **9**: p. 365-371.
13. Dietze, A., et al., *Transgene delivery and gelonin cytotoxicity enhanced by photochemical internalization in fibroblast-like synoviocytes (FLS) from rheumatoid arthritis patients.* Photochemical & Photobiological Sciences, 2005. **4**: p. 341-347.
14. Ndoye, A., et al., *Enhanced gene transfer and cell death following p53 gene transfer using photochemical internalisation of glucosylated PEI-DNA complexes.* The Journal of Gene Medicine, 2004. **6**: p. 884-894.
15. Ndoye, A., et al., *Sustained gene transfer and enhanced cell death following glucosylated-PEI-mediated p53 gene transfer with photochemical internalisation in p53-mutated head and neck carcinoma cells.* International Journal of Oncology, 2004. **25**: p. 1575-1581.
16. Prasmickaite, L., et al., *Photochemically enhanced gene transfection increases the cytotoxicity of the herpes simplex virus thymidine kinase gene combined with ganciclovir.* Cancer Gene Therapy, 2004. **11**: p. 514-523.
17. Hogset, A., et al., *Photochemical transfection: a new technology for light-induced, site-directed gene delivery.* Human Gene Therapy, 2000. **11**: p. 869-880.
18. Hellum, M., et al., *Photochemically enhanced gene delivery with cationic lipid formulations.* Photochemical & Photobiological Sciences, 2003. **2**: p. 407-411.
19. Maurice-Duelli, A., et al., *Enhanced cell growth inhibition following PTEN nonviral gene transfer using polyethylenimine and photochemical internalization in*

endometrial cancer cells. Technology in Cancer Research & Treatment, 2004. **3**: p. 459-465.
20. Kloeckner, J., et al., *Photochemically enhanced gene delivery of EGF receptor-targeted DNA polyplexes.* Journal of Drug Targeting, 2004. **12**: p. 205-213.
21. Nishiyama, N., et al., *Light-induced gene transfer from packaged DNA enveloped in a dendrimeric photosensitizer.* Nature Materials, 2005. **4**: p. 934-941.
22. Ndoye, A., et al., *Eradication of p53-mutated Head and Neck Squamous Cell Carcinoma Xenografts Using Nonviral p53 Gene Therapy and Photochemical Internalization.* Molecular Therapy, 2006. **In press**.
23. Shiraishi, T. and Nielsen, P.E., *Photochemically enhanced cellular delivery of cell penetrating peptide-PNA conjugates.* FEBS Letters, 2006. **580**: p. 1451-1456.
24. Folini, M., et al., *Photochemical internalization of a peptide nucleic acid targeting the catalytic subunit of human telomerase.* Cancer Research, 2003. **63**: p. 3490-3494.
25. Bøe, S. and Hovig, E., *Photochemical induced gene silencing with PNA-peptide conjugates.* Oligonucleotides, 2006. **In press**.
26. Berg, K., et al., *Site-specific drug delivery by photochemical internalization enhances the antitumor effect of bleomycin.* Clinical Cancer Research, 2005. **11**: p. 8476-8485.
27. Dietze, A., et al., *Enhanced photodynamic destruction of a transplantable fibrosarcoma using photochemical internalisation of gelonin.* British Journal of Cancer, 2005. **92**: p. 2004-2009.
28. Selbo, P.K., et al., *In vivo documentation of photochemical internalization, a novel approach to site specific cancer therapy.* International Journal of Cancer, 2001. **92**: p. 761-766.
29. Weyergang, A., et al., *Photochemically stimulated drug delivery increases the cytotoxicity and specificity of EGF-saporin.* Journal of Controlled Release, 2006. **111**: p. 165-173.
30. Selbo, P.K., et al., *Photochemical internalisation increases the cytotoxic effect of the immunotoxin MOC31-gelonin.* International Journal of Cancer, 2000. **87**: p. 853-859.
31. Selbo, P.K., et al., *5-Aminolevulinic acid-based photochemical internalization of the immunotoxin MOC31-gelonin generates synergistic cytotoxic effects in vitro.* Photochemistry and Photobiology, 2001. **74**: p. 303-310.
32. Moan, J. and Peng, Q., *An outline of the hundred-year history of PDT.* Anticancer Research, 2003. **23**: p. 3591-3600.
33. Brown, S.B., et al., *The present and future role of photodynamic therapy in cancer treatment.* The Lancet Oncology, 2004. **5**: p. 497-508.
34. Weishaupt, K.R., et al., *Identification of singlet oxygen as the cytotoxic agent in photoinactivation of a murine tumor.* Cancer Research, 1976. **36**: p. 2326-2329.
35. Moan, J., et al., *The mechanism of photodynamic inactivation of human cells in vitro in the presence of haematoporphyrin.* British Journal of Cancer, 1979. **39**: p. 398-407.
36. Kimel, S., et al., *Singlet oxygen generation of porphyrins, chlorins, and phthalocyanines.* Photochemistry Photobiology, 1989. **50**: p. 175-183.
37. Jori, G. and Spikes, J.D., *Photochemistry of porphyrins*, in *Topics in photomedicine*, Smith, K.C., Editor. 1984, Plenum Press: New York. p. 183-318.
38. Moan, J. and Berg, K., *The photodegradation of porphyrins in cells can be used to estimate the lifetime of singlet oxygen.* Photochemistry Photobiology, 1991. **53**: p. 549-553.
39. Berg, K., *Mechanisms of cell damage in photodynamic therapy*. Fundamental bases of phototherapy, ed. Honingsmann, H., et al. 1996, Milano.

40. Noodt, B.B., et al., *Primary DNA damage, HPRT mutation and cell inactivation photoinduced with various sensitizers in V79 cells.* Photochemistry Photobiology, 1993. **58**: p. 541-547.
41. Berg, K. and Moan, J., *Lysosomes as photochemical targets.* International Journal of Cancer, 1994. **59**: p. 814-822.
42. Prasmickaite, L., et al., *Evaluation of different photosensitizers for use in photochemical gene transfection.* Photochem Photobiol, 2001. **73**: p. 388-395.
43. Marchal, S., et al., *Necrotic and apoptotic features of cell death in response to Foscan((R)) photosensitization of HT29 monolayer and multicell spheroids.* Biochem Pharmacol, 2005. **69**: p. 1167-1176.
44. Plaetzer, K., et al., *Apoptosis following photodynamic tumor therapy: induction, mechanisms and detection.* Curr Pharm Des, 2005. **11**: p. 1151-1165.
45. Oleinick, N.L., et al., *The role of apoptosis in response to photodynamic therapy: what, where, why, and how.* Photochemical and Photobiological Sciences, 2002. **1**: p. 1-21.
46. Chiu, S.M., et al., *Photodynamic therapy-induced death of HCT 116 cells: Apoptosis with or without Bax expression.* Apoptosis, 2005. **10**: p. 1357-1368.
47. Kessel, D. and Luo, Y., *Mitochondrial photodamage and PDT-induced apoptosis.* Journal of Photochemistry Photobiology B: Biology, 1998. **42**: p. 89-95.
48. Noodt, B.B., et al., *Different apoptotic pathways are induced from various intracellular sites by tetraphenylporphyrins and light.* British Journal of Cancer, 1999. **79**: p. 72-81.
49. Hogset, A., et al., *Photochemical transfection: a technology for efficient light-directed gene delivery.* Somat Cell Mol Genet, 2002. **27**: p. 97-113.
50. Verma, I.M. and Weitzman, M.D., *Gene therapy: twenty-first century medicine.* Annuual Review of Biochemistry, 2005. **74**: p. 711-738.
51. Gardlik, R., et al., *Vectors and delivery systems in gene therapy.* Medical Science Monitor, 2005. **11**: p. RA110-121.
52. El-Aneed, A., *An overview of current delivery systems in cancer gene therapy.* Journal of Controlled Release, 2004. **94**: p. 1-14.
53. Bessis, N., et al., *Immune responses to gene therapy vectors: influence on vector function and effector mechanisms.* Gene Therapy, 2004. **11 Suppl 1**: p. S10-17.
54. Gebhart, C.L. and Kabanov, A.V., *Evaluation of polyplexes as gene transfer agents.* Journal of Controlled Release, 2001. **73**: p. 401-416.
55. Kashani-Sabet, M., *Non-viral delivery of ribozymes for cancer gene therapy.* Expert Opin Biol Ther, 2004. **4**: p. 1749-1755.
56. Zabner, J., et al., *Cellular and molecular barriers to gene transfer by a cationic lipid.* Journal of Biological Chemistry, 1995. **270**: p. 18997-19007.
57. Lungwitz, U., et al., *Polyethylenimine-based non-viral gene delivery systems.* European Journal of Pharmaceutics and Biopharmaceutics, 2005. **60**: p. 247-266.
58. Godbey, W.T., et al., *Tracking the intracellular path of poly(ethylenimine)/DNA complexes for gene delivery.* Proceedings of the National Acadademy of Sciences of the United States of America, 1999. **96**: p. 5177-5181.
59. Varga, C.M., et al., *Receptor-mediated targeting of gene delivery vectors: insights from molecular mechanisms for improved vehicle design.* Biotechnology and Bioengeneering, 2000. **70**: p. 593-605.
60. Chen, C.Y., et al., *Effect of herpes simplex virus thymidine kinase expression levels on ganciclovir-mediated cytotoxicity and the "bystander effect".* Human Gene Therapy, 1995. **6**: p. 1467-1476.

61. Jaattela, M., *Escaping cell death: survival proteins in cancer.* Experimental Cell Research, 1999. **248**: p. 30-43.
62. Cheung, H.H., et al., *Abnormalities of cell structures in tumors: apoptosis in tumors.* Exs, 2006: p. 201-221.
63. Ozturk, M., et al., *p53 as a potential target in cancer therapy.* Bone Marrow Transplantation, 1992. **9 Suppl 1**: p. 164-170.
64. Kagawa, S., et al., *Antitumor activity and bystander effects of the tumor necrosis factor-related apoptosis-inducing ligand (TRAIL) gene.* Cancer Research, 2001. **61**: p. 3330-3338.
65. Fischer, U. and Schulze-Osthoff, K., *New approaches and therapeutics targeting apoptosis in disease.* Pharmacological Reviews, 2005. **57**: p. 187-215.
66. Devi, G.R., *siRNA-based approaches in cancer therapy.* Cancer Gene Therapy, 2006. **In press**.
67. Kerr, J.F., et al., *Apoptosis: a basic biological phenomenon with wide-ranging implications in tissue kinetics.* British journal of Cancer, 1972. **26**: p. 239-257.
68. Broker, L.E., et al., *Cell death independent of caspases: a review.* Clinical Cancer Research, 2005. **11**: p. 3155-3162.
69. Jin, Z. and El-Deiry, W.S., *Overview of cell death signaling pathways.* Cancer Biology and Therapy, 2005. **4**: p. 139-163.
70. Fadeel, B. and Orrenius, S., *Apoptosis: a basic biological phenomenon with wide-ranging implications in human disease.* Journal of Internal Medicine, 2005. **258**: p. 479-517.
71. Majno, G. and Joris, I., *Apoptosis, oncosis, and necrosis. An overview of cell death.* The American Journal of Pathology, 1995. **146**: p. 3-15.
72. Fesik, S.W., *Promoting apoptosis as a strategy for cancer drug discovery.* Nature Reviews. Cancer, 2005. **5**: p. 876-885.
73. Ozoren, N., et al., *The caspase 9 inhibitor Z-LEHD-FMK protects human liver cells while permitting death of cancer cells exposed to tumor necrosis factor-related apoptosis-inducing ligand.* Cancer Research, 2000. **60**: p. 6259-6265.
74. Wang, S. and El-Deiry, W.S., *TRAIL and apoptosis induction by TNF-family death reseptors.* Oncogene, 2003. **22**: p. 8628-8633.
75. Ozoren, N. and El-Deiry, W.S., *Defining characteristics of Types I and II apoptotic cells in response to TRAIL.* Neoplasia, 2002. **4**: p. 551-557.
76. Igney, F.H. and Krammer, P.H., *Death and anti-death: tumour resistance to apoptosis.* Nature Reviews. Cancer, 2002. **2**: p. 277-288.
77. Zhang, L. and Fang, B., *Mechanisms of resistance to TRAIL-induced apoptosis in cancer.* Cancer Gene Therapy, 2005. **12**: p. 228-237.
78. Piette, J., et al., *Cell death and growth arrest in response to photodynamic therapy with membrane-bound photosensitizers.* Biochemical pharmacology, 2003. **66**: p. 1651-1659.
79. Matroule, J.Y., et al., *Mechanism of colon cancer cell apoptosis mediated by pyropheophorbide-a methylester photosensitization.* Oncogene, 2001. **20**: p. 4070-4084.
80. Reiners, J.J., Jr., et al., *Release of cytochrome c and activation of pro-caspase-9 following lysosomal photodamage involves Bid cleavage.* Cell Death and Differentiation, 2002. **9**: p. 934-944.
81. Cirman, T., et al., *Selective disruption of lysosomes in HeLa cells triggers apoptosis mediated by cleavage of Bid by multiple papain-like lysosomal cathepsins.* The Journal of Biological Chemistry, 2004. **279**: p. 3578-3587.

82. Granville, D.J., et al., *Nuclear factor-kappaB activation by the photochemotherapeutic agent verteporfin.* Blood, 2000. **95**: p. 256-262.
83. Prasmickaite, L., et al., *Photochemical Internalisation (PCI) of Transgenes Controlled by Heat-Shock Protein 70 Promoter.* Photochemistry and Photobiology, 2006. **82**: p. 809-816.
84. Boland, M.P., *DNA damage signalling and NF-kappaB: implications for survival and death in mammalian cells.* Biochemical Society Transactions, 2001. **29**: p. 674-678.
85. Nonaka, M., et al., *Inhibitory effect of heat shock protein 70 on apoptosis induced by photodynamic therapy in vitro.* Photochemistry and Photobiology, 2004. **79**: p. 94-98.
86. Ozoren, N. and El-Deiry, W., *Heat shock protects HCT116 and H460 cells from TRAIL-induced apoptosis.* Experimental Cell Research, 2002. **281**: p. 175-181.
87. Nylandsted, J., et al., *Heat shock protein 70 promotes cell survival by inhibiting lysosomal membrane permeabilization.* Journal of Experimental Medicine, 2004. **200**: p. 425-435.
88. Beere, H.M., *Death versus survival: functional interaction between the apoptotic and stress-inducible heat shock protein pathways.* The Journal of Clinical Investigation, 2005. **115**: p. 2633-2639.
89. Korbelik, M., et al., *Photodynamic therapy-induced cell surface expression and release of heat shock proteins: relevance for tumor response.* Cancer Research, 2005. **65**: p. 1018-1026.
90. Parcellier, A., et al., *Heat shock proteins, cellular chaperones that modulate mitochondrial cell death pathways.* Biochemical and Biophysical Research Communications, 2003. **304**: p. 505-512.
91. Kelley, S.K. and Ashkenazi, A., *Targeting death receptors in cancer with Apo2L/TRAIL.* Current Opinion in Pharmacology, 2004. **4**: p. 333-339.
92. Wiley, S.R., et al., *Identification and characterization of a new member of the TNF family that induces apoptosis.* Immunity, 1995. **3**: p. 673-682.
93. Ashkenazi, A., et al., *Safety and antitumor activity of recombinant soluble Apo2 ligand.* The Journal of Clinical Investigation, 1999. **104**: p. 155-162.
94. Ganten, T.M., et al., *Preclinical differentiation between apparently safe and potentially hepatotoxic applications of TRAIL either alone or in combination with chemotherapeutic drugs.* Clinical Cancer Research, 2006. **12**: p. 2640-2646.
95. Lawrence, D., et al., *Differential hepatocyte toxicity of recombinant Apo2L/TRAIL versions.* Nature Medicine, 2001. **7**: p. 383-385.
96. Pitti, R.M., et al., *Induction of apoptosis by Apo-2 ligand, a new member of the tumor necrosis factor cytokine family.* The Journal of Biological Chemistry, 1996. **271**: p. 12687-12690.
97. Nagane, M., et al., *The potential of TRAIL for cancer chemotherapy.* Apoptosis, 2001. **6**: p. 191-197.
98. MacFarlane, M., *TRAIL-induced signalling and apoptosis.* Toxicology Letters, 2003. **139**: p. 89-97.
99. Sanlioglu, A.D., et al., *Surface TRAIL decoy receptor-4 expression is correlated with TRAIL resistance in MCF7 breast cancer cells.* BioMedCentral Cancer, 2005. **5**.
100. Chu, L., et al., *Adenoviral Vector Expressing CYLD Augments Antitumor activity of TRAIL by Suppression of NF-kappaB Survival Signaling in Hepatocellular Carcinoma.* Cancer Biology and Therapy, 2006. **5, In press**.
101. Daniels, R.A., et al., *Expression of TRAIL and TRAIL receptors in normal and malignant tissues.* Cell Research, 2005. **15**: p. 430-438.
102. Xu, L.H., et al., *Synergistic antitumor effect of TRAIL and doxorubicin on colon cancer cell line SW480.* World Journal of Gastroenterology, 2003. **9**: p. 1241-1245.

103. El-Zawahry, A., et al., *Doxorubicin increases the effectiveness of Apo2L/TRAIL for tumor growth inhibition of prostate cancer xenografts.* BioMed Central Cancer, 2005. **5**.
104. Kang, J., et al., *Subtoxic concentration of doxorubicin enhances TRAIL-induced apoptosis in human prostate cancer cell line LNCaP.* Prostate Cancer and Prostatic Diseases, 2005. **8**: p. 274-279.
105. Kim, D.M., et al., *Rapid induction of apoptosis by combination of flavopiridol and tumor necrosis factor (TNF)-alpha or TNF-related apoptosis-inducing ligand in human cancer cell lines.* Cancer Research, 2003. **63**: p. 621-626.
106. Ganten, T.M., et al., *Enhanced caspase-8 recruitment to and activation at the DISC is critical for sensitisation of human hepatocellular carcinoma cells to TRAIL-induced apoptosis by chemotherapeutic drugs.* Cell Death and Differentiation, 2004. **11 Suppl 1**: p. S86-96.
107. Granville, D.J., et al., *Fas ligand and TRAIL augment the effect of photodynamic therapy on the induction of apoptosis in JURKAT cells.* International Immunopharmacology, 2001. **1**: p. 1831-1840.
108. Wu, X.X., et al., *TRAIL and chemotherapeutic drugs in cancer therapy.* Vitamins and Hormones, 2004. **67**: p. 365-383.
109. Zhu, H., et al., *Overcoming acquired resistance to TRAIL by chemotherapeutic agents and calpain inhibitor I through distinct mechanisms.* Molecular Therapy, 2004. **9**: p. 666-673.
110. Nicoletti, I., et al., *A rapid and simple method for measuring thymocyte apoptosis by propidium iodide staining and flow cytometry.* Journal of Immunological Methods, 1991. **139**: p. 271-279.
111. Twentyman, P.R. and Luscombe, M., *A study of some variables in a tetrazolium dye (MTT) based assay for cell growth and chemosensitivity.* British Journal of Cancer, 1987. **56**: p. 279-285.
112. Lowry, O.H., et al., *Protein measurement with the Folin phenol reagent.* The Journal of Biological Chemistry, 1951. **193**: p. 265-275.
113. Steel, G.G. and Peckham, M.J., *Exploitable mechanisms in combined radiotherapy-chemotherapy: the concept of additivity.* International Journal of Radiation Oncology, Biology, Physics, 1979. **5**: p. 85-91.
114. Wiseman, J.W., et al., *A comparison of linear and branched polyethylenimine (PEI) with DCChol/DOPE liposomes for gene delivery to epithelial cells in vitro and in vivo.* Gene Therapy, 2003. **10**: p. 1654-1662.
115. Kim, C.Y., et al., *Cancer gene therapy using a novel secretable trimeric TRAIL.* Gene Therapy, 2005.
116. Volanti, C., et al., *Distinct transduction mechanisms of cyclooxygenase 2 gene activation in tumour cells after photodynamic therapy.* Oncogene, 2005. **24**: p. 2981-2991.
117. Kim, H.R., et al., *Enhanced apoptotic response to photodynamic therapy after bcl-2 transfection.* Cancer Research, 1999. **59**: p. 3429-3432.
118. Rudner, J., et al., *Type I and type II reactions in TRAIL-induced apoptosis -- results from dose-response studies.* Oncogene, 2005. **24**: p. 130-140.
119. Yamaguchi, Y., et al., *Targeting of X-linked inhibitor of apoptosis protein or survivin by short interfering RNAs sensitize hepatoma cells to TNF-related apoptosis-inducing ligand- and chemotherapeutic agent-induced cell death.* Oncology Reports, 2005. **14**: p. 1311-1316.
120. Kim, D.W., et al., *Use of the human elongation factor 1 alpha promoter as a versatile and efficient expression system.* Gene, 1990. **91**: p. 217-223.

121. Wenger, T., et al., *Specific resistance upon lentiviral TRAIL transfer by intracellular retention of TRAIL receptors.* Cell Death and Differentiation, 2006. **In press**.
122. van Engeland, M., et al., *Annexin V-affinity assay: a review on an apoptosis detection system based on phosphatidylserine exposure.* Cytometry, 1998. **31**: p. 1-9.
123. Haywood-Small, S.L., et al., *Phthalocyanine-mediated photodynamic therapy induces cell death and a G0/G1 cell cycle arrest in cervical cancer cells.* Biochemical and Biophysical Research Communications, 2006. **339**: p. 569-576.
124. Davies, C.L., et al., *Relationship between changes in antigen expression and protein synthesis in human melanoma cells after hyperthermia and photodynamic treatment.* British Journal of Cancer, 1988. **58**: p. 306-313.
125. Furre, I.E., et al., *Targeting PBR by hexaminolevulinate-mediated photodynamic therapy induces apoptosis through translocation of apoptosis-inducing factor in human leukemia cells.* Cancer Research, 2005. **65**: p. 11051-11060.
126. Lakhani, S.A., et al., *Caspases 3 and 7: key mediators of mitochondrial events of apoptosis.* Science, 2006. **311**: p. 847-851.
127. Moor, A.C., *Signaling pathways in cell death and survival after photodynamic therapy.* Journal of Photochemistry and Photobiology B, 2000. **57**: p. 1-13.
128. Suliman, A., et al., *Intracellular mechanisms of TRAIL: apoptosis through mitochondrial-dependent and -independent pathways.* Oncogene, 2001. **20**: p. 2122-2133.
129. Mathur, A., et al., *Evaluation of fluorescent dyes for the detection of mitochondrial membrane potential changes in cultured cardiomyocytes.* Cardiovascular Research, 2000. **46**: p. 126-138.

Appendix

1 Buffers for SDS-PAGE and Western Blotting

1.1 SDS lysis buffer

Tris-HCl pH 6.8	62.5 mM
SDS	2 % w/v
Glycerol	10 %
DTT	50 mM
Bromphenol blue	0.01 %

Immediately before lysis, 945 µl of the SDS lysis buffer was supplemented with the following:

Protease inhibitor cocktail	10 µl
Phospatase inhibitor cocktail I	10 µl
Phospatase inhibitor cocktail II	10 µl
PMSF	5 µl
NaF (1 mM)	5 µl
Na_3VO_4	5 µl
β-Glycerolphosphate (1.5 M)	10 µl

1.2 RIPA-buffer

Tris-HCl	50 mM
Tergitol NP-40	1 %
Na-deoxycholate	0.25 %
NaCl	150 mM
EDTA	1 mM

Immediately before lysis, 967 µl of the RIPA-buffer was supplemented with the following:

Na_3VO_4 (1 mM)	5 µl
Protease inhibitor cocktail	10 µl
NaF (1 mM)	5 µl
β-glycerolphosphate (1.5 M)	14 µl

1.3 4x sample buffer

Tris-HCl, pH 6.8 (1.5 M)	46.6 ml
Glycerol	40.0 ml
SDS (30 % w/v)	26.7 ml
Bromphenol blue (1 %)	4.0 ml
dH_2O	2.7 ml

1.4 Running buffer (5x)

Tris-base	15 g
Glycine	72 g
Dilution up to 1000 ml with dH_2O	
SDS	5 g

Before use the buffer was diluted 1:5 in dH_2O

1.5 Transfer buffer

Tris-base 15.1 g
Glycine 74.1 g
Methanol 1000 ml
Dilution up to 5000 ml with dH_2O
SDS 3.75 g

1.6 10x Tris-buffered saline (TBS)

Tris-base 12.11 g
NaCl 87.66 g
Dilution up to 1000 ml with dH_2O, pH adjusted to 7.6

1.7 Wash buffer

10x TBS 100 ml
Tween20 (10 %) 10 ml
Dilution up to 1000 ml with dH_2O

1.8 Blocking buffer

Wash buffer 100 ml
Powdered skimmed milk 5 g

2 Preparation of cell lysates for DR5 analysis using the RIPA-buffer

HCT-116 cells were treated as described in Materials and methods, chapter 2.1.2. The cell samples were prepared 4, 8, 18 or 24 h after light exposure by the following procedure:

1. The medium containing the floating cells from two parallel wells on a 6-well-plate was transferred to a tube.
2. The adherent cells were detached by trypsinisation and collected into the same tube, which was put on ice.
3. The cells were then pelleted and kept on ice.
4. Finally the pellet was washed twice in PBS to remove trypsin and FCS before 50 µl of complete RIPA buffer was added to the cells. Mixed well with a pipette and let the samples stay on ice for about 20 min before they were put in –80°C..

Upon use the lysates were added 1 µl of benzonase and an O.D. measurement was performed to ensure equal loading. An appropriate amount of sample according to these measurements was added to 10 µl of 4x sample buffer and applied to the gel. The remaining procedure was performed as described in “materials and methods”.